Influence of Myc-interacting proteins on transcription and development

Der Einfluss von Myc-interagierenden Proteinen auf Transkription und Entwicklung

Doctoral thesis

for a doctoral degree

at the Graduate School of Life Sciences,

Julius-Maximilians-Universität Würzburg,

Section Integrative Biology

submitted by

Jennifer Marianne Gerlach

from **Rodalben**

Würzburg, 2017

Members of the Thesis Committee:

Chairperson: Prof. Dr. Alexander Buchberger

Primary Supervisor: Prof. Dr. Peter Gallant

Supervisor (Second): Prof. Dr. Christian Wegener

Supervisor (Third): Prof. Dr. Thomas Raabe

Submitted on: …………………………………………………..……..

Date of Public Defence: ……………………………………….…………

Date of Receipt of Certificates: ………………………………………….

Substantial parts of this thesis were submitted for publication in "The PAF1 complex component Leo1 recruits *Drosophila* Myc to promoters" (Gerlach *et al*., manuscript submitted).

---

[1] This figure was submitted for publication in similar form in (Gerlach *et al*., manuscript submitted) (see following pages).

Table of Contents

List of figures

List of tables

Summary

The transcription factor Myc interacts with several co-factors to regulate growth and proliferation and thereby enables normal animal development. Deregulation of Myc is associated with a wide range of human tumors. Myc binds to DNA together with its dimerization partner Max, preferentially to canonical E-box motifs, but this sequence-specific interaction is probably not sufficient for Myc's binding to target genes.

In this work, the PAF1 complex was characterized as a novel co-factor of Myc in *Drosophila melanogaster*. All components of the complex are required for Myc's recruitment to chromatin, but the subunit Atu has the strongest effect on Myc's binding to target genes through its direct physical interaction with Myc. Unexpectedly, the impact of Atu depletion on the expression of Myc target genes was weak compared to its effect on Myc binding. However, the influence of Atu becomes more prominent in situations of elevated Myc levels *in vivo* . Myc-repressed as well as Myc-activated targets are affected, consistent with the notion that Myc recruitment is impaired.

An independent set of analyses revealed that Myc retains substantial activity even in the complete absence of Max. The overexpression of Myc in Max^0 mutants specifically blocks their pupariation without affecting their survival, which raised the possibility that Myc might affect ecdysone biosynthesis. This connection was studied in the second part of this thesis which showed that Myc inhibits the expression of ecdysteroidogenic genes and thereby the production of ecdysone. Myc most likely affects the signaling pathways (PTTH and insulin signaling) upstream of the PG, the organ where ecdysone is produced. By combining existing ChIPseq, RNAseq and electronic annotation data, we identified five potential Max-independent Myc targets and provided experimental data that they might be involved in Myc's effect on Max mutant animals. Together our data confirm that some Myc functions are Max-independent and they raise the possibility that this effect might play a role during replication.

Zusammenfassung

Der Transkriptionsfaktor Myc interagiert mit verschiedenen Cofaktoren, um Wachstum und Proliferation zu regulieren, was die normale Entwicklung von Tieren ermöglicht. Die Fehlreguliereung von Myc wird mit einer großen Anzahl menschlicher Tumore in Verbindung gebracht. Myc bindet gemeinsam mit seinem Dimerisationspartner Max an DNA, bevorzugt an kanonische E-Box Motive. Allerdings ist diese sequenz-spezifische Interaktion wahrscheinlich nicht ausreichend für die Bindung von Myc an Zielgene.

In dieser Arbeit wurde der PAF1 Komplex als ein neuartiger Cofaktor von Myc in *Drosophila melanogaster* charakterisiert. Alle Komponenten des Komplexes sind für die Rekrutierung von Myc an Chromatin notwendig, jedoch hat die Untereinheit Atu, durch ihre direkte physische Interaktion mit Myc, den stärksten Effekt auf die Bindung von Myc an Zielgene. Verglichen mit dem Effekt auf die Bindung von Myc hatte die Depletion von Atu nur einen schwachen Einfluss auf die Expression der Myc Zielgene. *In vivo* ist der Einfluss von Atu stärker ausgeprägt in Situationen in denen die Myc Proteinlevel erhöht sind. Sowohl Myc-reprimierte als auch Myc-aktivierte Gene sind dadurch betroffen. Dies stimmt mit der Entdeckung überein, dass die Rekrutierung von Myc beeinträchtigt ist.

Unabhängige Versuche haben gezeigt, dass Myc eine deutliche Aktivität behält auch bei vollständiger Abwesenheit von Max. Die Überexpression von Myc in Max^0 Mutanten verhindert deren Verpuppung ohne ihr Überleben zu beeinträchtigen. Dies führt zu der Vermutung, dass Myc einen Einfluss auf die Biosynthese von Ecdyson hat. Diese Verbindung wurde im zweiten Teil der Arbeit untersucht und hat gezeigt, dass Myc die Expression von Genen, die an der Ecdyson-Synthese beteiligt sind, verhindert und dadurch die Produktion von Ecdyson selbst. Myc wirkt bevorzugt auf die Signalwege (PTTH und Insulin Signalkaskade) oberhalb der Prothorakaldrüse, dem Organ in dem Ecdyson produziert wird. Durch die Kombination von ChIPseq, RNAseq und der Auswertung elektronischer Daten wurden von uns fünf potentielle Max-unabhängige Zielgene von Myc identifiziert. Des weiteren haben experimentelle Daten gezeigt, dass diese in Zusammenhang mit dem Effekt von Myc auf Max^0 Mutanten stehen. Zusammenfassend haben unsere Daten bestätigt, dass einige Funktionen von Myc Max-unabhängig sind und es besteht die Möglichkeit, dass dieser Effekt eine Rolle während der Replikation spielen könnte.

1 Introduction

1.1 The transcription factor Myc

The transcription factor Myc is one of the most intensively studied proto-oncogenes. The strong interest is based on the fact that Myc is deregulated in a wide range of human tumors. The first Myc gene was identified in 1978 as a viral oncogene, called v-myc, which caused tumors (<u>my</u>elo<u>c</u>ytomatosis) in chicken (Sheiness *et al.*, 1978). Some years later, the verte-brate homologs c-Myc (Vennstrom *et al.*, 1982), N-Myc (Kohl *et al.*, 1983) and L-Myc (Nau *et al.*, 1985) were discovered. In rodents, two more homologs (B-Myc and s-Myc) were found (Ingvarsson *et al.*, 1988; Sugiyama *et al.*, 1989). Subsequent analyses demonstrated that Myc is highly conserved during evolution and found in all vertebrates and many invertebrates (Mahani *et al.*, 2013), including *Drosophila melanogaster* (Gallant *et al.*, 1996; Schreiber-Agus *et al.*, 1997). The Myc family codes for transcription factors, which are involved in sev-eral molecular processes like cellular growth and proliferation, apoptosis and cell cycle pro-gression (Dang, 2013; Eilers and Eisenman, 2008).

1.1.1 Molecular functions of Myc

The Myc proteins (c-, L- and N-Myc) contain several domains which mediate their diverse functions. Four motifs, known as Myc boxes I–IV (MBI–MBIV) (Figure 1.1), are highly con-served even between different species. The N-terminal transactivation domain (TAD) is im-portant for the transcriptional activity of Myc and contains the MBI and MBII (Luscher and Vervoorts, 2012). The Myc boxes III and IV are centrally located. MBIII has been shown to affect Myc stability, repression and apoptosis (Herbst *et al.*, 2005; Herbst *et al.*, 2004) but above all, the binding to WDR5 (Thomas *et al.*, 2015). For MBIV the claims are similarly broad (Cowling *et al.*, 2006). Furthermore, Myc possesses a nuclear localization signal (NLS) mediating its transport into the nucleus. The C-terminus harbors the basic region for DNA binding, and the helix-loop-helix-leucine zipper (bHLHZ) domain for the interaction with se-quence-specific co-factors (Luscher and Vervoorts, 2012). Therefore, Myc belongs to the bHLH superfamily of transcriptional regulators. Such proteins require the formation of homo- or heterodimers for their binding to DNA (Kiessling *et al.*, 2006). Myc needs a partner for het-erodimerization since it does not homodimerize under physiological conditions (Dang *et al.*, 1991; McDuff *et al.*, 2009). This partner is Max (Myc-associated protein X), another bHLHZ protein (Blackwood and Eisenman, 1991). *In vitro* these Myc:Max dimers bind specific DNA sequences (CACGTG), so-called E-boxes (enhancer-boxes) (Blackwell *et al.*, 1990). In addi-tion, Myc can bind to variants of this sequence (CANNTG) but with a lower affinity (Blackwell *et al.*, 1993). Many *in vivo* Myc targets contain such E-boxes but Myc does not bind to all of them indiscriminately. The genes must be located in open chromatin, i. e. in active promot-

ers, which are typically marked by methylation marks at histone H3 lysine 4 (K4) and 79 (K79) (Guccione *et al.*, 2006; Guo *et al.*, 2014; Lin *et al.*, 2012; Sabo *et al.*, 2014). However, Myc also binds to many promoters lacking an E-box motif (Guo *et al.*, 2014). This can be partially explained by the recently reported interaction with WDR5, which recruits Myc to chromatin in a sequence-independent manner (Thomas *et al.*, 2015). Such sequence-independent recruitment to open chromatin has been observed in particular in situations of supraphysiological Myc level, where it was reported to invade virtually all promoters and stimulate their activity (Lin *et al.*, 2012; Nie *et al.*, 2012; Sabo *et al.*, 2014; Walz *et al.*, 2014). After the binding of Myc:Max heterodimers to the DNA, they recruit additional co-activator complexes, which leads to the activation of nearby genes. Among such co-activators are for example p300 or the adaptor protein TRRAP, a component of the TIP60 and GCN5 histone acetyltransferase (HAT) complexes (Hann, 2014; Luscher and Vervoorts, 2012; McMahon *et al.*, 1998). HAT enzymes recruited by Myc catalyze the acetylation of H3 and H4 histones, which leads to a change in chromatin structure. This allows the transcriptional access to DNA or the binding of chromatin remodeling complexes (Bouchard *et al.*, 2001; Frank *et al.*, 2003; McMahon *et al.*, 2000). Furthermore, the ATPases TIP48 and TIP49 were shown to be co-factors of Myc. These proteins belong to several chromatin remodeling complexes and exhibit helicase activity (Hann, 2014; Wood *et al.*, 2000). In addition, Myc:Max dimers recruit the positive transcription elongation factor b (P-TEFb) to Myc target genes *in vivo*. The recruitment of P-TEFb leads to the phosphorylation of RNA pol II thereby allowing efficient transcription elongation (Gargano *et al.*, 2007; Rahl *et al.*, 2010). Recently, Myc was shown to associate with the PAF1 complex and this leads subsequently to the inhibition of Myc target gene expression (Jaenicke *et al.*, 2016).
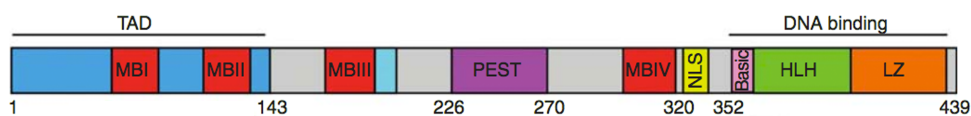
Figure 1.1: Myc protein structure

The Myc protein contains four conserved Myc boxes (MB I-IV), a nuclear localization signal (NLS) and at the C-terminus a basic region, a helix-loop-helix domain (HLH) and a leucine zipper (LZ). Shown is the human c-Myc which consists of 439 amino acids (modified form Farrell and Sears, 2014).

Myc activates the expression of many target genes but can also repress the transcription of genes. Therefore, Myc interacts with additional transcription factors like SP1 or Miz1 (Hann, 2014; Peukert *et al.*, 1997). These transcription factors promote transcription in the absence of Myc, whereas binding of Myc turns them into repressors. Most probably, the interaction of Myc with Miz1 or SP1 leads to an exchange of co-factors. Co-repressors, like DNA methyl-

transferases or HDACs, are recruited and replace the co-activators leading to subsequent repression of the corresponding genes (Hann, 2014; Luscher and Vervoorts, 2012).

1.1.2   Myc in *Drosophila*

The existence of three different Myc variants complicates studies in the vertebrate background. *Drosophila* represents a good system for evaluating Myc functions due to its simpler genetics. The fly genome encodes single Myc and Max proteins, and only one member of the MAD/MXD/MNT family, called Mnt (Gallant, 2009; Gallant, 2013; Gallant *et al.*, 1996). Calvin Bridges discovered the first Myc mutation already in 1935. He called the mutation "*diminutive*" (*dm*) due to the reduced size of the adult flies (Bridges, 1935). Many years later, it was shown that this mutation corresponds to the Myc locus (Gallant *et al.*, 1996; Schreiber-Agus *et al.*, 1997). Comparison of the amino acid sequence of *Drosophila* Myc (dMyc) and the three different vertebrate proteins shows only a moderate overall similarity of 26%, but the genomic structure and most functional domains are highly conserved. This is the case for MB II and III as well as the bHLHZ motif, whereas MB I shows only poor conservation (Gallant, 2013; Gallant *et al.*, 1996).

Besides the conservation of the structure during evolution, it was shown that *Drosophila* and vertebrate Myc proteins are able to substitute for each other. The lethality of a Myc mutation in the fly can be rescued by an isoform of c-Myc (Benassayag *et al.*, 2005). Furthermore, a proliferation defect of murine fibroblasts lacking c-Myc can be rescued by dMyc (Trumpp *et al.*, 2001). In addition, the interaction of dMyc with activated Ras can transform rat fibroblasts (Schreiber-Agus *et al.*, 1997).

Taken together, *Drosophila* is a good model to study the Myc/Max network and each discovery in the fly can help to understand the vertebrate system.

1.2   Co-factors of Myc

1.2.1   Max

The Myc binding partner Max is a small bHLHZ protein (Blackwood and Eisenman, 1991). Besides participating in the formation of Myc:Max heterodimers, Max was also shown to homodimerize and form heterodimers with Mxd proteins (Mxd1-4) (Ayer *et al.*, 1993; Hurlin *et al.*, 1995), Mnt (Hurlin *et al.*, 1997) and Mga (Hurlin *et al.*, 1999). All these proteins belong to the bHLHZ superfamily and the heterodimers with Max also bind E-boxes. In contrast to Myc:Max complexes, they potentially repress the expression of the corresponding genes by competing with Myc for the binding to Max. Furthermore, the resulting dimers compete with Myc:Max dimers for the binding to targets sites and after the binding to target genes, they

recruit transcriptional co-repressors. Thereby they antagonize the function of Myc (Gallant, 2009; Gallant, 2013).

The genome of *Drosophila melanogaster* contains a single Max gene coding for a protein of 161 amino acids. The comparison of the amino acid sequence of human and *Drosophila* Max revealed a high conservation with an overall identity of 52% (Gallant *et al.*, 1996). In addition, only one homolog for Mnt is present in *Drosophila*. It shows similarity to the vertebrate Mnt and Mxd proteins, even though the similarity with Mnt is higher. Max can form homodimers as well as heterodimers with Mnt, and these dimers repress the transcription of many Myc target genes, as already described for the vertebrate system (Loo *et al.*, 2005; Pierce *et al.*, 2008).

1.2.2 Max-independent functions

It was generally assumed that all of Myc's activities are Max dependent because Myc cannot bind to DNA on its own, it needs to form a heterodimer with Max (McDuff *et al.*, 2009). In addition, several Myc functions were shown to be dependent on Max, e. g. the transcriptional activation and repression by Myc (Kretzner *et al.*, 1992; Mao *et al.*, 2003), and Max was found to bind to Myc target sites, wherever investigated. However, several reports demonstrate the existence of Max-independet functions of Myc: Myc overexpression in PC12 cells from rats was able to induce apoptosis in the complete absence of Max (Vaque *et al.*, 2008; Wert *et al.*, 2001), and a derivative of Myc (Myc-nick) retains a function even though it lacks the bHLHZ and therefore cannot interact with Max (Conacci-Sorrell *et al.*, 2010). In *Drosophila*, such activities were revealed by extensive studies of Max *in vivo* (Steiger *et al.*, 2008). Null mutants of Myc (dm^4) die already shortly after hatching (Pierce *et al.*, 2004). In contrast null mutants of Max, herein termed Max^0, are able to undergo metamorphosis and about 70% of the animals develop to pharate adult stage (Steiger *et al.*, 2008). Such animals are smaller than wildtype at all stages (larvae, pupae and pharate adults) and show a prolonged larval development. Wildtype animals pupariate around day 5 after egg deposition (AED) whereas mutant larvae need 8 – 10 days to start pupariation. Even though Max^0 animals can develop to morphologically normal pharate adults, they are not able to eclose (Steiger *et al.*, 2008). Further investigations of Myc functions in a Max^0 background revealed that uncondi-tional and ubiquitous overexpression of Myc with the strong driver actin-GAL4 killed all ani-mals during L2 to L3 molt (Steiger, 2007). High expression levels of Myc are known to induce apoptosis (de la Cova *et al.*, 2004; Montero *et al.*, 2008; Schwinkendorf and Gallant, 2009). Therefore, co-expression of the caspase inhibitor p35 was thought to rescue lethality by blocking apoptosis but this was not the case. Unexpectedly, when expression of Myc and p35 in a Max^0 mutant background is initiated after the L3 molt, no lethality was observed. Such larvae did not pupariate at all and survived up to 33 days AED. In contrast, sole ex-

pression of Myc or p35 during L3 stage did not affect pupariation and resulted in pupae comparable to Max^0 mutants (Steiger, 2007).

The observed pupariation block caused by Myc and p35 overexpression is similar to the phenotype previously described for *ecdysoneless* (*ecd^1*) mutants, which cannot produce ecdysone. These mutants are unable to pupariate and remain living larvae for up to three weeks (Garen *et al.*, 1977). Feeding of 20-hydroxyecdysone (20E) is able to rescue their pupariation. This also worked for Max^0 animals overexpressing Myc and p35 consistent with the assumption that ecdysone production or signaling is disrupted in this genotype (Steiger, 2007).

These findings served as the starting point for the project "Myc affects ecdysone synthesis and developmental transitions" investigated during this thesis. Since Max is required for the binding of Myc to some target genes, this project is expected to identify a class of Myc targets that do not rely on Max for Myc's DNA binding, but on a potentially novel mechanism.

1.2.3 The RNA Polymerase II-associated factor (PAF1) complex

The complex was originally found over 20 years ago in a screen to identify novel RNA polymerase II (RNA pol II) associated factors in *Saccharomyces cerevisiae* (Wade *et al.*, 1996). Therefore, the first identified protein from the screen was termed Polymerase-associated factor 1 (Paf1) (Shi *et al.*, 1996). Subsequently, it was shown that Paf1 is one component of a multimeric complex. In yeast and *Drosophila*, this complex consists of five subunits Paf1, Cdc73, Leo1, Rtf1 and Ctr9 (Figure 1.2). In humans, the complex contains an additional component, Ski8 (Zhu *et al.*, 2005). Some of the homologues in *Drosophila* have different names: Paf1 is called antimeros, Cdc73 is known as hyrax and Leo1 as Atu (Another transcription unit). Furthermore, Parafibromin is the human homolog of Cdc73. Even though the complex is conserved from yeast to human, it is not essential in yeast and after complex elimination the expression of only few genes is affected (Jaehning, 2010). In contrast, all genes encoding the different PAF1 complex components were shown to be essential in *Drosophila* (Bahrampour and Thor, 2016; Mosimann *et al.*, 2006; Spradling *et al.*, 1999; Tenney *et al.*, 2006).
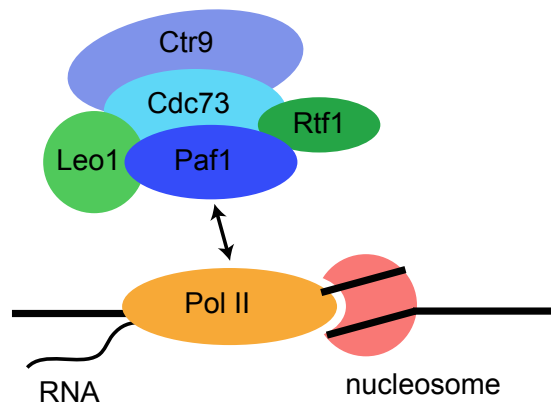
Figure 1.2: The PAF1 complex

The PAF1 complex consists of five subunits in yeast and *Drosophila*. These components are Paf1, Leo1, Cdc73, Rtf1 and Ctr9. Some *Drosophila* homologs have different names: Paf1 = antimeros; Cdc73 = hyrax; Leo1 = Atu. The organization within the complex is not finally resolved yet. The complex interacts with Pol II in transcription regulation (adapted from (Kim *et al.*, 2010)).

The physical interaction between the PAF1 complex and RNA pol II, which was shown in the original screen, suggested a function in transcription. This was supported by several studies that revealed an association of PAF1 with different transcription elongation factors. In *Drosophila* it was shown that the recruitment of the factors Spt6 and FACT (Facilitates Chromatin Transcription) is reduced after the depletion of Paf1 (Adelman *et al.*, 2006). An association with the Spt4-Spt5 complex and FACT was also demonstrated in yeast (Squazzo *et al.*, 2002). A recent study with human leukemia cells showed that the positive transcription elongation factor b (P-TEFb) plays a direct role in the recruitment of the PAF1 complex (Yu *et al.*, 2015) and that the complex has a positive effect on RNA pol II pause release and transcriptional elongation (Tomson and Arndt, 2013; Yu *et al.*, 2015). In contrast, a negative influence on elongation was ascribed to the PAF1 complex by several other publications (Chen *et al.*, 2015; Crisucci and Arndt, 2012; Jaenicke *et al.*, 2016). Different models have been proposed for PAF1's effect on transcription. Either the complex is recruited to specific genes via a sequence-specific transcription factor, e.g. GCN4 (Qiu *et al.*, 2006), or the PAF1 complex recruits the corresponding transcription factor, like STAT3 (Youn *et al.*, 2007). Recently, Jaenicke *et al.* (2016) showed an interaction of the transcription factor Myc and the PAF1 subunit Cdc73 and proposed that the PAF1 complex is recruited by Myc. After depletion of Cdc73 the expression of Myc targets is increased by about 10%, which suggests a negative effect of the complex on the investigated targets (Jaenicke *et al.*, 2016).

The PAF1 complex was also discovered independently in an RNAi screen for novel Myc cofactors in S2 cells (Furrer, 2008; Furrer *et al.*, 2010). In the screen, a firefly luciferase report-

er was used to determine levels of Myc-dependent transcription. *Drosophila* S2 cells were co-transfected with the reporter and a single dsRNA for knockdown of a candidate co-factor gene. In total, 752 transcription-associated factors were tested. The screen revealed 33 proteins that showed an influence on reporter activity, including several components of the PAF1 complex (Furrer, 2008).

Another objective of this work was to understand how the PAF1 complex contributes to the biological and molecular activities of Myc in *Drosophila melanogaster*.

1.3 Biological functions of Myc

Myc is an essential gene in vertebrates as well as in *Drosophila*. Myc deletion leads to embryonic lethality in mice (Davis *et al.*, 1993) and flies carrying a null mutation of Myc (*dm^4*) die during early development in the first larval stage (Pierce *et al.*, 2004; Steiger *et al.*, 2008). The first discovered hypomorphic Myc mutation (*dm^1*) revealed already the influence of Myc on final body size (Bridges, 1935). This was confirmed in later studies showing that *dm1* mutants grow more slowly at larval stages and develop to smaller adult flies (Gallant *et al.*, 1996; Schreiber-Agus *et al.*, 1997). In such flies, cell size is reduced whereas cell number is not affected (Johnston *et al.*, 1999). Conversely, elevated Myc levels result in an increase in body size of adult flies of almost 30% (de la Cova *et al.*, 2004). Together, these findings demonstrate that the most prominent function of Myc in *Drosophila* is the control of growth. Furthermore, Myc has been reported to be involved in several other processes: Myc triggers regenerative growth of imaginal discs after damage, it affects the rate of endoreplication in polyploidy tissues (e. g. fat body, salivary gland, ovary) and it influences the production of a fat-body-derived signal, which promotes systemic growth (Gallant, 2013). After overexpression, Myc also influences apoptosis in a non cell autonomous manner. The cells which overexpress Myc actively eliminate the neighboring, slower-growing wildtype cells. This process is called cell competition (Gallant, 2013).

Like its vertebrate counterpart, *Drosophila* Myc activates or represses numerous target genes. Many of these genes play a role in ribosome biogenesis and are regulated directly by Myc:Max complexes since they contain a canonical E-box (CACGTG) near their transcriptional start site. Besides these RNA pol II targets, the transcription by RNA polymerase I and III is also controlled by Myc and thereby the expression of ribosomal RNAs (rRNAs) and small non-coding RNAs, like tRNAs and 5S rRNA (Gallant, 2013; Grewal *et al.*, 2005; Hulf *et al.*, 2005; Steiger *et al.*, 2008). Myc was shown to activate Pol I activity and rRNA synthesis indirectly by increasing the levels of RNA pol I co-factors (Grewal *et al.*, 2005). In contrast, the activity of RNA pol III is directly promoted by Myc via the physical interaction with the co-factor Brf1 and this process is independent of the dimerization with Max (Gallant, 2013; Steiger *et al.*, 2008).

1.4 Developmental timing in *Drosophila melanogaster*

The development of *Drosophila melanogaster* is strongly influenced by environmental conditions such as temperature, availability and quality of food. Under optimal conditions, the development from egg to adult takes about 10 days. After embryogenesis, the animals develop through three larval stages (L1 to L3). In late L3 the larvae leave the food and prepare for pupariation. In the pupal case they undergo metamorphosis and eclose as adult flies (Figure 1.3).
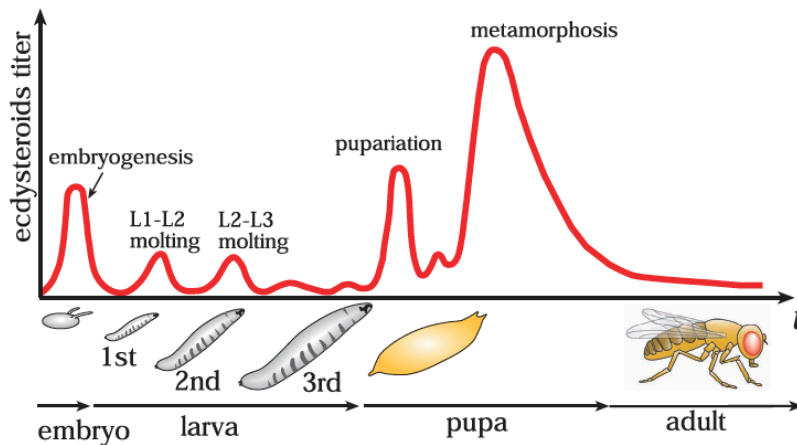
Figure 1.3: Ecdysteroid levels throughout *Drosophila* development

The different developmental stages of *Drosophila melanogaster* and the corresponding levels of ecdysteroids. The hormone pulses trigger the developmental transitions of the animal. The depicted titers result from 20E equivalents in whole body homogenates (Niwa and Niwa, 2014; Riddiford, 1993).

In holomometabolous insects such as *Drosophila*, growth is restricted to the larval period whereas maturation takes place during metamorphosis (Delanoue *et al.*, 2010). The final size of a larva, and thereby the size of the resulting adult, is determined by the duration of the growth phase (i.e. the timing of pupariation). The temporal coordination of organismal developmental is therefore crucial to produce reproductively mature adults. Several neuropeptides and hormones are involved in this control, but the steroid hormone ecdysone is the master regulator (Yamanaka *et al.*, 2013).

1.4.1 The steroid hormone ecdysone

During insect development the steroid hormone ecdysone is produced and released in pulses to trigger developmental transitions (Figure 1.3). The biosynthesis of the hormone takes place in the major endocrine organ of the larvae, the prothoracic gland (PG), which is part of a composite tissue called the ring gland (Colombani *et al.*, 2005). Here, dietary cholesterol is converted stepwise to ecdysone by enzymes encoded by the Halloween gene family (Figure

1.4). These genes were originally discovered in 1984 in a large mutant screen causing embryonic lethality and impairing cuticle formation (Kluding, 1984). The members of the Halloween class are *neverland* (*nvd*), *shroud* (*sro*), *spook* (*spo*), *spookier* (*spok*), *phantom* (*phm*), *disembodied* (*dib*) and *shadow* (*sad*). Except for *nvd* and *sro* all of them code for cytochrome P450 enzymes (Gilbert, 2004; Gilbert *et al.*, 2002; Warren *et al.*, 2002; Warren *et al.*, 2004). After the release from the PG another cytochrome P450 enzyme, shade (*shd*), converts ecdysone into its active form, 20-hydroxyecdysone (20E) (Figure 1.4). This step takes place in the peripheral tissues (Petryk *et al.*, 2003). All these sequential oxidation and hydroxylation steps from cholesterol to 20-hydroxyecdysone are termed ecdysteroidogenesis (Nakaoka *et al.*, 2017).

After the activation by shade in the peripheral tissue, 20E binds to its receptor, the ecdysone receptor (*EcR*), which forms a heterodimer with Ultraspiracle (*USP*) (Hill *et al.*, 2013). The dimer complex induces the expression of target genes, first the so-called early response genes *Broad-Complex* (*BR-C*), *Ecdysone-induced gene 74* (*E74*) and *Ecdysone-induced gene 75* (*E75*). Subsequently, late genes are induced which control the biological responses to each ecdysone pulse. This leads to the morphological changes specific for each developmental stage (Delanoue *et al.*, 2010).
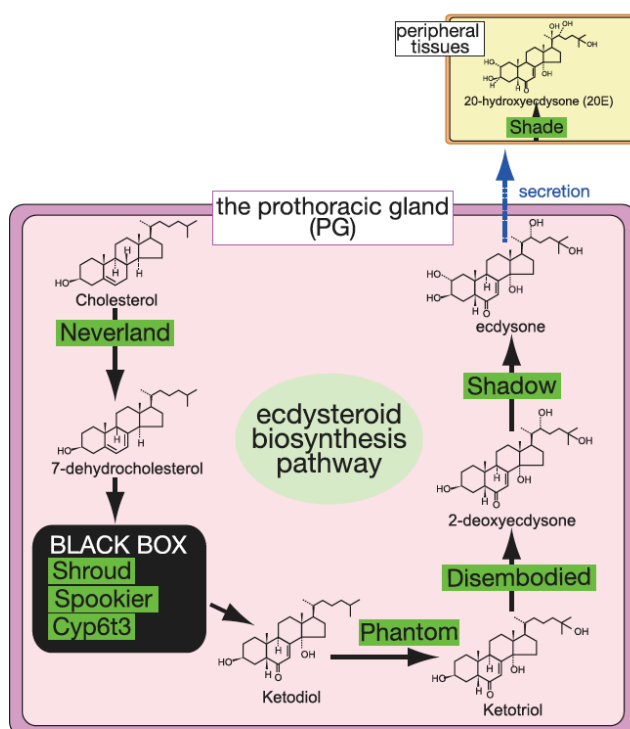
Figure 1.4: Ecdysteroidogenesis in *Drosophila*

Conversion of dietary cholesterol to 20-hydroxyecdysone. The identified intermediates and involved enzymes are shown (adapted from Niwa and Niwa, 2014).

1.4.2   Regulation of ecdysone biosynthesis

The biosynthesis of ecdysone is controlled by several molecular pathways and transcription factors. A schematic overview of the pathways is shown in Figure 1.5 and a detailed description follows in the chapters below.
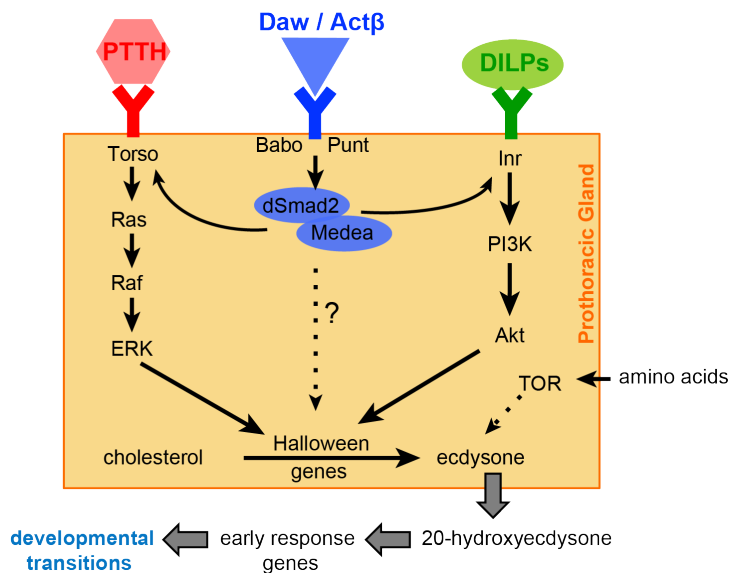
Figure 1.5: Pathways controlling ecdysone production

Schematic overview of the pathways involved in the control of ecdysone biosynthesis in the prothoracic gland. Shown are the ligands, their receptors and the downstream effectors of the different pathways in a facilitate form (adapted from Gibbens *et al.*, 2011).

1.4.2.1   The PTTH pathway

The prothoracicotropic hormone (PTTH) is a brain-derived neuropeptide. PTTH is produced by two pairs of neurosecretory cells (PTTH-producing neurons), which directly innervate the PG (McBrayer *et al.*, 2007). Torso, a receptor tyrosine kinase, was identified as the PTTH receptor. In larvae, *torso* is specifically expressed in the PG (Rewitz *et al.*, 2009). The binding of PTTH to its receptor leads to the activation of downstream Ras/Raf/MAP kinase signaling (Figure 1.5). This promotes ecdysone biosynthesis by stimulating the transcription of ecdysone biosynthetic genes (Gibbens *et al.*, 2011; McBrayer *et al.*, 2007). The loss of PTTH (by ablating the PTTH-producing neurons or blocking downstream signaling) causes a developmental delay which results in larger adult flies (McBrayer *et al.*, 2007; Rewitz *et al.*, 2009). Consistent with this, ubiquitous overexpression of PTTH or PG-specific overactivation of Ras or Raf reduces body size (Caldwell *et al.*, 2005; McBrayer *et al.*, 2007).

These findings demonstrate that PTTH regulates the timing of ecdysone synthesis and thereby final animal size but it is not absolutely required for metamorphosis (Yamanaka *et al.*, 2013).

1.4.2.2 The TOR pathway

The protein kinase Target of Rapamycin (TOR) in the PG senses the nutritional status of the animal, especially the availability of amino acids (Layalle *et al.*, 2008). Even though a cross-talk between the IIS and the TOR pathway has been reported previously (Dan *et al.*, 2002; Manning *et al.*, 2002), Layalle *et al.* showed that both pathways retain distinct functions in animal growth control (Layalle *et al.*, 2008). Inhibition of the Target of rapamycin complex 1 (TORC1) in the PG resulted in a prolonged larval development and delayed expression of ecdysteroidogenic genes (Layalle *et al.*, 2008). Recently, two downstream effectors of TORC1 were identified, REPTOR and REPTOR-BP (Tiebe *et al.*, 2015). During the larval stages when the animals feed and grow, TORC1 levels are high causing the phosphorylation and thereby repression of REPTOR. The activity of TORC1 is reduced under starvation conditions whereby REPTOR becomes active. REPTOR translocates from the cytoplasm to the nucleus and binds to its partner REPTOR-BP. This leads to the induction of target genes involved, for example, in the response to nutrient stress (Tiebe *et al.*, 2015). It is possible that REPTOR mediates the effect on Halloween gene expression after TORC1 inhibiton, although the PG has so far not been explicitly investigated for the contribution of REPTOR on TORC1 dependent activities.

1.4.2.3 The insulin/insulin-like growth factor signaling (IIS) pathway

The best studied pathway is the insulin/insulin-like growth factor signaling (IIS) pathway. The nutritional status of the animal is sensed by the fat body which emits some humoral signals (fat-body-derived signals) and thereby regulates the release of *Drosophila* insulin-like peptides (DILPs) (Geminard *et al.*, 2009; Rajan and Perrimon, 2012). In *Drosophila* eight insulin-like peptides (DILP 1 - 8) are known (Colombani *et al.*, 2012; Garelli *et al.*, 2012; Gronke *et al.*, 2010). Several of them (DILP 2, 3 and 5) are expressed and secreted from two clusters of seven neurosecretory cells in the brain, the insulin producing cells (IPCs) (Ikeya *et al.*, 2002; Luo *et al.*, 2014). After release, the DILPs bind to a single insulin-like receptor (InR). This in turn leads to the activation of the downstream kinases PI3K and Akt in the target tissues (Figure 1.5) (Colombani *et al.*, 2005). PI3K signaling has two roles: in peripheral tissues it regulates growth and metabolism, in the PG it contributes to ecdysone synthesis and cellular growth (Colombani *et al.*, 2005). The loss of PI3K in the PG results in bigger larvae and subsequently adult flies and reduces the expression of the Halloween genes *phm* and *dib* (Colombani *et al.*, 2005). Decreased insulin signaling affects developmental timing and produces large flies (Caldwell *et al.*, 2005; Colombani *et al.*, 2005; Mirth *et al.*, 2005) but does not prevent metamorphosis.

1.4.2.4   The TGFβ / Activin pathway

In contrast to the pathways described above, TGFβ / Activin signaling is absolutely required for ecdysteroidogenesis in the PG, and disruption of the pathway leads to a developmental arrest and inhibits pupariation (Gibbens *et al.*, 2011). Actβ, Dawdle and Myoglianin belong to the Activin / TGFβ ligands which bind to two receptors, a type I receptor (*baboon*) and a type II receptor (*punt*). Here, *baboon* (*babo*) is the one which mediates the specificity for the pathway. Downstream signaling is transduced by dSmad2 and Medea, which form a complex to influence transcription (Figure 1.5) (Gibbens *et al.*, 2011). Knockdown of *dSmad2* reduces the transcript levels of several Halloween genes and causes the abrogation of the 20E peak in the third larval stage (Gibbens *et al.*, 2011). Further investigations revealed that the PTTH as well as the IIS pathway is affected by the loss of *dSmad2*. In both pathways, the expression of the corresponding receptor (Torso or InR) was reduced (Gibbens *et al.*, 2011). Since animals impaired in either pathway are still able to undergo metamorphosis (Colombani *et al.*, 2005; McBrayer *et al.*, 2007; Mirth *et al.*, 2005), it is likely that the pathways can partially substitute for each other. In contrast, the elimination of *dSmad2* causes the simultaneous knockdown of both pathways and results in a complete developmental arrest. This might explain the absolute requirement of the TGFβ / Activin pathway for metamorphosis. Furthermore, it is possible that the TGFβ / Activin pathway has additional essential targets, which affect the transcription of the ecdysone biosynthetic genes and thereby prevent pupariation (Gibbens *et al.*, 2011).

1.5 Objectives of the thesis

Myc affects numerous cellular processes, as described above. The association with co-factors is essential to regulate transcription and subsequently organismal growth, which is the most obvious function of Myc in *Drosophila*. The conservation of Myc between vertebrates and the fly in combination with a much simpler genome and the availability of a huge number of tools for genetic manipulations, make *Drosophila* a good model organism to study the impact of different co-factors on Myc's function.

1) Myc:Max heterodimers were shown to bind most efficiently to E-box motifs. However, several findings suggest that the primary DNA sequence is not sufficient for Myc recruitment to target genes and suggest a requirement for additional proteins. Therefore, M. Furrer carried out an RNAi screen to find factors that play a role in Myc recruitment, or afterwards in trans-activation or -repression. This search identified the PAF1 complex as a potential co-factor of Myc.

The objective of this project was to understand how the PAF1 complex component Atu is involved in Myc's activities. Specific aims of the project involve analyzing the physical interaction of Myc and Atu and characterizing essential protein sequences for this. Furthermore, it will be investigated if Myc recruits the PAF1 complex to target genes or if Atu, and presumably the whole complex, helps to recruit Myc. Finally, the target genes which are affected by this mechanism should be elucidated as well as the impact of Atu on global gene expression in S2 cells and *in vivo*.

2) The characterization of Max mutant flies suggested that Myc affects ecdysone biosynthesis in a Max-independent fashion (Steiger *et al.*, 2008).

During this project it will be investigated how the overexpression of Myc affects ecdysone biosynthesis. In detail, this includes the identification of the larval organ where Myc's action takes place and the confirmation of impaired ecdysone production after Myc overexpression. Furthermore, the determination of the pathway that mediates this effect as well as the specific Myc target(s) involved. Finally, it would be interesting to identify a natural condition, which requires Myc's action in the absence of Max.

2 Materials

2.1 Strains and cell lines

2.1.1 Bacterial strain

XL1 blue   *Escherichia coli*; recA1, endA1, gyrA96, thi-1, hsdR17, supE44, relA1, lac [F' proAB lacIqZΔM15 Tn10(Tetr)]; used for generation and amplification of plasmids

2.1.2 *Drosophila melanogaster* strains

Table 2.1: List of Drosophila strains

Strain	Genotype	Figure
JL115	y w; act-FRT-CD2-FRT-GAL4 hs-FLP; +; CG5033WT-FLuc	4.1
V60100	w	4.1
MF-20	y w; UAS-atms-IR [VDRC 20876] (2nd)	4.1
MF-21	w; UAS-Rtf1-IR [VDRC 27341] (3rd)	4.1
MF-22	w; UAS-Atu-IR [VDRC 17490] (3rd)	4.1
MF-32	w; UAS-Myc-IR [VDRC 2948] (2nd)	4.1
JL118	y w; UAS-hyx-IR/ CyO, GFP (2nd)	4.1
P796	yw hs-FLP; UAS-Myc[132]; act>CD2>GAL4 UAS-GFP/ TM6B	4.9
P560	y w hs-FLP; + ; act>CD2>GAL4 UAS-GFP/ TM6B	4.9
JL112	yw; Atu-IR; act>CD2>Gal4 max/ TM6B	4.9
JL113	yw; Atu-IR; UAS-p35	4.9
DS48	(y) w; UAS-p35	4.9
JL81	y w hs-FLP; Sp/ CyO y+; act>CD2>Gal4 max/ TM6B	4.9
JL1	y w UAS-mCD8-GFP hs-FLP;; actin>CD2>GAL4 max[1]/ TM6B	4.10; 4.11; 4.13 C; 4.14; 4.15 B
P968	y w; UAS-Myc[132]; max[1] UAS-p35/ TM6B	4.10; 4.11; 4.13 A&C; 4.14; 4.15 B
DS12	y w; +; max[1]/ TM6B	4.10; 4.11; 4.13 A&C; 4.14; 4.15 B
JL2	y w; +; max[1] phm-GAL4 UAS-GFP/ TM6B	Tab. 4.2.1; Fig. 4.11
JL31	y w; Feb36-GAL4/ CyO y+; max[1]/ TM6B	Tab. 4.2.1

JL88	y w; P5015-GAL4; max[1]/ TM6B	Tab. 4.2.1
JL77	hs-FLP; phm-GAL80; act-FRT-CD2-FRT-GAL4 max[1]/ TM6B	Tab. 4.2.1
DS68	y w; P0206-GAL4; max[1]/ TM6B, Tb, Hu	Tab. 4.2.1
JL5	y w; Aug21-GAL4; max[1]/ (SM5; TM6B)	Tab. 4.2.1
JL14	y w; C929-GAL4; max[1] UAS-GFP/ TM6B	Tab. 4.2.1
JL27	y w;+ ;386y-GAL4 max[1]/ TM6B	Tab. 4.2.1
JL25	y w; (elav-GAL4; max[1])/ (SM5 /TM6B)	Tab. 4.2.1
JL32	y w; CG-GAL4; max[1]/ TM6B	Tab. 4.2.1
y w	y w	4.13 A&C; 4.15 B
JL109	y w act-FRT-CD2-FRT-GAL4 hs-FLP; +; max[1] unk-FLuc [y+ w+]/ TM6B	4.13 A
JL82	y w; tGPH; act-FRT-CD2-FRT-GAL4 max[1]/ TM6B	4.13 B
JL26	y w hs-FLP; +; max[1] UAS-p35/TM6B	4.9; 4.13 B
JL76	y w hs-FLP; UAS-Myc[132]; max[1] UAS-p35/TM6B	4.9; 4.13 B
JL11	y w/ y w hs-FLP; max[1] UAS-p35/ TM6B; UAS-HA-Myc[ΔZ, ZH-102]	4.14

2.1.3 *Drosophila melanogaster* cell lines

Drosophila Schneider 2 (S2) cells	A primary culture which derived from late stage embryos of Oregon-R (Schneider, 1972)
S2 pMT181-HA-Atu	Stable S2 cell line with $CuSO_4$ inducible HA-Atu expression (under the control of the *Drosophila* metallothionein promotor); generated for this project

17

2.2 Cultivation media and supplements

2.2.1 Media and antibiotics for bacterial cell culture

LB-medium

10% (w/v) Bacto tryptone

0.5% (w/v) yeast extract

1% (w/v) NaCl

LB-agar

1.2% (w/v) Bacto agar was added to LB-medium, then autoclaved and cooled down to 50°C, antibiotics were added and 20 ml were poured into 10 cm dishes

Antibiotics

Ampicillin (100 µg/ml) was added to LB-medium or LB-agar plates

2.2.2 Media for cell culture

Full Medium

Schneider's Insect Medium (Sigma)

10% (v/v) fetal bovine serum (FBS; PAN Biotech), heat inactivated at 56°C for 30 min before usage

1% (v/v) Penicillin / Streptomycin (Sigma)

Freezing Medium

45% (v/v) Full Medium

45% (v/v) Conditioned Medium

10% (v/v) DMSO

2.2.3 Further supplements

$CuSO_4$

125 µM to induce the expression of stably transfected plasmids

Puromycin (InvivoGen)

10 µg/ml for the selection of stable transfected cells

2.3 Nucleic acids

2.3.1 Oligonucleotides

All oligonucleotides were designed with the free software Primer3 (http://bioinfo.ut.ee/primer3-0.4.0/primer3/) or adopted from the DRSC FlyPrimerBank and purchased from Sigma-Aldrich. As far as possible, the oligonucleotides were designed to be exon-spanning to avoid amplification of genomic DNA.

F, for = forward; R, rev = reverse; L = left

Table 2.2: List of oligonucleotides for dsRNA

Name	Application	Sequence (5' → 3')
YF_T7_Atu_L2	dsRNA	TAATACGACTCACTATAGGGAGA**CAAGCTCAC-TTTCCGTCCTC**
YF_T7_Atu_R2	dsRNA	TAATACGACTCACTATAGGGAGA**CTTCCACTGG-CAGACTTGCT**
Atu_T7_cl_F	dsRNA	TAATACGACTCACTATAGGGAGA<u>GAATTC</u>**CTG-CAGACCTGGGAAAAGAG**
Atu_T7_cl_R	dsRNA	TAATACGACTCACTATAGGGAGA<u>TCTAGA</u>**GAGGAC-GGAAAGTGAGCTTG**
Paf1_T7_F	dsRNA	TAATACGACTCACTATAGGGAGA**ATCAAA-GCCATCGAGAAGAC**
Paf_T7_R	dsRNA	TAATACGACTCACTATAGGGAGA**TGGTGTTGTT-GGGTTGCTG**
hyx_T7_F	dsRNA	TAATACGACTCACTATAGGGAGA**C-CATCAAGGCAAAGCGTC**
hyx_T7_R	dsRNA	TAATACGACTCACTATAGGGAGA**GCTCCCGC-TATTACACCC**
Ctr9_T7_F	dsRNA	TAATACGACTCACTATAGGGAGA**GCAACTTGAA-GATGGCAAAG**
Ctr9_T7_R	dsRNA	TAATACGACTCACTATAGGGAGA**TTTGAA-TATGGCCAAAGCCT**
Rtf1_T7_F	dsRNA	TAATACGACTCACTATAGGGAGA**AACGCATGG-CAGAAAAAGA**
Rtf1_T7_R	dsRNA	TAATACGACTCACTATAGGGAGA**ATGAACTCGAG-TCGGAAGA**
T7dmyc5	dsRNA	TAATACGACTCACTATAGGGAGACCAC**CCGGCTCT-GATAGTGACTCC**
T7dmyc3	dsRNA	TAATACGACTCACTATAGGGAGACCAC**TGCTCAT-CATGGAGCTATGC**
GFP-L	dsRNA	TAATACGACTCACTATAGGGAGA**TGAG-CAAGGGCGAGG**
GFP-R	dsRNA	TAATACGACTCACTATAGGGAGA**GCGGCGGTCAC-GAAC**
dmaxT7.5	dsRNA	TAATACGACTCACTATAGGGAGA**TTT-GCGCGCAATCCGTG**

dmaxT7.3	dsRNA	TAATACGACTCACTATAGGGAGA**TAAGGTCGATT-GGGTGGG**

All oligonucleotides contain the sequence of the T7 promoter ("TAATACGACTCAC-TATAGGGAGA"). The specific sequence of each oligonucleotide is displayed in bold letters. An enzymatic restriction site in the sequence is underlined.

Table 2.3: List of oligonucleotides for qPCR and ChIP

Name	Application	Sequence (5' → 3')
PG_act5C_F1	qPCR	GCCCATCTACGAGGGTTATGC
PG_act5C_R1	qPCR	AATCGCGACCAGCCAGATC
DB_Atu_qPCR_F1	qPCR	ATGGGCAGCCAAAACTCGGACGA
DB_Atu_qPCR_R1	qPCR	CGCACTACCTCCTTGCGGCG
DB_Atu_qPCR_F2	qPCR	AAGTGGAAGCCGCAGTGTCACG
DB_Atu_qPCR_R2	qPCR	CGGGAACGATCGCTGCCACT
Paf1_qPCR_F3	qPCR	CTGGTTGTCAAGCATCGTCC
Paf1_qPCR_R3	qPCR	ACTTCTTCCACGATCTCCTCC
hyx_qPCR_F	qPCR	GCCAGATTATCTTCGGCGAG
hyx_qPCR_R	qPCR	GCCCTTCTTACCGGATCCAT
Ctr9_qPCR_F	qPCR	TCCAACTGCATAGAGATCCCTT
Ctr9_qPCR_R	qPCR	CAACACCTCTGGACAGTCGG
Rtf1_qPCR_F	qPCR	CGGACGCAATCCCTGATCG
Rtf1_qPCR_R	qPCR	CCGTTTGGGGCTTCTTTCG
Myc_qRTPCR_F2	qPCR	CAACGATATGGTGGACGATG
Myc_qRTPCR_R2	qPCR	CACGAGGGATTTGTGGGTAG
Max_qPCR_F3	qPCR	CGTGAGCAGACAACAACAAAA
Max_qPCR_R3	qPCR	GATTATTCCACTAAGTTGGTAAGTTT
Pka-C1-cod for	ChIP	CATGACACGGCCAAAGGAGC
Pka-C1-cod rev	ChIP	GGACAAGTGGCGACGCAATC
Uhg1-E2 for	ChIP	CGATTCTTGGAACTACCCTCT
Uhg1-E2 rev	ChIP	GTGACCGCACTACGATTCTG
Uhg2-ES1 for	ChIP	CCGCCATCTTTTCACAGAAT
Uhg2-ES1 rev	ChIP	CGAAGAGCACACAACTTACCA
Nacα_ChIP_F	ChIP	GCATACGTTCACACTGACAGA
Nacα_ChIP_R	ChIP	AGAAATATGGCGGAGGGGAG
BR-C for	qPCR	GCCCTGGTGGAGTTCATCTA

BR-C rev	qPCR	CAGATGGCTGTGTGTGTCCT
Eig75B for	qPCR	GCGGTCCAGAATCAGCAG
Eig75B rev	qPCR	GAGGATGTGGAGGAGGATGA
phm_for	qPCR	TGCCGACCGTAGTCCTCTC
phm_rev	qPCR	GCGCAGATGATGCCAAATCC
dib_for	qPCR	TATTCCTGGCTAAGATTGCACCA
dib_rev	qPCR	TACAACCAGACAATGTCCTGC
shd_for	qPCR	TGGAATTGTGAACGAGCAAGG
shd_rev	qPCR	CCTGGGAGAAGTAATGCTGGA
spo_for	qPCR	TGGCGATTTTACTGAGTGTTCTG
spo_rev	qPCR	TCCTGGAGCCTGGGTATATTTTT
spok_for	qPCR	CTTTGGCGGTGATCGAAACAA
spok_rev	qPCR	GCAGTGTCGCCGAGCTAAA
sad_for2	qPCR	GGACACTTGTGGATCTTATAGCC
sad_rev2	qPCR	TCCCGGAAAATGGGACCATAC
PTTH_qPCR_F	qPCR	AGGCTGCGACTGCAAAGTTA
PTTH_qPCR_R	qPCR	ACGGCATTCATCAGAAAGCGA
mld_qPCR_F1	qPCR	CGACAGAAGCAGAAACCGAAA
mld_qPCR_R1	qPCR	GAGATGATGTAGCTTTAGTCCCG
EcR_qPCR_F1	qPCR	GTCCCGGAGAACCAATGTG
EcR_qPCR_R1	qPCR	GGCGAAGTGGTCATTTTGTCC
Krh1_qPCR_F1	qPCR	CAGATCCCTATCAGTGCAATGTT
Krh1_qPCR_R1	qPCR	GCACCTGGAGGTTCTCCTTC
rpr_qPCR_F1	qPCR	TGGCATTCTACATACCCGATCA
rpr_qPCR_R1	qPCR	CCAGGAATCTCCACTGTGACT
EcR_ChIP_F1	ChIP	TCCGTTGTACAGCACCATCT
EcR_ChIP_R1	ChIP	GGCGCTTTACCATCAACATG
mld_ChIP_F1	ChIP	GCGCTCTACTTCTGCCATCT
mld_ChIP_R1	ChIP	GCATGGAGAGCACGTTGAAA
Eip75B_ChIP_F1	ChIP	CTATTCTCGGCGAGCACAAA
Eip75B_ChIP_R1	ChIP	CCTTCAGGCGATCGTTCATT
rpr_ChIP_F1	ChIP	ACCATGCCGCTCGAAAATC
rpr_ChIP_R1	ChIP	AAGAGGTGTTGGCTAGTCGT
Krh1_ChIP_F1	ChIP	CATGGGTTTTCGACTCGCTC
Krh1_ChIP_R1	ChIP	GTGAGGCTGTCGAAAACTCG

2.3.2 Plasmids

2.3.2.1 Empty vectors

pMT181   Insect expression vector, *Drosophila* metallothionein gene
                         promoter controls expression of genes (CuSO$_4$ inducible),
                         puromycin resistance as selectable marker

pUAST   Insect expression vector,
                         P element-based vector for Gal4-regulated expression of
                         genes in *Drosophila*

2.3.2.2 Expression vectors

pMT181_HA-Atu   pMT181 expression vector with an N-terminal 3x HA-tag and
                         CDS of Atu

pMT181_HA-MycWT   pMT181 expression vector with an N-terminal 3x HA-tag and
                         CDS of Myc

pMT181_HA-MycDZ   pMT181 expression vector with an N-terminal 3x HA-tag and
                         CDS of Myc lacking the leucine zipper domain

pUAS-HA-MycWT   pUAST expression vector with an N-terminal 3x HA-tag and
                         CDS of Myc

pUAS-HA-MycD1-293   pUAST expression vector with an N-terminal 3x HA-tag and
                         CDS of Myc lacking aa 1-293

pUAS-HA-MycDBox2   pUAST expression vector with an N-terminal 3x HA-tag and
                         CDS of Myc lacking Myc Box2 domain

pUAS-HA-MycDBox3   pUAST expression vector with an N-terminal 3x HA-tag and
                         CDS of Myc lacking Myc Box3 domain

pUAS-HA-MycDC   pUAST expression vector with an N-terminal 3x HA-tag and
                         CDS of Myc lacking basic helix-loop-helix and leucine zipper
                         domain

pUAS-HA-MycDZ   pUAST expression vector with an N-terminal 3x HA-tag and
                         CDS of Myc lacking leucine zipper domain

pUAS-HA-AtuWT   pUAST expression vector with an N-terminal 3x HA-tag and
                       CDS of Atu

pUAS-Au1-AtuWT   pUAST expression vector with an N-terminal AU1-tag and
                       CDS of Atu

pUAS-Au1-AtuD2   pUAST expression vector with an N-terminal AU1-tag and
                       CDS of Atu lacking aa 371-725

pUAS-Au1-AtuD3   pUAST expression vector with an N-terminal AU1-tag and
                       CDS of Atu lacking aa 591-725

pUAS-Au1-AtuD211_511   pUAST expression vector with an N-terminal AU1-tag and
                       CDS of Atu lacking aa 442-473

pUAS-Au1-AtuD4   pUAST expression vector with an N-terminal AU1-tag and
                       CDS of Atu lacking aa 1-189

pUAS-Au1-AtuD5   pUAST expression vector with an N-terminal AU1-tag and
                       CDS of Atu lacking aa 1-369

pUAS-Au1-AtuD501   pUAST expression vector with an N-terminal AU1-tag and
                       CDS of Atu lacking aa 1-440

2.4 Antibodies

ChIP = Chromatin-Immunoprecipitation; IP = Immunoprecipitation; WB = Western blot

2.4.1 Primary antibodies

Table 2.4: List of primary antibodies

Antibody	Application	Host / Isotype	Source of supply
Au1-tag	IP, WB	mouse, monoclonal IgG2a	BioLegend, B901902
Au1-tag	IP, WB	rabbit, polyclonal IgG	Bethyl, A190-125A
Atu	IP, WB	rabbit, polyclonal IgG	produced by Group Gallant
CDC73	WB	rat, polyclonal	Gift from John Lis
HA-tag	ChIP, IP, WB	rabbit, polyclonal IgG	Abcam, ab9110
HA-tag	WB	rabbit, polyclonal IgG	ICL, RHGT-45A-Z
IgG	ChIP	mouse, polyclonal	Dianova
IgG	ChIP	rabbit, polyclonal	Dianova
Myc-N	ChIP	rabbit, polyclonal IgG	Santa Cruz, sc-28208
Myc (P4C4-B10)	WB	mouse, monoclonal	produced by Group Gallant
Rtf1	WB	rabbit, polyclonal	Gift from John Lis
α-Tubulin	WB	mouse, monoclonal IgG1 (clone B-5-1-2)	Sigma, T5168

2.4.2 Secondary antibodies

anti-mouse-HRP   goat anti-mouse immunoglobulin, coupled with horseradish peroxidase (Jackson)

anti-rabbit-HRP   donkey anti-rabbit immunoglobulin, coupled with horseradish peroxidase (GE Healthcare)

anti-rat-HRP   goat anti-rat immunoglobulin, coupled with horseradish peroxidase (GE Healthcare)

2.5 Chemicals

All chemicals were purchased from the companies Ambion, AppliChem, Invitrogen, Life Technologies GmbH, Merck, Roth and Sigma-Aldrich. Buffers and solutions were prepared in ddH$_2$O if not indicated otherwise.

2.6 Enzymes, standards, beads and kits

2.6.1 Enzymes

Absolute qPCR SYBR Green Mix	Thermo Scientific
Antarctic phosphatase	New England Biolabs
Benzonase	Merck Millipore
Mini protease inhibitor cocktail tablets	Roche
Omniscript reverse transcriptase	Qiagen
Proteinase K	Roth
Q5 polymerase	New England Biolabs
Restriction endonuclease	New England Biolabs
RNase A	Roth
RNase-free DNase I	Qiagen
RNasin® ribonuclease inhibitor	Promega
T4 DNA ligase	New England Biolabs
Taq polymerase	New England Biolabs
Turbo DNase	Life technologies

2.6.2 Standards

GeneRuler 1 kb Plus DNA Ladder	Thermo Scientific
GeneRuler 100 bp DNA Ladder	Thermo Scientific
GeneRuler 50 bp DNA Ladder	Thermo Scientific
PageRuler Prestained Protein Ladder	Thermo Scientific

2.6.3   Beads for purification

Dynabeads® Protein A / G	Life Technologies
Pierce™ Anti-HA Magnetic Beads and HA Synthetic Peptide	Life Technologies

2.6.4   Kits

dNTPs	Roth
Effectene® Transfection Reagent	Qiagen
Experion DNA 1K Analysis Kit	Bio-Rad
Experion RNA HighSense Analysis Kit	Bio-Rad
Experion RNA StdSense Analysis Kit	Bio-Rad
GenElute Plasmid MiniPrep Kit	Sigma Aldrich
GeneJET Gel Extraction Kit	Thermo Scientific
Immobilon Western HRP Substrate	Millipore
MEGAscript® T7 Transcription Kit	Life Technologies
MinElute PCR Purification Kit	Qiagen
NEBNext® ChIP-Seq Library Prep Master Mix Set for Illumina®	NEB
NEBNext® Poly(A) mRNA Magnetic Isolation Module	NEB
NEBNext® Ultra™ RNA Library Prep Kit for Illumina®	NEB
NEBNext® Multiplex Oligos for Illumina® (Dual Index Primers Set 1)	NEB
Omniscript RT Kit	Qiagen

Plasmid Midi Kit   Qiagen

QIAquick PCR Purification Kit   Qiagen

Quant-iT PicoGreen dsDNA Assay Kit   Life Technologies

Random Hexamers   Roche

RiboMinus™ Eukaryote Kit for RNA-Seq   Thermo Scientific

RNase-free DNase Set   Qiagen

RNeasy Mini Kit   Qiagen

2.7 Buffers and solutions

Ammonium persulfate (10%)

      5 g ammonium persulfate were dissolved in 50 ml ddH_2O,

      aliquots were stored at -20°C

Ampicillin stock solution

      10 g ampicillin were solubilized in 100 ml ddH_2O and sterile filtered;

      aliquots were stored at -20°C

Blocking solution for nitrocellulose membranes

      5% (w/v) skim milk powder in TBS

Bradford solution

      8.5% (v/v) phosphoric acid solution

      4.75% (v/v) ethanol

      0.01% (w/v) Coomassie G250 stain

      solution was filtered and stored in the dark

Blue DNA loading dye (6x)

      0.2% (v/v) Bromphenol blue

      60% (v/v) Glycerin

      60 mM EDTA

ChIP elution buffer

       1% (w/v) SDS

       100 mM $NaHCO_3$

ChIP lysis buffer I

       5 mM PIPES, pH 8.0

       85 mM KCl

       0.5% (v/v) NP40

ChIP lysis buffer II

       10 mM Tris-HCl, pH 7.5

       150 mM NaCl

       1% (v/v) NP40

       1% (w/v) DOC

       0.1% (w/v) SDS

       1 mM EDTA

ChIP wash buffer I

       20 mM Tris, pH 8.1

       150 mM NaCl

       2 mM EDTA

       0.1% (w/v) SDS

       1% (v/v) Triton X-100

ChIP wash buffer II

       20 mM Tris, pH 8.1

       500 mM NaCl

       2 mM EDTA

       0.1% (w/v) SDS

       1% (v/v) Triton X-100

ChIP wash buffer III

       10 mM Tris, pH 8.1

       250 mM LiCl

       1% (v/v) NP40

       1% (w/v) SDS

       1 mM EDTA

Extraction buffer A

  0.1 M Tris-HCl, pH 9.0

  0.1 M EDTA

  1% (v/v) SDS

HEGN lysis buffer (2x)

  40 mM HEPES KOH, pH 7.8

  20% (v/v) glycerol

  0.4 mM EDTA

  0.2% (v/v) NP40

  2 mM Na-ß-glycerophosphat

  20 mM NaF

  20 mM $Na_4P_2O_7$

  sterile filtered (0.2 µm) and stored at 4°C

  freshly added 140 mM KCl and aqua dest ad 1x

Hoechst 33342 (Molecular Probes Inc.)

  used 1:500 in PBS

Laemmli buffer (2x)

  3% (v/v) SDS

  10% (v/v) Glycerol

  62.5 mM Tris, pH 6.8

  0.001% (v/v) Bromphenol blue

  5% (v/v) β-mercaptoethanol

NP40 lysis buffer

  150 mM NaCl

  50 mM Tris-HCl, pH 8.0

  5 mM EDTA, pH 8.0

  0.5% (v/v) NP40

Orange DNA loading dye (6x)

  0.4% (w/v) Saccharose

  10 mM EDTA, pH 8.0

  10 µl (v/v) Orange G

PBS (1x)

  137 mM NaCl

  2.7 mM KCl

  10.1 mM Na_2HPO_4

  1.76 mM KH_2PO_4

BSA-PBS

  5 mg/ml BSA in 1x PBS

PBTw

  0.1% Tween-20 in 1x PBS

PLB (1x)

  5x passive lysis buffer (Promega) diluted in ddH_2O

Protease inhibitor (PI)

  cOmplete^{TM}, Mini protease inhibitor cocktail (Roche, 11836153001),
  used 1:100

Proteinase K

  10 mg/ml in ddH_2O

RNase A (10 mg/ml)

  100 mg RNase A (Roth) in

  27 µl 3 M sodium acetate, pH 5.2

  9 ml ddH_2O

  aliquots à 450 µl

  boiled for 30 min at 100°C to inactivate DNases

  50 µl 1M Tris, pH 7.4 added per aliquot

  stored at -20°C

SDS running buffer

  25 mM Tris base

  250 mM Glycin

  0.1% (v/v) SDS

Separating gel 10-15%

      10 – 15% (v/v) acrylamide / bisacrylamide

      375 mM Tris-HCl, pH 8.8

      0.1% (v/v) SDS

      0.1% (v/v) APS

      0.1% (v/v) TEMED

Stacking gel 5%

      5% acrylamide / bisacrylamide

      125 mM Tris-HCl, pH 6.8

      0.1% (v/v) SDS

      0.1% (v/v) APS

      0.1% (v/v) TEMED

Stripping buffer

      62.5 mM Tris-HCl, pH 6.8

      2% (v/v) SDS

      0.1 M β-mercaptoethanol

TAE (50x)

      2 M Tris base

      5.7% acetic acid

      50 mM EDTA, pH 8.0

TBS (10x)

      250 mM Tris base

      1.4 M NaCl

      adjusted to pH 7.4

TE

      10 mM Tris-HCl, pH 8.0

      1 mM EDTA

Transfer buffer

       48 mM Tris base

       390 mM Glycine

       3.5 mM SDS

       20% (v/v) methanol

Vectashield mounting medium

       ready-to-use solution

       VEC-H-1000 (Biozol Diagnostica Vertrieb GmbH)

2.8 Consumables and equipment

Consumables such as cell culture dishes, reaction tubes and other disposable plastic items were purchased from the companies Applied Biosystems, B. Braun, Eppendorf, Greiner, Kimberley-Clark, Millipore, Nunc, Sarstedt, Schleicher und Schüll and VWR international.

2.8.1 Equipment

Binocular	Olympus SZ61
Chemiluminescence imaging	LAS-4000 mini (Fujifilm)
Cell culture incubator	Incu-Line (VWR)
Centrifuges	Eppendorf 5415 R (Eppendorf)
	Biofuge 15 (Heraeus)
	Avanti J-26 XP (Beckman Coulter)
Heating block	Thermomixer comfort (Eppendorf)
Heat Sealing	ALPSTM 50V (Thermo)
Incubator for flies	Binder
Luminometer	GloMax 96 Microplate Luminometer (Promega)
Magnetic Stirrer	Combimag RCH (IKA)
Microplate reader	TECAN Infinite® 200 PRO
Microscope for	DMI 6000 B (Leica)

immunofluorescence	TCS SP5 (Leica)
	Discovery V8 (Zeiss)
	Nikon Ti-Eclipse (confocal microscope)
Microscope for cell culture	Axiovert 40CFL (Zeiss)
PCR thermal cycler	C1000 Thermal Cycler (Bio-Rad)
Phosphorimager	Typhoon 9200 (GE healthcare)
Photometer	UltrospecTM 3100 pro UV/Visible (Amersham Biosciences)
Power supply	PowerPac 300 (Bio-Rad)
Quantitation of RNA and DNA	Experion Automated Electrophoresis System (Bio-Rad)
	NanoDrop 3000 (Thermo Scientifc)
Quantitative real-time PCR machine	MXp3000P qPCR system (Stratagene)
	StepOne^{TM} Realtime Cycler (Applied Biosystems)
SDS-PAGE system	Mini Trans-Blot (Bio-Rad)
Sterile bench	Lamin Air (Heraeus)
Ultrasonifier	W-250 D (Heinemann)
UV fluorescent table	Maxi UV fluorescent table (PEQLAB)
Universal shaker	SM-30 (Edmund Bühler GmbH)
	Titramax 101(Heidolph)
Vortex mixer	Vortex-Genie 2 (Scientifc Industries)
Waterbath	ED-5M heating bath (Julabo)
Western blot transfer chamber	Mini-PROTEAN Tetra Cell (Bio-Rad)

2.9 Software and online programs

ApE plasmid editor   M. Wayne Davis

Bedtools   (Quinlan and Hall, 2010)

Bowtie v.0.12.8   www.bowtie-bio.sourceforge.net

Illustrator™, Photoshop™, Acrobat™   Adobe Inc.

Image Studio Lite v4.0.21   LI-COR Inc.

Mac OS X   Apple Inc.

MACS v1.4.2   (Zhang *et al.*, 2008)

Microsoft Office 2011 Mac   Microsoft Inc.

Multi Gauge   Fujifilm

MxPro qPCR Software   Stratagene

Primer3web v4.0.0   http://primer3.ut.ee/

Prism4   GraphPad Software Inc.

pubmed   https://www.ncbi.nlm.nih.gov/pubmed

R 3.1.1   R foundation

Samtools   (Li *et al.*, 2009)

StepOne™ Software v2.3   Applied Biosystems

UCSC Genome Bioinformatics   http://genome.ucsc.edu

3 Methods

3.1 Molecular biology methods

3.1.1 Transfection of bacteria with plasmid DNA and plasmid purification

Competent bacteria were thawed on ice and mixed with the ligation mix (3.1.9) or 0.5 – 1 µg of plasmid DNA. After an incubation of 30 min on ice, a heat shock was given for 2 min at 42°C. 1 ml of LB medium without antibiotics was added and the culture was incubated for 45 – 90 min at 37°C. Afterwards the bacterial suspension was centrifuged, resuspended in 100 µl medium and plated on LB agar plates containing the appropriate antibiotic for selection. The plates were incubated upside down at 37°C over night.

3.1.2 Isolation of plasmid DNA from bacteria

For preparative isolation of plasmid DNA (Midiprep), 50 ml of a bacterial overnight culture were treated according to the manufacturer's protocol (Plasmid Midi Kit, Qiagen) until the step of isopropanol precipitation. After removal of the isopropanol, the pellet was air dried and resuspended in 400 µl ddH$_2$O followed by an ethanol precipitation (3.1.3). The mix was incubated for 30 – 60 min at -20°C and then centrifuged (30 min, 4°C, 13200 rpm). The DNA pellet was washed with 70% ethanol, air dried and solubilized in 50 µl ddH$_2$O.

A Miniprep was performed to isolate small amounts of the plasmid DNA. Therefor 3 ml of cultivated bacteria were processed according to the manufacturer's instructions (GenElute Plasmid MiniPrep Kit, Sigma-Aldrich). The DNA pellet was resuspended in 50 µl ddH$_2$O.

3.1.3 Ethanol precipitation of nucleic acids

An ethanol precipitation was performed to concentrate and purify nucleic acids. 2.5 volumes of 100% ethanol and 0.1 volumes of 3 M sodium acetate (pH 5.2) were added to the aqueous solution, mixed thoroughly by vortexing and incubated at -20°C for 30 min or over night. After centrifugation (30 min, 4°C, 13200 rpm), the precipitate was washed once with cold ethanol (70%) and dissolved in an appropriate volume of ddH$_2$O.

3.1.4 Nucleic acid quantitation

3.1.4.1 NanoDrop

The NanoDrop 1000 (Peqlab) was typically used to measure the concentration of DNA or RNA in solution. The absorbance was measured at 260 nm. The ratio of absorbance at 260 and 280 nm was determined, which reflects the purity of the nucleic acid solution. For pure DNA a ratio of ~ 1.8 was expected and for pure RNA ~ 2.

3.1.4.2 PicoGreen

The concentration of double-stranded DNA (dsDNA) was determined with the Quant-iT™ PicoGreen® dsDNA reagent (Invitrogen). The fluorescence can be measured at an excitation wavelength of 485 nm and emission at 535 nm due to the fact that PicoGreen intercalates into dsDNA. The measurement was performed according to the manufacturer's protocol. Chromatin samples after ChIP, which were used for ChIP-Sequencing, were quantified with PicoGreen to determine the DNA concentration.

3.1.4.3 Bioanalyzer

The quality and concentration of RNA, which was used for library preparation for RNA-Sequencing, was determined with the Experion™ Automated Electrophoresis System from Bio-Rad. In addition, the DNA libraries were quantified with this method.

3.1.5 Phenol / chloroform extraction of nucleic acids

To extract DNA, one volume of phenol / chloroform / isoamylalcohol (25:24:1) was added to each sample and the samples were vortexed vigorously. After centrifugation (5 min, RT, 13200 rpm) the upper phase was transferred into a new tube and mixed with 1 µl glycogen (Glycoblue), 50 µl of 3 M NaAc (pH 5.2) and 1 ml of ice cold ethanol (100%). The samples were vortexed, incubated for at least 30 min at -20°C and then centrifuged (30 min, 4°C, 13200 rpm). The pellet was washed once with 500 µl of cold 70% ethanol and subsequently dried at RT before resuspension in an appropriate volume of TE or RNase free water.

3.1.6 Restriction analysis of DNA

Sequence specific hydrolysis of DNA was performed with restriction endonucleases from New England Biolabs (NEB) or Roche using the recommended restriction buffers. A digestion was incubated for 1 – 2 hours at 37°C and set up according to the following table.

Restriction digest mix: 1 – 2 µg DNA
0.5 µl restriction endonuclease 1
0.5 µl restriction endonuclease 2
2 µl 10x reaction buffer
ad 20 µl ddH$_2$O

3.1.7 Separation of DNA and RNA fragments via gel electrophoresis

Gel electrophoresis was used to separate DNA or RNA fragments according to their size. Depending on the expected fragment size, a 1 – 2% agarose gel was prepared. For this pur-

pose the agarose was boiled in 1x TAE buffer, supplemented with 0.3 µg/ml ethidium bromide and poured into a gel chamber with combs. The samples were mixed with loading buffer and transferred into the pockets of the gel. A suitable DNA ladder (Thermo Scientific) was loaded next to the samples to determine the size of the fragments. The separation was performed at 120 – 150 V for 1 – 2 hours and the fragments were visualized using a UV transilluminator, which detects the intercalated ethidium bromide.

3.1.8 Extraction and purification of DNA fragments and PCR products

For purification of DNA fragments from agarose gels, the fragment was cut out of the gel and extracted with the GeneJet Gel Extraction Kit (Thermo Scientific) according to the manufacturer's protocol.

PCR products were purified with the QIAquick PCR Purification Kit (Qiagen) following the manufacturer's instructions.

3.1.9 Ligation of DNA fragments

Ligation was used to attach two DNA fragments covalently with each other. The DNA fragment (insert) was used in 3 – 5x molar excess to the linearized vector. The Insilico ligation calculator (http://www.insilico.uni-duesseldorf.de/Lig_Input.html) was used to calculate the needed amounts of insert and vector to get the optimal molar ratio.

Ligation mix: 100 ng linearized vector

                          x ng DNA fragment (insert)

                          1 µl T4 DNA ligase (NEB)

                          1 µl 10x ligation buffer

                    ad 10 µl ddH$_2$O

The ligation mix was incubated for 1 – 3 hours at RT or over night at 16°C and then transformed into competent bacteria.

Prior to ligation, linearized plasmids were treated with Antarctic phosphatase (NEB) according to the manufacturer's protocol to prevent self-ligation.

3.1.10 Isolation of total RNA from larvae or tissue culture

For the isolation of RNA from larvae, up to 21 larvae were completely homogenized in 100 µl Qiazol (Qiagen) using a pestle. The sample was leveled up to 700 µl with Qiazol and vigorously vortexed. Afterwards the samples were either frozen in liquid nitrogen and stored at -80°C or directly processed with the miRNeasy Mini Kit (Qiagen) following manufacturer's protocol.

RNA from cells was isolated using the RNeasy Mini Kit (Qiagen). Cells were harvested, washed once with cold PBS and pelleted. The pellet was resuspended in the recommended volume of RLT buffer and further processed according to the manufacturer's instructions or stored at -80°C.

All samples were additionally treated with an on-column DNase digestion to get rid of DNA contaminations. For this purpose, DNase I (Qiagen) was used and handled according to the instructions in Appendix B of the protocol belonging to the miRNeasy Mini Kit. RNA concentration was determined by Nanodrop (for cDNA preparation) or Experion RNA Analysis Kit (Bio-Rad) before RNA-Sequencing. The RNA samples were stored at -80°C.

3.1.11 cDNA synthesis

The extracted total RNA (3.1.10) was reverse transcribed into complementary DNA (cDNA) to analyze the expression of individual genes. For this purpose the Omniscript RT kit (Qiagen) was used according to the table below. The cDNA synthesis mix and a control (without reverse transcriptase) were incubated for one hour at 37°C. Afterwards the samples were stored at -20°C.

cDNA synthesis mix:
  1 µg total RNA
  2 µl 10x reverse transcription buffer
  2 µl dNTP mix
  0.2 µl random hexamers (final conc. 10 µM)
  0.25 µl RNasin® ribonuclease inhibitor (40 U/µl, Promega)
  1 µl reverse transcriptase
  ad 20 µl RNase free water

The cDNA was diluted up to 1000 µl with ddH_2O (1:50) and 10 µl of diluted cDNA was used per quantitative real-time PCR reaction (3.1.13.2).

3.1.12 dsRNA synthesis

Double stranded RNA-mediated interference was used to target the expression of specific genes. Linear DNA was amplified by PCR (3.1.13) serving as template for the *in vitro* transcription of the dsRNA. For this purpose, the Megascript T7 Kit (Ambion) was used.

Synthesis mix for dsRNA: 0.2 – 0.4 µg template DNA

                   4 µl 10x reaction buffer

                   4 µl of each dNTP

                   4 µl enzyme mix

                ad 40 µl RNase free water (provided)

The transcription mix was incubated for 4 hours at 37°C, mixed with 1 µl TURBO DNase (Ambion) and further incubated for 15 min. Phenol / chloroform extraction followed by isopro-panol precipitation (according to manufacturer's protocol) was used to purify the transcripts. The pellet was dissolved in 40 µl RNase free water, heated up to 65°C and slowly cooled down to RT to allow reannealing of the complementary strands. The dsRNA was stored at -80°C and investigated on an agarose gel before use.

3.1.13 Polymerase chain reaction (PCR)

The polymerase chain reaction (Mullis *et al.*, 1986) was used to amplify specific regions of DNA for different purposes.

3.1.13.1 PCR to amplify cDNA for cloning or dsRNA synthesis

The gene of interest was amplified from an existing expression vector or genomic DNA to generate a new expression vector. This allowed the addition of tags to the gene or the inser-tion of new restriction sites.

The resulting cDNA was also used as a template for the synthesis of dsRNA (3.1.12).

Standard PCR reaction: 20 – 200 ng DNA template

                   10 µl 5x Q5 reaction buffer

                   2.5 µl forward primer (10 µM)

                   2.5 µl reverse primer (10 µM)

                    1 µl dNTP mix (10 mM)

                   0.5 µl Q5 polymerase (NEB)

                ad 50 µl nuclease free water

Table 3.1: PCR thermal cycling profile

Cycle step	Temperature	Time	Cycles
Initial denaturation	98°C	30 s	1x
Denaturation	98°C	15 s	
Annealing	$T_m - 3°C$	30 s	25 – 35 x
Extension	72°C	30 s / kb	
Final extension	72°C	7 min	1 x

3.1.13.2 Quantitative real-time PCR (qPCR)

Quantitative PCR was performed to analyze the abundance of mRNAs (quantitative reverse transcriptase PCR; qRT-PCR) or the enrichment of DNA fragments after chromatin immuno-precipitation (3.3.7) (quantitative real-time PCR; qPCR). The amount of newly synthetized DNA can be quantified in real time using a dye which fluoresces only when intercalated into double-stranded DNA during amplification.

The measurement was carried out with the Mx3000P qPCR system (Stratagene) or the StepOne™ Realtime Cycler (Applied Biosystems).

qPCR reaction: 10 µl diluted cDNA (3.1.11) or chromatin (3.3.7)

        5 µl SYBR Green Mix with ROX (Thermo Scientific)

     0.5 µl forward primer (10 µM)

     0.5 µl reverse primer (10 µM)

      4 µl RNase free water

Table 3.2: qPCR thermal cycling profile

Cycle step	Temperature	Time	Cycles
Initial denaturation	95°C	15 min	1x
Denaturation	95°C	15 s	
Annealing	60°C	20 s	40 x
Extension	72°C	15 s	
	95°C	15s	
Melting curve	60°C	1 min	1 x
	95°C	15 s	

Abundance of mRNA (analysis of cDNA) was always compared to an appropriate control and the housekeeping gene Actin5c was used for normalization. For the calculation, the threshold cycle (CT) was determined, which indicates at which PCR cycle the fluorescence signal rises

above a certain threshold. For each primer pair the threshold is selected such that all amplification curves intersect it in their exponential phase.

$$\Delta CT = CT^{\text{housekeeping gene}} - CT^{\text{gene of interest}}$$

$$\Delta\Delta CT = \Delta CT_{\text{control}} - \Delta CT_{\text{sample}}$$

$$\text{Relative expression} = 2^{-\Delta\Delta CT}$$

All qPCR reactions were measured in duplicates or triplicates and the average as well as the standard deviation was calculated.

3.2 Cell biology methods

The S2 cells were cultivated at 25°C in a cell incubator under constant temperature. All cell culture work was performed in a sterile workbench.

3.2.1 Passaging of cells

The semi-adherent cells were passaged every 2 – 3 days, when they covered the surface of the flask completely and started to detach and float in the medium. The cells were diluted depending on the future application. For this purpose, a part of the cells was transferred into one or more fresh flasks and mixed with full medium. (Capacity of the flasks: 15 ml for 75 cm^2; 24 ml for 175 cm^2).

3.2.2 Freezing and thawing cells

The day before freezing, cells were split in a 1:1 ratio (cells:medium) to expand the culture. Cells were harvested and counted in a Neubauer chamber. After centrifugation (5 min, RT, 1100 rpm) the pellet was resuspended in freezing medium (2.2.2) to obtain $2*10^7$ cells / ml. Aliquots of 1 ml each were prepared in cryovials and slowly cooled to -80°C using a MrFROSTY freezing container filled with isopropanol at RT. After 24 hours the vials were transferred to the liquid nitrogen storage tank.

Cells were quickly thawed by putting them in a 37°C water bath and washed once with full medium to get rid of the freezing medium. Then they were plated in 5 ml full medium in a fresh 25 cm^2 flask (Greiner).

3.2.3   Transfection of plasmid DNA

3.2.3.1   Transfection using Effectene

The cells were split in a 1:1 ratio 24 hours before the transfection to expand the culture. In 6-well plates $5*10^6$ cells per well were plated and incubated for 2 – 3 hours to allow them to settle. A transfection mix (see table below) was prepared using the Effectene® Transfection Reagent (Qiagen). The number of cells and the amount of transfection agent were adjusted appropriately when using dishes with a different surface area. The transfection mix was incubated for 5 min at RT, afterwards 10 µl of Effectene Reagent was added and incubated for further 5 – 10 min at RT to allow the formation of transfection complexes.

After washing the cells once with 1x PBS 1.6 ml of full medium was added. The transfection mixture was mixed with 600 µl of full medium and added dropwise to the cells. 16 h later the medium was exchanged with 3 ml of fresh medium. The cells were harvested 24 – 48 h after transfection.

Effectene transfection mix: 0.4 µg plasmid DNA

0.2 µg tub-Gal4

3.2 µl enhancer

ad 100 µl EC buffer

3.2.4   Transfection of dsRNA

To expand the culture, the cells were split in a 1:1 ratio 24 hours before the transfection. In 6-well plates, $5*10^6$ cells per well were plated and incubated for 2 – 3 hours to allow them to adhere. The cells were washed once with serum free medium and then transfected with 1 ml serum free medium containing 10 µg of corresponding dsRNA. 2 ml of full medium were added after a 30 min incubation at 25°C. After 24 – 72 h, depending on the efficiency of the dsRNA, the cells were harvested and processed further.

3.2.5   Induction of inducible cell lines

In stably transfected cell lines a final concentration of 125 µM $CuSO_4$ was used to induce the expression of constructs under the control of a metallothionein promotor. The cells were harvested 24 hours after induction.

For a treatment with dsRNA and $CuSO_4$, the cells were processed as described in 3.2.4 and full medium containing $CuSO_4$ was added after the incubation time of 30 min.

3.2.6 Hypoxia stress test

To investigate the consequences of hypoxia stress on gene expression, several 6 cm petri dishes were plated with $1.5*10^7$ cells and incubated for one hour at 25°C so that the cells had time to settle. Afterwards the medium was replaced with fresh full medium and half of the plates were transferred to a hypoxia chamber (Whitley H35 Hypoxystation) at 26.5°C and 0.5% O_2. 4 hours and 24 hours after the start of the experiment one plate from each condition was harvested (hypoxia and normoxia as reference). The cells were washed once with 1x PBS, resuspended in 700 µl Qiazol, flash frozen in liquid nitrogen and stored at -80°C. Subsequently, the RNA was isolated (3.1.10) and the gene expression analyzed by qPCR (3.1.13.2).

3.3 Protein biochemistry methods

3.3.1 Generation of protein lysates from whole cells

For total protein lysates the cells were carefully harvested, washed once with 1x PBS and centrifuged (5 min, 4°C, 1200 rpm). The pellet was dissolved in NP40 lysis buffer (10 µl buffer / mio cells) with freshly added proteinase inhibitors (PI; 1:100) and incubated for 30 min on ice. Afterwards, lysates were treated with 1 µl of Benzonase for 30 min at 37°C or centrifuged (15 min, 4°C, 13200 rpm) to clear them from debris, or a combination of both. The lysates were mixed with an equal volume of Laemmli buffer and stored at -20°C.

3.3.2 Protein determination by the Bradford method

Protein lysates were quantified according to the Bradford method (Bradford, 1976). 500 µl of Bradford reagent were mixed with an equal volume of ddH_2O and transferred into 1 ml cuvettes. 2 µl of the protein lysate were added and the reaction was mixed by vortexing. The absorbance was measured at 595 nm. A reaction containing 2 µl of the lysis buffer served as reference. The protein concentration was determined according to the absorbance of the standard curve established with known concentrations of Bovine Serum Albumine.

3.3.3 SDS polyacrylamide gel electrophoresis (SDS-PAGE)

SDS polyacrylamide gel electrophoresis was used to separate proteins according to their molecular weight. The protein lysates (3.3.1) were boiled for 5 min at 95°C, quickly spun down and loaded on a SDS polyacrylamide gel. The gel consisted of a 5% stacking gel and a variably concentrated separating gel (between 8% and 15%, depending on the protein to be visualized). The PageRuler Pre-Stained Protein Ladder (Fermentas) served as a size marker. Separation of the proteins was performed using SDS-PAGE chambers (Bio-Rad) filled with SDS running buffer at 80 – 120 V.

3.3.4 Western blot

After separation by SDS-PAGE (3.3.3), the proteins were transferred onto a nitrocellulose membrane or a PVDF membrane. Nitrocellulose membranes were first incubated in water for 30 sec and then in tank blot buffer for another 30 sec. PVDF membranes had to be activated in methanol for 1 min and then equilibrated in blot buffer. The gel was layered on the membrane followed by wet Whatman filter papers on each side and fixed in a tank blot transfer chamber (Bio-Rad). The chamber was completely filled with 1x transfer buffer containing 20% methanol. The transfer was carried out in the cold room (4°C) usually at 225 mA for 2 hours and 20 minutes. The duration of the transfer was adjusted based on the protein of interest. Subsequently, the membrane was blocked for 1 h in blocking buffer and cut into parts for the incubation with different primary antibodies over night at 4°C. After washing (3 x 10 min in TBS) the membrane was incubated with the corresponding secondary antibody in blocking solution for 3 – 4 h at RT followed by another three washing steps with TBS. All incubation steps were carried out under gentle shaking. Chemiluminescence signals generated by the HRP coupled to the secondary antibodies were visualized using the Immobilon Western Substrate (Millipore) according to the manufacturer's instructions. The signal was detected with the LAS-4000 imager (Fujifilm Global).

3.3.5 Stripping antibodies from nitrocellulose membranes

To remove antibodies from nitrocellulose membranes, the membranes were incubated in tubes with freshly prepared stripping buffer for 10 – 30 min at 65°C in a water bath. Afterwards, membranes were washed three times with TBS (10 min each), incubated for 1 hour in blocking buffer and incubated again as described in 3.3.4.

3.3.6 Immunoprecipitation

3.3.6.1 Immunoprecipitation of transiently transfected constructs

Immunoprecipitations (IPs) of tagged proteins were used to study protein-protein interactions. S2 cells were transfected with different constructs (3.2.3) 24 hours before starting the IP. For each IP 1 – 2 wells of a 6-well plate were used seeded with 5 mio cells. Dynabeads A or G (7.5 µl of a 50% suspension per IP) were washed three times with BSA-PBS (5 mg/ml) and then incubated with 500 µl BSA-PBS containing 1 µg of the appropriate antibody for 6 – 8 h at 4°C on a rotating wheel. Cells were harvested 24 h after transfection, washed once with cold PBS with proteinase inhibitors (PI; 1:100) and lysed for 30 min on ice in 300 µl pre-chilled NP40 lysis buffer containing PI. Afterwards, each lysate was supplemented with 1 µl of Benzonase and incubated for another 30 min at 37°C. The lysates were centrifuged for 15 min at 4°C and 13200 rpm to remove cell debris. 10% of every lysate were put aside as input control. After three washing steps with lysis buffer, the beads were mixed with the lysates

and incubated over night at 4°C on a rotating wheel, followed by three more washing steps with lysis buffer. The beads were resuspended in 20 µl NP40 lysis buffer and an equal volume of 2x Laemmli. The samples were either stored at -20°C or directly processed by SDS-PAGE and Western blotting. The samples were boiled for 10 min at 95°C to elute and denature the proteins prior to loading. 3 – 4% of input samples were mixed with Laemmli buffer and boiled for 5 min at 95°C as well.

3.3.6.2   Immunoprecipitation of endogenous proteins

For the endogenous-like immunoprecipitation the stably transfected HA-Atu cell line was used. 24 h before the start of the experiment about $300*10^6$ cells were treated with $CuSO_4$ to induce HA-Atu expression. The Protein A Dynabeads (50 µl per IP) were prepared before starting the experiment by three washes with BSA-PBS. Afterwards the beads were incubated with 8 µg antibody (specific or control IgG) in 1 ml BSA-PBS for 6 – 8 h at 4°C on a rotating wheel. The beads were washed three times with HEGN buffer, then they were mixed with the lysates. The cells were harvested, washed once with cold PBS containing PI (1:100) and lysed for 30 min on ice in 2 ml cold HEGN buffer with PI. The lysate was sonicated 8x for 5 sec with an amplitude of 20% and centrifuged (15 min, 4°C, 13200 rpm). As reference, 5% of the lysate were set aside and stored at -20°C. The samples were mixed with the antibody coupled beads and incubated over night at 4°C on a rotating wheel. Afterwards the beads were washed three times using HEGN buffer with PI and resuspended in 30 µl of this buffer and an equal volume of 2x Laemmli buffer. The samples were boiled for 10 minutes at 95°C before being analyzed on a 10% SDS gel, followed by Western blotting.

3.3.7   Chromatin immunoprecipitation (ChIP)

Interactions between proteins and DNA were investigated using chromatin immunoprecipitation (ChIP). For this purpose, cells were plated on 10 cm dishes and treated according to the experimental setup. For each IP approximately $4*10^7$ cells were used. First, the proteins were cross-linked to the DNA by addition of formaldehyde to the medium (final conc. 1%), followed by an incubation for 10 min at 37°C. To stop this process 50 mM glycine were added and the plates were incubated for 5 min at RT. Afterwards the cells were transferred to falcon tubes and washed three times with cold PBS containing proteinase inhibitors (PI, 1:100). The samples were either frozen in liquid nitrogen and stored at -80°C or directly lysed.

The lysis consisted of two steps. First, the pellet was resuspended in 3 ml ChIP lysis buffer I with PI (1:100) and incubated on ice for 20 min to swell the cell nuclei. In the second step, samples were centrifuged (5 min, 4°C, 1200 rpm) and the cells were lysed in 2 ml ChIP lysis buffer II with PI (1:100) for 10 min on ice to disrupt the cellular membranes. Afterwards the

samples were sonicated in order to obtain DNA fragments between 200 – 300 bp. Sonication was carried out for 15 – 20 min at 15% amplitude (10 sec pulse, 20 sec pause).

To verify successful fragmentation, a 50 µl aliquot was taken out at each of three time points: prior to sonication, after half the sonication time and at the end. To revert the crosslinking, the samples were mixed with 450 µl TE, 160 mM NaCl and 20 µg/ml RNase A and incubated on a shaker for 1 h at 37°C and over night at 65°C. 5 mM EDTA and 200 µg/ml proteinase K were added and further incubated for 2h at 45°C to digest the proteins. The chromatin was then isolated via phenol / chloroform extraction (3.1.5) and the size of fragments checked on a 2% agarose gel (3.1.7).

In case of sufficient fragmentation of the chromatin, 15 µl of Dynabeads Protein A and Protein G were mixed for each ChIP, washed three times with BSA-PBS and incubated with 1 ml BSA-PBS containing 3 µg of specific antibody or control IgG over night at 4°C on a rotating wheel. The next day the beads were washed again three times and resuspended in 30 µl BSA-PBS. The chromatin was centrifuged once (5 min, 4°C, 1200 rpm), 1% of each sample was set aside as input control and the supernatant was incubated with the prepared beads for 6 h at 4° C on a rotating wheel. Afterwards the beads were washed three times with ChIP wash buffer I – III, respectively, and once with TE before the chromatin was eluted from the beads. For this purpose, beads were incubated twice with 150 µl ChIP elution buffer for 15 min at RT and the eluates were merged. The same amount of elution buffer was added to the input samples and crosslinking was reverted. The samples were supplemented with 14 µl 1 M Tris (pH 6.8), 1.2 µl 5 M NaCl and 1 µl RNase A (10 mg/ml) and incubated over night as described before, followed by the addition of 3.5 µl 0.5 M EDTA and 7 µl proteinase K (10 mg/ml) and an incubation for 2h at 45°C. Finally, the chromatin was purified with phenol / chloroform (3.1.5), the pellet dissolved in 750 µl RNase free water and the samples were analyzed via qPCR (3.1.13.2).

3.3.8 Re-ChIP

For Re-ChIP experiments $2*10^8$ cells expressing HA-Atu and the same amount of naïve S2 cells were fixed and processed as described for ChIP. For the first ChIP 60 µl Anti-HA Magnetic beads (Life Technologies) per IP were used and incubated with the fragmented chromatin over night at 4°C on a rotating wheel. Protein A and G Dynabeads were prepared as described for ChIP (3.3.7); 15 µl each per IP were incubated with 3 µg specific antibody, control IgG or empty beads as additional control. After the over night incubation the first ChIP was washed three times with each wash buffer and once with TE. The chromatin was eluted twice with 50 µl HA peptides (Life Technologies; 0.8 mg/ml in 1x RIPA buffer) for 15 minutes at 37°C. The eluates were merged and made up to 900 µl with ChIP lysis buffer II. The beads for the second ChIP were washed and mixed with an equal part of the eluates. 5% of

each sample were kept as input control. Subsequently, the samples were processed as described for ChIP and analyzed with qPCR (3.1.13.2).

3.4 Next-generation sequencing

3.4.1 ChIP for deep sequencing

For ChIP-Sequencing the standard ChIP procedure was performed with a few exceptions. The amount of cells ($1.2*10^8$), antibody (10 µg) and Dynabeads (50 µl each) were increased per IP. The purified chromatin pellet was solubilized in 40 µl RNase free water and quantified using the Quant-iT™ PicoGreen® dsDNA Assay Kit (Life Technologies).

3.4.2 RNA treatment for RNA sequencing

For RNA sequencing (RNAseq), total RNA was isolated using the miRNeasy Mini Kit (Qiagen) and an additional on-column DNase digest was performed (3.1.10). The concentration and quality of the RNA was analyzed with the Experion™ Automated Electrophoresis System (Bio-Rad) using RNA standard sense Chips according to the manufacturer's instructions. Only RNA which was not degraded was further processed. The RNA was treated with the RiboMinus™ Eukaryote Kit for RNA-Seq (Thermo Scientific) to remove ribosomal RNAs. For this purpose 10 µg of total RNA were used as starting material. For the isolation of mRNA 1 µg of total RNA was processed with the NEBNext® Poly(A) mRNA Magnetic Isolation Module following the manufacturer's protocol. Agencourt AMPure XP Beads (Beckman Coulter) were used for the purification of the double stranded cDNA and during library preparation.

3.4.3 Library preparation

3.4.3.1 NEBNext® ChIP-Seq Library Prep Master Mix Set for Illumina®

For the preparation of ChIP-Seq libraries usually 3 ng of chromatin were treated according to the instruction manual. Subsequently, the libraries were size-selected (~200 bp) with the help of an agarose gel and purified via gel extraction (Qiagen). Libraries were amplified with 15 PCR cycles. The Experion Automated Electrophoresis System (Bio-Rad) was used for the quantification and size determination of the libraries. An equimolar mix of all libraries was prepared prior to sequencing.

3.4.3.2 NEBNext® Ultra™ RNA Library Prep Kit for Illumina®

The RNA was treated as described in 3.4.2 and the libraries were prepared following the manufacturer's protocol. Size-selection was performed with the Agencourt AMPure XP Beads followed by amplification with 13 PCR cycles. These libraries were also analyzed with

the Experion Automated Electrophoresis System (Bio-Rad) and mixed in equimolar ratios before sequencing.

3.4.4 Bioinformatics and downstream data analyses

For data analysis, FASTQ-files were generated and mapped to the *Drosophila* genome version dm6 using Bowtie 2.2.4. The resulting .sam files were converted to .bam files with Samtools. ChIPseq peaks were identified with macs 1.4.0 and the statistical analyses were done with R and GraphPad Prism.

All analyses of deep-sequencing data were performed by Peter Gallant and described in more detail in the manuscript Gerlach *et al.* (submitted).

3.5 Fly specific methods

3.5.1 Fly culturing

Fly stocks were kept on *Drosophila* standard medium. All crosses and experiments were performed in a fly incubator at 25°C if not indicated otherwise.

3.5.2 Heat shock conditions for overexpression experiments

The vials containing larvae or adult flies were incubated for 2 h at 37°C in a water bath to induce heat shock dependent gene expression. After that, the vials were put back to 25°C.

3.5.3 Images of fluorescent tissue

3.5.3.1 Imaging using Discovery V8

The expression of GFP or RFP in larvae under the control of a specific Gal4 driver was documented with a binocular microscope (Discovery V8, Zeiss) equipped with a GFP filter (475 nm) and an RFP filter (561 nm), respectively. For this purpose the larvae were floated with a 20% sucrose solution, washed once with PBS and immobilized on a plastic lid of a cell culture plate cooled on ice. If desired, the larvae were placed in a fresh vial for further development.

3.5.3.2 Imaging using confocal microscope

For confocal images different larval tissues were fixed. For this purpose, larvae were dissected and inverted in 1x PBS, fixed with 4% paraformaldehyde (in PBTw) for 20 min at RT and washed three times with PBTw (20 min, RT). During the first washing step Hoechst 33342 (1:500; final conc. 10 µg/ml) was added to the PBTw to stain the cell nuclei. Afterwards the tissue of interest was carefully dissected and mounted on a slide in a drop of Vectashild Mounting Medium (Biozol). The samples were covered with a coverslip and sealed

with transparent nail polish. The slides were stored at 4°C and documented with a confocal microscope using appropriate laser settings.

3.5.4 Extraction of genomic DNA

For the extraction of genomic DNA, 1 – 5 adult flies or larvae were collected. Animals were homogenized with a pestle in 100 µl of extraction buffer A. The double amount of buffer was used for higher numbers of animals. The solution was incubated for 30 min at 70°C shaking at 350 rpm, subsequently 14 µl of 8 M sodium acetate were added, mixed and kept on ice for 30 min. The solution was cleared from debris by centrifugation (15 min, 4°C, 13200 rpm) and the supernatant was transferred to a new tube. The centrifugation step was repeated. Cold isopropanol (0.5x volume) was added, the tube inverted several times and centrifuged (5 min, RT, 13200 rpm) to precipitate the nucleic acids. The pellet was washed once with 70% ethanol and finally dissolved in 20 – 50 µl elution buffer (Qiagen) or water.

3.5.5 Pupariation assay

Pupariation was monitored once or twice a day and pupariated larvae were marked. 6 – 7 days after egg deposition (AED), after the majority of wildtype animals were already pupariated, Max^0 mutants were floated with 20% sucrose solution, counted and transferred to a fresh vial. Monitoring went on until all animals were pupariated or dead.

3.5.6 Luciferase reporter gene assay

For this assay larvae of different genotypes were collected and single prothoracic glands (PGs) were isolated. To monitor mTOR activity all animals carried a transgene expressing firefly luciferase under the control of the mTOR-repressed *unkempt* promotor (unk-FLuc; (Tiebe *et al.*, 2015)). A single PG was lysed in 10 µl of 1x PLB and vigorously vortexed for 2 minutes to disrupt the cells. The samples were stored at -20°C or directly measured. For this purpose, 10 µl of each sample were pipetted into one well of a black 96-well plate and placed into the Glomax 96 Microplate Luminometer. The reagents (Dual-Luciferase® Reporter Assay System, Promega) were prepared according to the manufacturer's instructions. After starting the program, the luminometer automatically put 50 µl of each solution per well and measured light emission at 562 nm in relative light units (RLU).

4 Results

4.1 Influence of the PAF1 complex on Myc–regulated transcription

4.1.1 The PAF1 complex affects Myc target genes *in vivo*

Furrer *et al*. performed an RNAi screen in *Drosophila* S2 cells to identify novel Myc co-factors (Furrer *et al.*, 2010). For this screen, a reporter expressing firefly luciferase under the control of the CG5033 promoter, a confirmed Myc target, was constructed. S2 cells were co-transfected with the reporter and different dsRNAs. The luciferase activity was subsequently analyzed. This screen identified 33 potential new Myc co-factors, including the different components of the PAF1 complex.

Subsequently, we focused on the characterization of the PAF1 complex and its role as Myc co-factor (Gerlach *et al*., manuscript submitted). To assess the influence of the complex on Myc dependent transactivation, the different components were depleted. This showed no strong impact on Myc protein levels but reduces the gene expression of endogenous CG5033, the gene from which the reporter is derived (experiment carried out by M. Furrer; see Gerlach *et al*., manuscript submitted).

The luciferase reporter was also introduced into flies for *in vivo* experiments. These flies were crossed with RNAi lines to knock down the different PAF1 complex components. Ubiquitous dsRNA expression was induced by a heat-shock of 2 hours at 37°C. Larvae were collected 48 hours after induction and processed for luciferase assays. Since Paf1 depletion killed all animals within 48 h, for this particular knockdown the reporter activity was already measured after 24 h. All tested RNAis reduced the activity of the reporter (Figure 4.1), but the effects were rather mild. Paf1 depletion caused the strongest reduction, which was even stronger then after Myc knockdown. Knockdown of Atu had the weakest effect in this setup.

Surprisingly, after depletion of the different PAF1 complex components (except Paf1) most of the animals survived to pharate adult stage and even some adult escapers were found. Probably the efficiency of the different knockdowns was low because null mutants of hyx or Ctr9 show much stronger phenotypes.

Taken together these results suggest that the PAF1 complex plays a positive role in Myc-dependent transcription regulation.
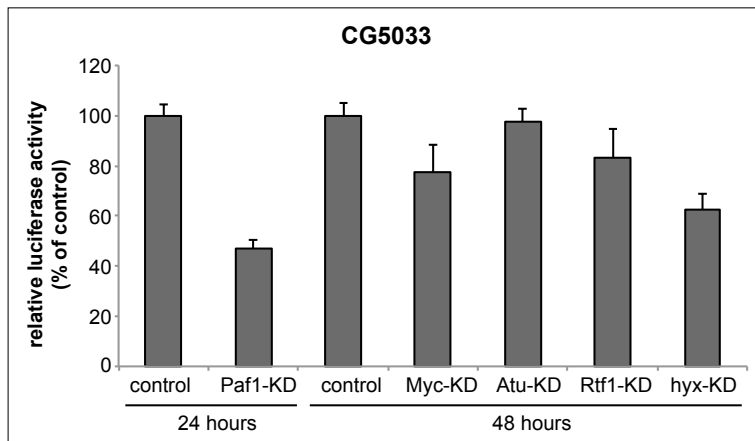
Figure 4.1: Luciferase activity in larvae after knockdown of PAF1 complex components

Larvae carrying a firefly luciferase transgene under the control of the CG5033 promoter were treated with a heat shock for 2 hours at 37°C, leading to ubiquitous expression of GAL4 and the indicated knockdown of different PAF1 complex components. The larvae were collected after 24 or 48 hours and processed for a luciferase assay. Average and SEM are shown for 5 individual animals per genotype.

Genotypes: „hs-FLP actin5C-FRT-stop-FRT-GAL4 CG5033-FLuciferase UAS-X-IR"

("X" stands for dsRNA targeting the respective PAF1 complex component).

4.1.2   Myc interacts physically with the PAF1 complex component Atu

In vitro experiments were performed to understand how the PAF1 complex is influencing Myc-regulated transcription. Immunoprecipitations (IPs) were carried out to test if Myc and PAF1 complex components interact physically. An HA-tagged variant of Atu was already available, therefore it was the first investigated subunit. HA:Atu and wildtype HA:Myc were transfected in S2 cells and showed a strong interaction in the IP (Figure 4.2 B and Gerlach *et al*., manuscript submitted).

To study the binding site of the two proteins, the interaction of Atu with different Myc variants (Figure 4.2 A) was examined. For this purpose, S2 cells were co-transfected with HA-tagged wildtype Atu and different HA-tagged Myc mutants. 24 h later the cells were lysed and processed for co-immunoprecipitation. Input samples were analyzed to ensure the correct expression of all transfected plasmids (Figure 4.2 B lower panel). The co-immunoprecipitations (CoIPs) showed that none of the described Myc domains is required for the association with Atu (Figure 4.2 B upper panel): neither loss of Myc Box 1 or 2, located at the N-terminus, nor loss of the centrally located Myc Box 3 affected the binding to Atu. A truncation of the C-terminus, which is essential for the association with Max, had also no effect. However, a central region of Myc between amino acids 294 and 403 was shown to be important for the binding of Myc to Atu (experiment carried out by D. Birkel; see Gerlach *et al*., manuscript submitted). No function has previously been attributed to this region but it is immediately adjacent to MBIII that has recently been found to interact with WDR5 (Thomas *et al.*, 2015).

To find out which part of Atu is necessary for the interaction with Myc, AU1-tagged mutant forms of Atu had been generated. Again cells were transfected with the indicated plasmids and processed 24 h later. Input controls confirmed the expression of the constructs (Figure 4.2 C middle + lower panel). CoIPs using an antibody against AU1 revealed that the region between the amino acids 442 and 474 is essential for the association with Myc (Figure 4.2 C upper panel). So far, nothing is known about this region.

Overexpressed Myc and Atu showed a strong interaction *in vitro*, which is mediated by a central region of each protein.
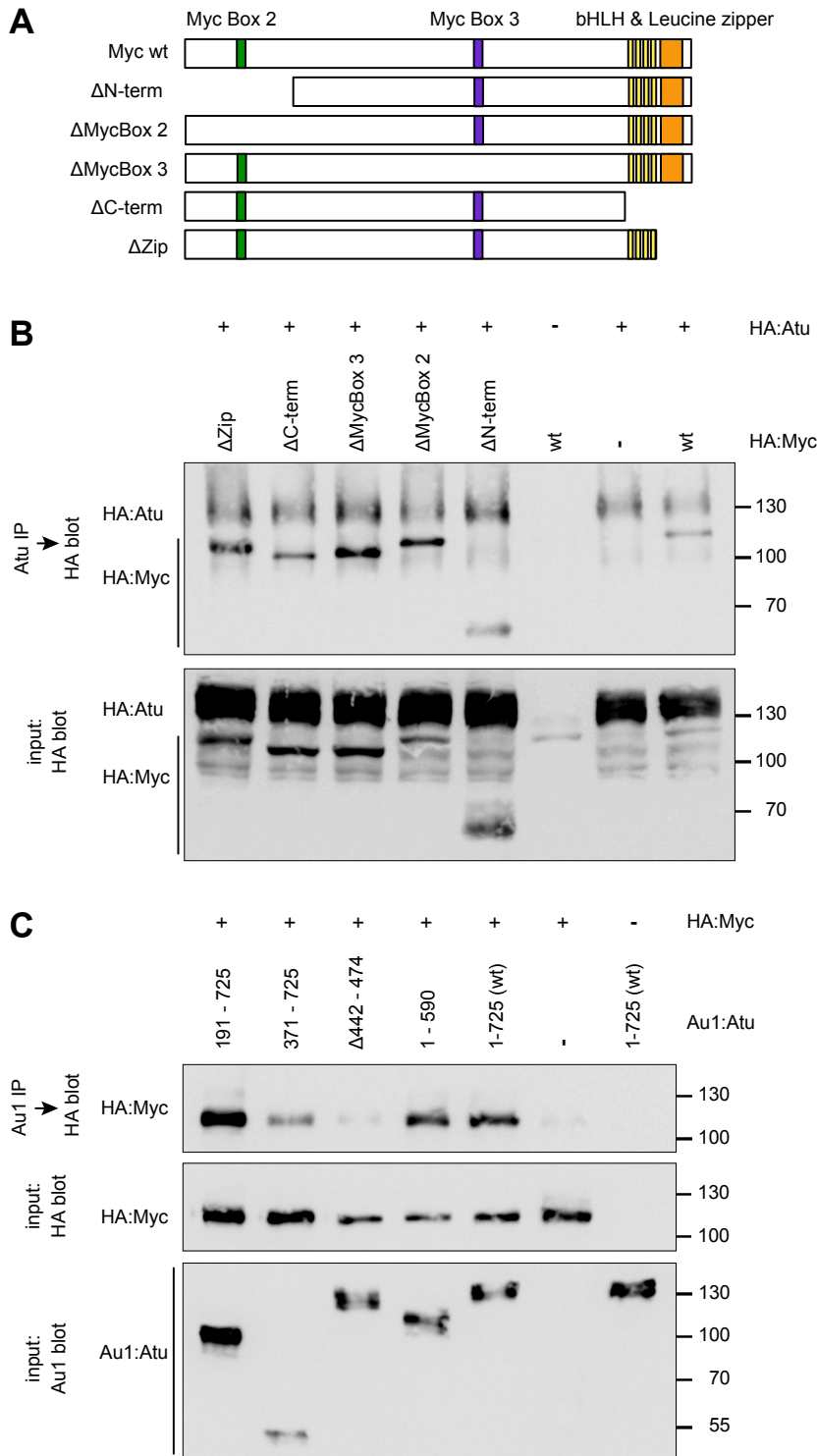
Figure 4.2: Exogenous Myc and Atu interact physically[1]

A) Scheme of wildtype Myc and Myc deletions that were used to explore the interaction with Atu.

B) Co-Immunoprecipitations of different HA:Myc variants with wildtype HA:Atu. The constructs were transiently expressed in S2 cells for 24 h and immunoprecipitated with a rabbit anti-Atu antibody. Precipitated proteins were analyzed by Western blot with an anti-HA antibody.

C) Co-Immunoprecipitations of wildtype HA:Myc with HA:Atu deletions. S2 cells were transiently transfected with HA-tagged wildtype Myc and Au1-tagged Atu constructs. 24 h after transfection cell lysates were prepared and immunoprecipitations were performed with a mouse anti-Au1 antibody. Immunoprecipitated proteins were detected by Western blot with the indicated antibodies.

To examine if Myc and Atu also interact with each other under physiological conditions, co-immunoprecipitations of endogenous proteins were attempted. This approach failed because the antibody against Atu is probably not strong enough. Therefore, a stable cell line was generated which carries a $CuSO_4$-inducible plasmid for the expression of HA-tagged Atu. In the absence of $CuSO_4$, the cell line shows some leaky expression of HA:Atu and after induction with $CuSO_4$ the cells express HA:Atu at levels which are close to physiological Atu levels (Figure 4.3 B). This cell line enables the use of an anti-HA antibody and the expression of HA:Atu at equally low levels as the endogenous protein.

First, the cell line was used for CoIPs of HA:Atu and endogenous Myc. For this purpose, cells were exposed to 125 µM $CuSO_4$ for 24 h, lysed and incubated with the prepared beads. The efficiency of the IP itself was investigated as control (Figure 4.3 A lower panel) showing that a substantial amount of HA:Atu was precipitated in the IP, but only background levels in the control. Moreover, the analysis showed that endogenous Myc co-precipitates together with HA:Atu (Figure 4.3 A upper panel) confirming the interaction seen above between the over-expressed proteins. Second, a proximity-ligation assay was performed with the inducible cell line to verify the association of HA:Atu and endogenous Myc. The assay showed that both proteins lie in close vicinity confirming the association of HA:Atu with endogenous Myc (experiment performed by A. Baluapuri; see Gerlach *et al.*, manuscript submitted).

To examine if this interaction takes place directly on the DNA, re-chromatin-immunoprecipitations (Re-ChIP) were performed. For this purpose, control S2 cells and HA:Atu inducible cells were processed as described above for CoIPs. Figure 4.3 B shows that comparable levels of Myc were present in naïve and in HA:Atu expressing S2 cells, and that the levels of HA:Atu were strongly increased after $CuSo_4$ induction. In HA:Atu expressing cells, two bands were detected with the anti-Atu antibody corresponding to endogenous Atu and HA:Atu, respectively. Untreated HA:Atu cells served as additional control and showed some leaky expression of HA:Atu. Protein levels of endogenous Myc and endogenous Atu were similar to naïve S2 cells. For Re-ChIP the chromatin was first incubated with an HA-specific antibody, precipitated material was eluted with HA-peptides and re-precipitated with a rabbit anti-Myc antibody. The binding was evaluated via qPCR and signals were normalized to the one of Uhg1 from HA:Atu expressing cells. The results showed that Myc targets are enriched compared to non-immune IgGs and the negative control region Pka-C1 (Figure 4.3 C). The specificity of the experiment is attested by the very low signal from control S2 cells.

Altogether these experiments demonstrate a physical interaction between Atu and Myc in cell culture. The association involves a central region of Myc (between 294 and 403 aa) and the amino acids between 442 and 474 of Atu and this interaction was shown to take place directly on the DNA.
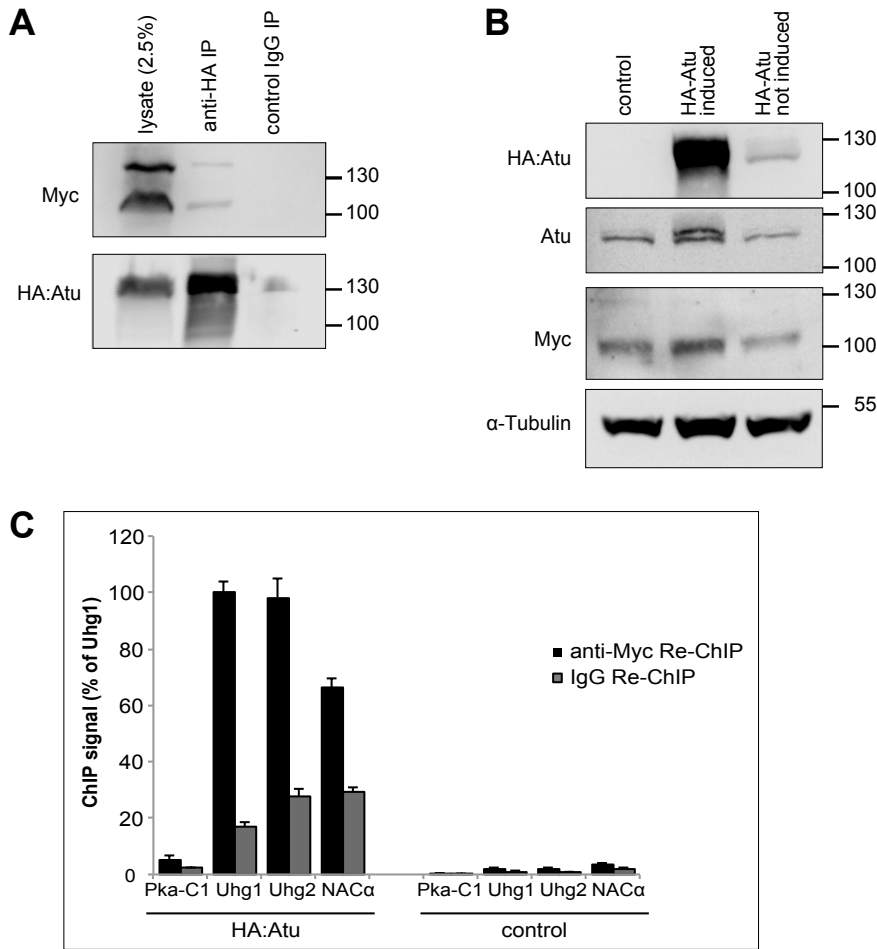
Figure 4.3: Myc and Atu associate at physiological levels and bind to at least three common targets[1]

A) Co-immunoprecipitation of endogenous Myc with HA-tagged Atu. Cells with a stably integrated HA:Atu plasmid were treated with 125 µM CuSO4 to induce expression of HA:Atu. 24 h later cell lysates were prepared and an immunoprecipitation was performed with either a rabbit anti-HA antibody or unspecific rabbit IgGs. 2.5% of the input and half of the immunoprecipitated samples were analyzed by Western blotting.

B & C) Naïve S2 cells (control) and cells carrying an inducible HA:Atu plasmid were incubated with or without $CuSO_4$. The cells were harvested 24h after induction and further processed for analysis by Western blot (B) or Re-ChIP (C).

B) Western blot attesting the successful induction of HA:Atu. The blot was probed with anti-HA, anti-Atu and anti-Myc antibodies. α-Tubulin served as loading control.

C) Re-Chromatin-immunoprecipitation of control cells or cells expressing HA:Atu. The chromatin was first precipitated with an anti-HA antibody and eluted with HA peptides. The eluates were precipitated again either with anti-Myc or rabbit IgGs as control. Averages and SEMs result from technical triplicates and were normalized to the signal of Uhg1 from HA:Atu expressing cells.

4.1.3 The PAF1 complex helps to recruit Myc to its targets

The findings that Myc and Atu interact physically raised the question how the PAF1 complex is involved in Myc's activities. Two alternatives are conceivable. Either Myc binds to its target genes and subsequently recruits the PAF1 complex or the PAF1 complex first localizes to the DNA and helps to recruit Myc to its targets.

To address the first possibility, the binding of Atu to Myc target genes in the presence and absence of Myc was analyzed. For this experiment an HA-specific antibody was used since chromatin immunoprecipitations (ChIPs) with the available anti-Atu antiserum did not work. For this purpose, HA:Atu inducible cells and naïve S2 cells were treated for 24 h with 125 µM $CuSO_4$ and, where indicated, Myc-dsRNA. Successful induction of HA:Atu expression and Myc depletion was verified via Western blot (Figure 4.4 A). The samples for the ChIPs were incubated with beads coupled to a rabbit anti-HA antibody followed by qPCR analysis. Naïve S2 cells were used to determine background signals. The ChIP signals were all normalized to Uhg1 levels of HA:Atu expressing control cells. Binding of Atu to the investigated Myc targets was moderately reduced after Myc depletion (Figure 4.4 B). Binding of HA:Atu to Uhg1 was reduced by 26.9% (± 8.3%) after Myc knockdown while the binding to Uhg2 was reduced by 30.4% (± 10.5%) and to Nacα by 25.0% (± 8.1%). Pka-C1 was used as a negative control since this region shows low associated Myc binding and its expression is not affected after Myc depletion (Furrer *et al.*, 2010). Cells expressing HA:Atu showed increased binding to Pka-C1 but the signal is still much lower than for the other targets. This suggests that Atu might bind to Pka-C1, but in a Myc-independent fashion. In conclusion, Myc may contribute to the recruitment of Atu (and the PAF1 complex), but even in the almost complete absence of Myc, Atu still strongly associates with Myc targets, suggesting that it relies mostly on other means to get there.

To investigate whether the PAF1 complex first localizes to the DNA and helps to recruit Myc, the binding of endogenous Myc to its target genes was analyzed after Atu knockdown. For this purpose, S2 cells were incubated with dsRNA against Atu or left untreated. The cells were harvested 48 h later and further processed for Western blot or ChIP. Atu protein levels were reduced by approximately 85% (Figure 4.4 C). Afterwards, the chromatin was precipitated with a Myc-specific antibody or control IgGs. All values were normalized to Uhg1 of control cells. In control cells a strong enrichment over IgG was observed confirming the success of the ChIP (Figure 4.4 D). The knockdown of Atu caused a strong reduction of Myc's binding to its targets. Binding capacity to Uhg1 was reduced by 71.2% (± 6.0%) and the effect on the other two targets was in the same range (71.0 ± 6.8% for Uhg2, 72.6 ± 2.5% for NACα).
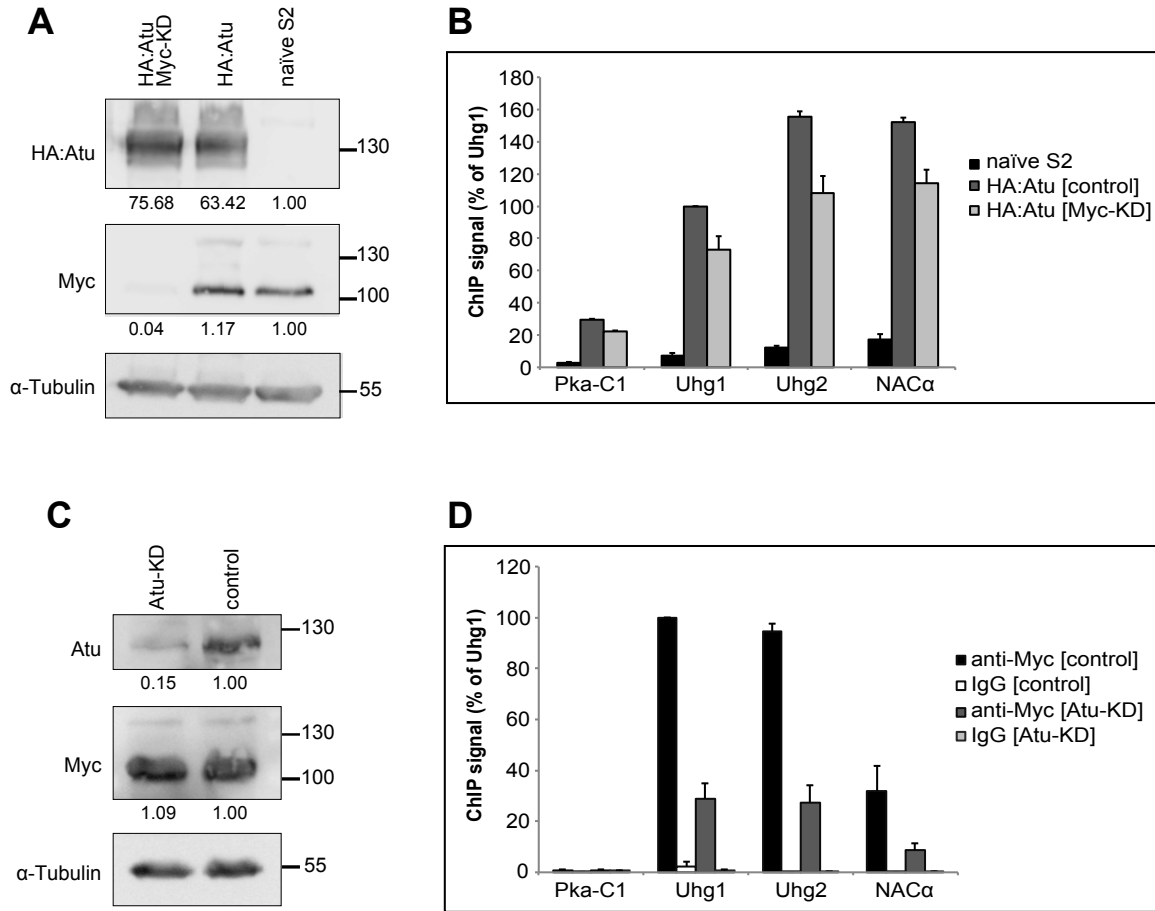
Figure 4.4: Influence of Myc or Atu depletion on chromatin binding[1]

A & B) S2 cells and cells carrying an inducible HA:Atu plasmid were treated with $CuSO_4$ and Myc-dsRNA respectively. 24 h later the cells were harvested and further processed for Western blot (A) or ChIP (B).

A) Western blot displaying HA:Atu induction and Myc depletion. The proteins were visualized with anti-HA and anti-Myc antibodies. α-Tubulin was used as a loading control. One representative example of two biological repeats is shown.

B) ChIP-qPCR of naïve S2 cells and HA:Atu expressing cells with or without Myc knockdown. Averages and SEMs result from two biologically independent experiments. All values were normalized to the signal of Uhg1 from HA:Atu expressing control cells.

C & D) Control S2 cells and cells treated with dsRNA against Atu were harvested 48 h after transfection for Western blot or ChIP.

C) Western blot confirming Atu depletion. The blot was probed with antibodies against Atu and Myc. α-Tubulin served as loading control. One representative blot of three repeats is shown.

D) ChIP-qPCR of Atu depleted cells and control cells. Samples were incubated with a rabbit anti-Myc antibody or rabbit IgGs as control. Shown are averages and SEMs from two (control) or three (Atu-KD) biological replicates. Signals were normalized to the one obtained for Uhg1 from control cells.

To examine if the binding of Myc is also reduced after the knockdown of other PAF1 complex components cells were transfected with the corresponding dsRNA and processed 48 h later. Untreated cells were used as control. Western blot analyses were performed to ensure Myc protein levels were not reduced after the different knockdowns (Figure 4.5 B upper panel) and the depletion of hyx and Rtf1 was confirmed (Figure 4.5 B lower panel). The reduction of transcript levels for all components 48 h after transfection was measured via qPCR since no antibodies for Paf1 or Ctr9 were available (Figure 4.5 C). ChIPs were performed as described above for Atu knockdown and binding of Myc was analyzed for the same targets. This showed that depletion of any PAF1 complex component reduced Myc binding as well (Figure 4.5 A) even though the reduction was not as strong as after Atu knockdown.

The results from the different manual ChIPs suggest that the second hypothesis is more likely, meaning that the PAF1 complex first localizes to open promoters through its interaction with the transcription machinery and subsequently recruits Myc.
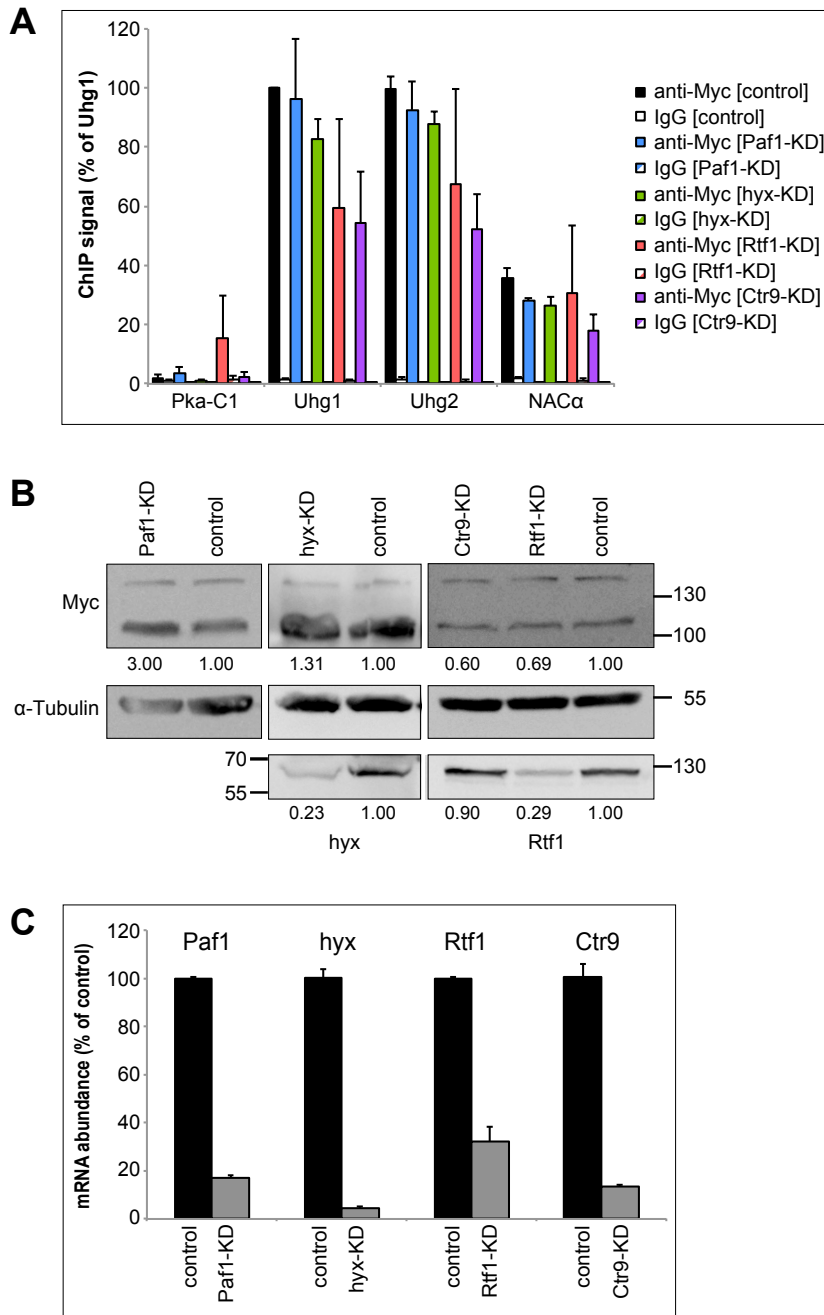
Figure 4.5: Chromatin binding of Myc is reduced after depletion of PAF1 complex components[1]

A & B & C) S2 cells were incubated with or without dsRNA against the indicated PAF1 complex component and harvested 48 h later.

A) ChIP-qPCR of control cells and cells with the indicated knockdown. Samples were precipitated with a rabbit anti-Myc antibody or rabbit IgGs as control. Shown are averages and SEMs from two (each knockdown) or six (control) biological replicates. All samples were normalized to the signal of Uhg1 from control cells.

B) Western blot analysis of endogenous Myc levels after depletion of different PAF1 complex components and confirmation of the knockdown. The blots were probed with the indicated antibodies. α-Tubulin was used as loading control. One representative blot for each knockdown sample is shown.

C) Level of mRNA in control cells and after knockdown analyzed by qRT-PCR. Results from two independent experiments are given as mean ± SEM.

4.1.4   Myc binding to target genes is reduced after Atu depletion

ChIP sequencing experiments were performed to get an overview about global effects of Atu depletion on Myc binding.

Cells were transfected with dsRNA against Myc or Atu and harvested 48 h later and processed for anti-Myc ChIP. Naïve S2 cells served as control. Western blotting of cells processed in parallel confirmed efficient knockdown of Myc and Atu, respectively (Figure 4.6 A). The control cells from the right panel and both knockdown samples were further processed. All values were normalized to Uhg1 of control cells. The results validate a binding reduction of 21.5% (± 2.6%) after Atu knockdown and 95.1% (± 0.2%) after Myc knockdown.

To identify the regions bound by Atu, chromatin from the stable HA:Atu cell line was included in the sequencing. For this purpose, cells carrying the inducible HA:Atu plasmid and naïve S2 cells were treated with 125 µM $CuSO_4$ for 24 h and then processed for Western blot and ChIP. The levels of HA:Atu, endogenous Atu and Myc were determined (Figure 4.6 C). The expression of HA:Atu is strongly elevated after $CuSO_4$ treatment whereas endogenous Atu and Myc levels are only slightly increased compared to control. An HA-ChIP was performed and binding capacity was analyzed by qPCR (Figure 4.6 D). The signal for Uhg1 in HA:Atu was used for normalization. Binding of HA:Atu cells to Uhg1 was almost five times stronger than background binding and the binding to Pka-C1 was increased indicating that Pka-C1 is also specifically bound by Atu. These results prove that the quality of the ChIP samples is good. Consequently all samples were processed for sequencing.
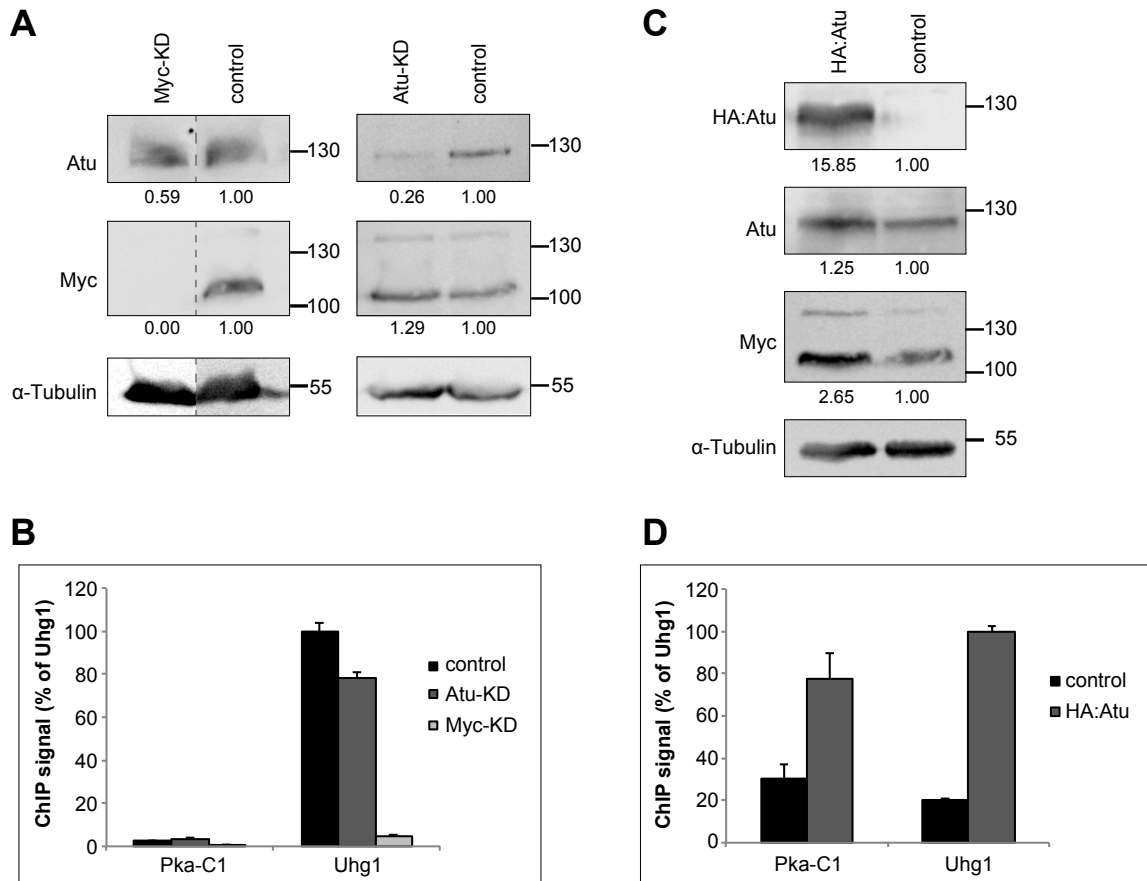
Figure 4.6: Preparation of ChIP-Seq samples[1]

A) Western blot confirming the depletion of Myc (left panel) and Atu (right panel) 48 h after transfection. Both blots were analyzed with mouse anti-Myc and rabbit anti-Atu antibodies. α-Tubulin served as a loading control. From the left panel only the Myc-KD sample was processed, the Atu-KD sample and control were taken from the right panel.

B) Anti-Myc ChIPs of the samples from panel A that were later used for ChIP-Seq (see below). Results were normalized to Uhg1 of control cells. Shown are averages ± SEM from technical triplicates.

C) Induction of HA:Atu expression was verified via Western blotting. Cells were processed 24 h after addition of $CuSO_4$ to induce expression of HA:Atu. Naïve S2 cells were used as control. Levels of HA:Atu, endogenous Atu and endogenous Myc were checked and α-Tubulin was used as loading control. The samples were processed for ChIP and results are depicted in panel D.

D) Anti-HA ChIP followed by qPCR from cells expressing HA:Atu or from naïve S2 cells as control. Shown are averages and SEMs of technical triplicates normalized to the signal for Uhg1 from HA:Atu expressing cells.

The reads from the sequencing (7'847'000 for each condition) were mapped onto the reference genome (dm6) and peaks were called with macs. Myc binding sites were defined as those that did not have increased read numbers after Myc knockdown and did not overlap with background sites (the ones detected in the anti-HA ChIP from naïve S2 cells). This revealed 714 specific Myc binding sites in naïve S2 cells. 296 of them are located in promoter regions within 100 bp of the transcriptional start site and 166 overlap with enhancer sites, as defined by (Arnold *et al.*, 2013). Myc depletion strongly reduced the binding to its target genes whereas Atu knockdown caused only a moderate reduction (Figure 4.7 A). This is consistent with the previous results from the ChIPs (Figure 4.6 B) which showed a reduction of Myc binding to Uhg1 by 21.5 ± 2.6% after Atu knockdown and by 95.1 ± 0.2% after Myc knockdown. Myc depletion caused the same reduction at both sites (Figure 4.7 B upper panel & Figure 4.7 C). In contrast, Atu knockdown significantly reduced Myc binding to promoter sites but did not affect enhancer sites. The anti-HA ChIP of cells expressing HA:Atu showed that promoters and enhancers are similarly bound by Atu (Figure 4.7 B lower panel). Therefore, differences resulting from a differential Atu occupancy can be excluded suggesting that Myc recruitment to enhancers is independent of Atu.

Since Myc:Max complexes are known to bind to E-box sequences, it was investigated if the impact of Atu is different in the presence or absence of such sequences. 115 of the 296 identified promoter sites contain an E-box and the binding of Myc to these sites is affected more strongly by Atu knockdown than to promoters without E-boxes (Figure 4.7 D). No differences were observed for enhancers, whether they contain an E-box or not.

Taken together, the ChIP experiments as well as the ChIP sequencing showed that Atu, and probably the whole PAF1 complex, is involved in the recruitment of Myc to its target genes, specifically to their promoter sites.
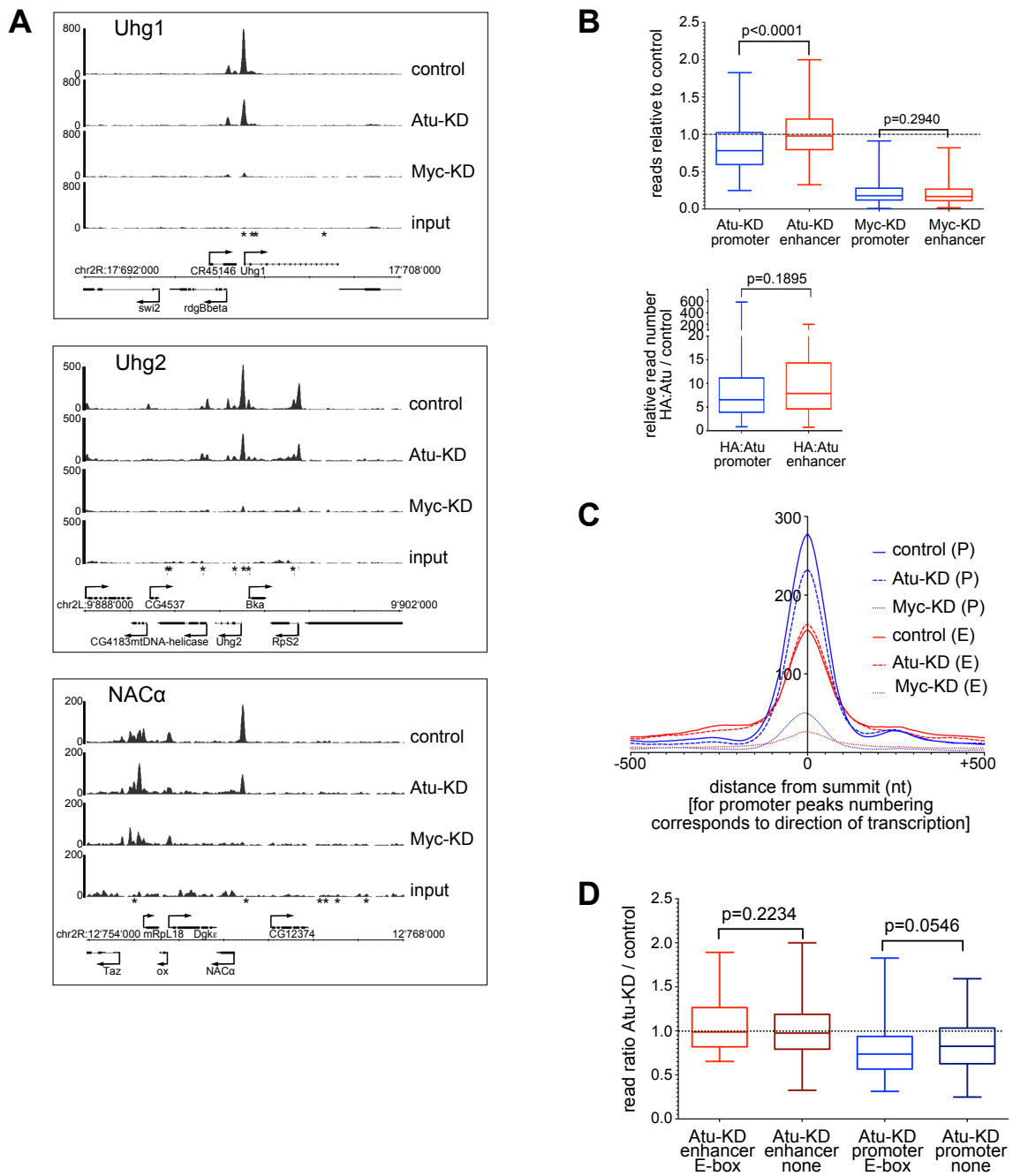
Figure 4.7: ChIP sequencing reveals the effect of Atu-knockdown on Myc's binding to targets[1]

A) ChIPseq profiles of the Myc targets previously examined via ChIP in Figure 4.4. Canonical E-boxes are marked with an asterisk (*).

B) Box plots displaying the effect of Atu or Myc depletion on promoter and enhancer sites (upper panel). Myc binding after the knockdown was compared to naïve S2 cells. The significance of the difference between promoter and enhancer sites was calculated with a two tailed t-test. Box plot showing the binding of HA:Atu at enhancer and promoter sites (lower panel).

C) Average distribution of reads over Myc binding sites located in promoters (P) or enhancers (E) in control cells or after Myc or Atu knockdown. Reads were counted over 50-nt windows for the indicated conditions, followed by subtraction of input reads for the corresponding window.

D) Effects of Atu depletion on enhancers or promoters, containing or lacking E-boxes.

4.1.5   The expression of direct Myc targets is reduced after Atu depletion

Atu promotes the recruitment of Myc to its target promoters, which suggests a role for Atu in Myc-regulated transcription. To investigate the effects of Atu knockdown on global gene expression of S2 cells, RNA sequencing experiments were performed. Cells were incubated with dsRNA against Atu or GFP (control) and harvested 48 h later. Three biologically independent samples for each condition were prepared. The first sequenced sample originates from the experiment shown in Figure 4.4 C and D. Atu protein levels of the other two samples were efficiently reduced as confirmed by Western blots (Figure 4.8 A). The sequencing generated a total of 6'757'000 reads that were mapped to the genome dm6. For final analysis, 9'123 genes were kept with at least 1 read in each of the six samples and at least 1 read per million in average for either control or Leo1 knockdown condition. R (package edgeR) was used for subsequent statistical analyses.

The $\log_2$ fold change of reads from the control samples (GFP-KD) and the Atu-KD samples were plotted against each other (Figure 4.8 B). Atu-KD does not differ strongly from the control sample as reflected by the calculated Spearman correlation coefficient of 0.9973 (Figure 4.8 B). which is very close to the theoretical maximum of 1. This shows that Atu depletion had very little effect on global gene expression.

In contrast, Figure 4.8 C shows that Atu depletion reduced the expression of direct Myc targets (58 genes) that were defined as genes, which are bound by Myc over an E-box in the promoter region and that show a decreased expression after Myc knockdown. Also the expression of genes containing an E-box within 100 nt downstream of their transcriptional start site (170 genes) is reduced. Hulf *et al*. 2005 showed that the vast majority of these genes are Myc targets. Both gene lists probably consist of Myc targets and the expression of these genes is reduced after Atu depletion.

Figure 4.8 D illustrates the effect of Atu on direct Myc targets in a different way. All expressed genes that resulted from the sequencing (9123) were ordered according to their relative expression after Atu knockdown and the 58 direct Myc targets were mapped onto them showing that they are preferentially downregulated after Atu knockdown.

In conclusion, after Atu depletion no big differences in the expression of the whole transcriptome were observed but a closer look at direct Myc targets revealed a mild reduction. These findings are consistent with the slight effect of Atu knockdown on CG5033 expression *in vivo* (Figure 4.1).

A

B

C

D
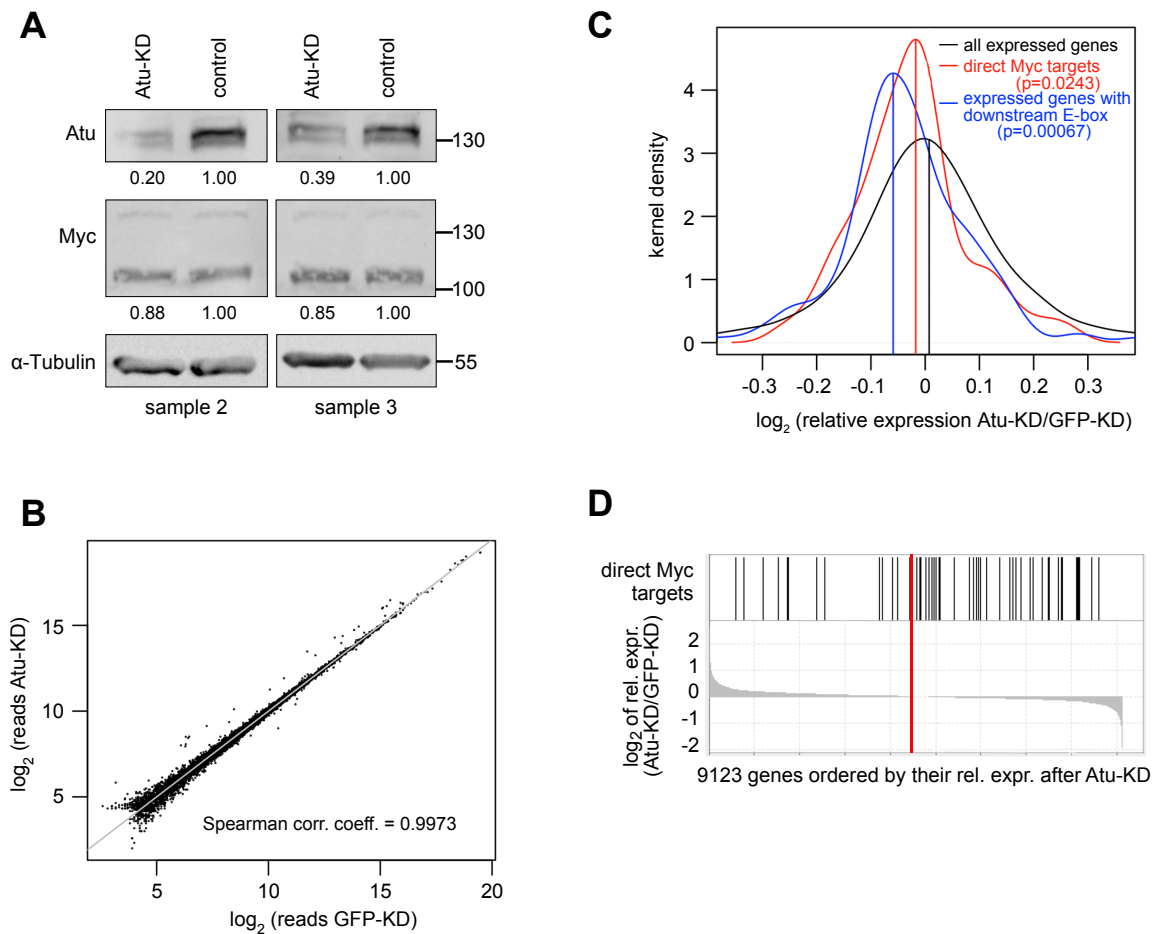
Figure 4.8: Effect of Atu-knockdown on the expression of Myc targets in S2 cells[1]

A) Western blot documenting the depletion of Atu after treatment with dsRNA for 48 h. Endogenous Atu and Myc levels are displayed; α-Tubulin serves as loading control. Both samples as well as the one shown in Fig. 4.4 C were used for RNA sequencing.

B) Dot blot displaying the expression levels ($\log_2$ of read numbers) after Atu knockdown compared to the mock depleted control sample (GFP-KD). Shown is the average of three biological replicates for Atu-KD and control. Only genes that were expressed above a minimum threshold in S2 cells were blotted (9123 genes).

C) Distribution of relative expression levels of all genes (9123 genes; black), direct Myc targets (58 genes; red) and genes with a downstream E-box (170 genes; blue).

D) All 9123 genes were ordered according to the relative expression after Atu-KD (lower part) and direct Myc targets (58 genes) were mapped on these genes (upper part). Genes bound by Myc over an E-box situated in the promoter region and downregulated after Myc depletion were defined as direct Myc targets.

4.1.6   Myc-dependent gene expression is reduced after loss of Atu or Max *in vivo*

In vivo, the depletion of PAF1 complex components had a much stronger effect in a setting where Myc is overexpressed. Wing disc clones overexpressing Myc are much larger than controls. Simultaneous knockdown of PAF1 complex components strongly reduced this overgrowth but had no effect on the size of control clones (experiment performed by M. Furrer; see Gerlach *et al*., manuscript submitted). Furthermore, overexpression of Myc in the eye discs induces growth and apoptosis in this tissue. This results in bigger adult eyes with bigger individual ommatidia but their arrangement is disturbed which leads to a rough appearance. Depletion of Atu reduced the roughness of these eyes suggesting that Atu impairs Myc-dependent apoptosis. No effect of Atu was observed in eyes without Myc overexpression (experiment performed by M. Gallant; see Gerlach *et al*., manuscript submitted). This suggests that Atu is more relevant in a situation of Myc overexpression, and hence that the knockdown of Atu in such a situation would have clearer effects on gene expression.

Therefore, the consequences of simultaneous Myc overexpression and Atu knockdown were investigated in imaginal discs by RNA sequencing. Furthermore, Myc-dependent transcription was investigated after the complete loss of Max since our previous data suggest that Max and Atu may play similar roles in Myc recruitment. Also a combination of both lesions was analyzed to address potential redundancies between Atu and Max.

For the sequencing, expression of the UAS transgenes was induced by a heat-shock 48 hours prior to sample collection. Afterwards, wing discs were dissected and RNA was isolated (3.1.10). For each genotype three independent biological replicates were prepared (in total 24 samples). Finally, the RNA was processed for sequencing. The obtained reads were mapped to the reference genome dm6 and this resulted in an average of 6.3 million reads for each sample. For final analysis, only genes expressed above a minimum threshold (as described for the RNAseq in S2 cells) were kept resulting in a list of 8251 genes. Statistical analysis was performed with R (package edgeR).

First, the read numbers of Atu and Max transcripts were evaluated to see how well the Atu knockdown worked and how much Max transcripts are reduced in Max^0 mutants (Figure 4.9 A). For this analysis, samples were combined independently of Myc status (with or without Myc overexpression) resulting in a total number of six independent samples. Atu transcripts were reduced by more than 70% and Max levels are virtually undetectable (Figure 4.9 A).

Expression levels from genotypes with or without Myc overexpression were blotted to investigate differences caused by elevated Myc levels. Genes which were significantly ($p<0.05$) deregulated by Myc and whose expression changed by at least 1.5-fold as compared to the identical genotype without Myc-overexpression are marked in red (Figure 4.9 B). In a wildtype background Myc overexpression led to the induction of 977 genes and the repression of 1176 genes (Figure 4.9 B, upper left & 4.9 C, left panel). Upon further analysis of the

activated genes typical classes of Myc targets were identified by GSEA e.g. genes involved in ribosome biogenesis, translation etc. Furthermore, a good overlap was observed between these genes and the genes bound by Myc in promoter regions in S2 cells (identified by ChIP sequencing, Figure 4.7). Unexpectedly, the analysis revealed a high number of repressed genes. Several publications reported less than 500 Myc-repressed genes *in vivo* or in S2 cells and all found a much smaller number of repressed genes than induced ones (Bonke *et al.*, 2013; Herter *et al.*, 2015; Hulf *et al.*, 2005; Orian *et al.*, 2003). However, the genes previously identified as being Myc-repressed are also enriched here amongst the Myc-repressed genes. The expression changes due to Myc overexpression were reduced by Atu depletion (17% less induction and 26% less repression) while the elimination of Max had an even stronger effect (almost no induction and 33% less repression). The combination of both lesions (Max and Atu) resulted in no additional effect compared to Max depletion only (Figure 4.9 B & C, left panel).

Comparison of the 2152 differentially expressed genes (977 activated and 1175 repressed) after Myc overexpression in imaginal discs with the ones bound by Myc in S2 cells resulted in a list of 221 induced and 25 repressed genes. This subset was also analyzed regarding the effects resulting from the different genotypic conditions (Figure 4.9 C; central panel). The results were very similar to the effects observed for all expressed genes (Figure 4.9 C; left panel).

Furthermore, the depletion of Atu had a slightly stronger effect on Myc targets containing an E-box (19% reduction) then on targets lacking an E-box (15% reduction) (Figure 4.9 C, right panel). This is consistent with the observation that Myc binding is more affected on promoters with an E-box than lacking an E-box in S2 cells (Figure 4.7 D). In a Max^0 background Myc overexpression was not able to induce expression of target genes with an E-box, in contrast genes without E-box were still slightly upregulated (Figure 4.9 C, right panel).

Taken together, the data show that Myc is able to induce the expression of some targets even in the complete absence of Max (Figure 4.9 C & Steiger *et al.*, 2008). Even though the RNAi against Atu did not completely eliminate all transcripts (Figure 4.9 A), Atu knockdown has a significant effect on Myc-dependent gene activation and repression (Figure 4.9 C).

Here, we showed that Atu interacts physically with Myc and this association takes place directly on the DNA. Depletion of Atu and other PAF1 complex components reduced the recruitment of Myc to its target genes in S2 cells and affected their expression in S2 cells and *in vivo*. Overall, we characterized the PAF1 complex as novel co-factor of Myc.

In addition, Myc overexpression in Max^0 mutants still allows the induction and repression of a few genes, raising the question if this is enough to still have any biological effect. This will be addressed in the following chapter.
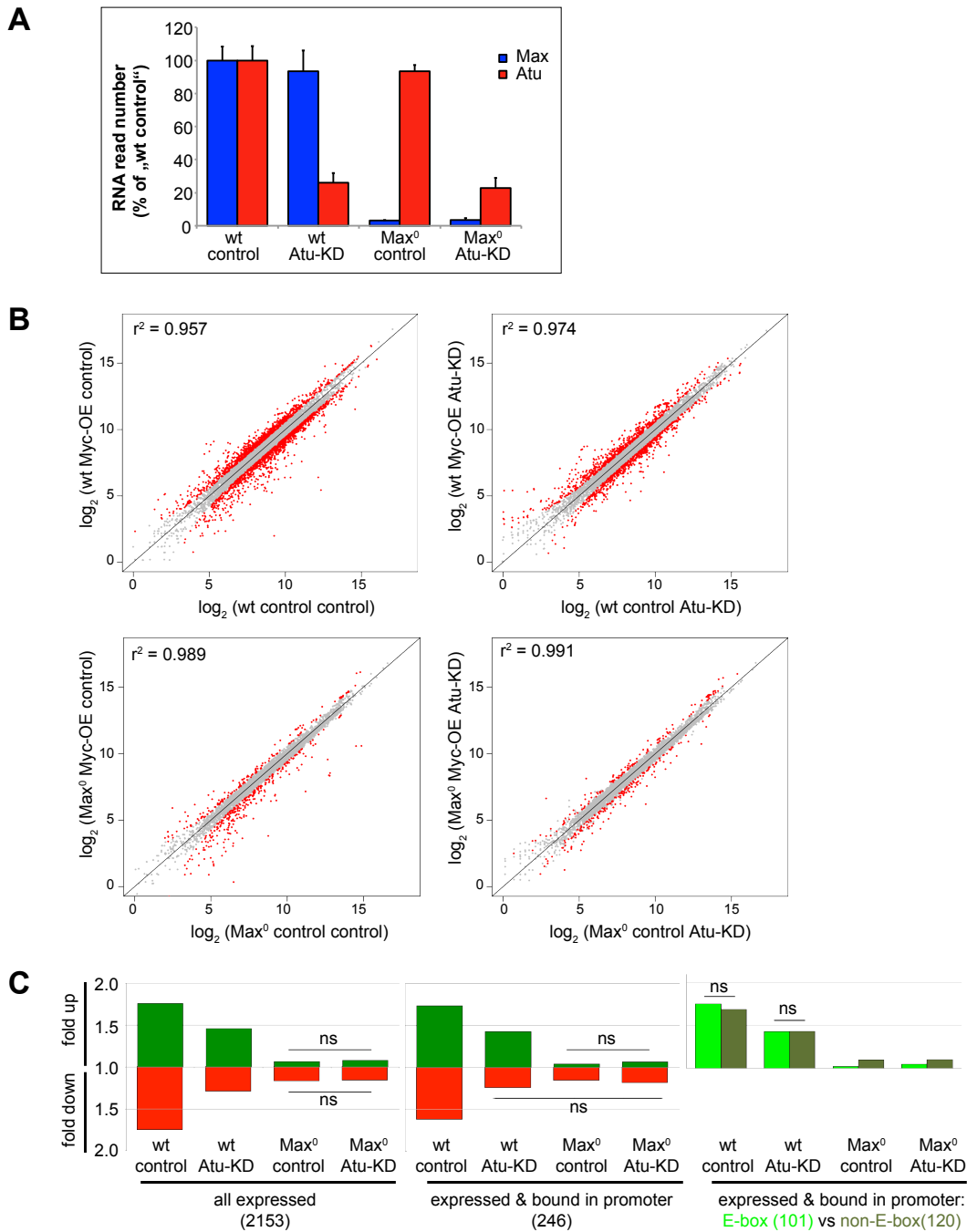
Figure 4.9: Effect of Atu or Max depletion on the expression of Myc targets in wing discs[1]

A) Relative read numbers for the mRNA of Atu and Max in *Drosophila* wing discs. Each column result-ed from six biological independent samples of the indicated genotype. Error bars show SEMs.

B) Dot blots representing the log2 fold change of read numbers in imaginal discs of the shown geno-types. For each genotype the average resulting from three biological replicates is depicted. Only genes that were expressed above a minimum threshold were blotted (8251 genes). Genes significant-ly deregulated by overexpression of Myc are shown in red.

C) Expression changes caused by overexpression of Myc in the different genotypes. All genes (977 induced and 1175 repressed ones) which showed differential expression after Myc overexpression in a wildtype background (left panel). Analysis restricted to the genes that overlap with Myc bound genes in promoter regions from S2 cells (221 induced and 25 repressed) (central panel). In addition, the 221 Myc-induced genes were discriminated by the presence or absence of a canonical E-box (right panel). All bars show median expression ratios, and the bars significantly differ from each other (Mann-Whitney test, $p < 0.01$), except the ones indicated with "ns".

4.2 Myc affects ecdysone synthesis and developmental transitions

4.2.1 Myc overexpression in Max^0 mutants causes pupariation block

Under physiological conditions the formation of Myc homodimers is not possible, but it dimerizes with Max. However, the study of Steiger *et al*. found evidence for Max-independent Myc functions (Steiger *et al.*, 2008). In an unpublished crucial experiment, D. Steiger showed that ubiquitous co-overexpression of Myc and the caspase inhibitor p35 in Max^0 mutants leads to a block of pupariation (Steiger, 2007).

These findings served as starting point for the current project. To ensure that the fly strains haven´t changed over time and that the phenotype is still present, the experiment was repeated several times. For this purpose, ovipositions for 4 – 6 hours were performed and 4 days later a heat-shock for 2 hours at 37°C was applied to induce ubiquitous expression of the transgenes. This time point for the heat-shock was chosen to ensure that all Max^0 mutants have reached L3 larval stage. 2 – 4 days later the mutant animals were floated with glucose, counted and put into a fresh vial. Pupariation was monitored every day or every second day.

Most of the Max^0 larvae pupariated between day 10 and 14. In contrast, only 10% of the Max^0 animals overexpressing Myc and p35 (hereafter called: Max^0 + Myc) pupariated up to day 16, and the fraction does not increase later on (Figure 4.10). These results confirm the earlier findings from D. Steiger.

The data indicate that Myc overexpression has an influence on the ecdysone system and this effect is independent from Max.
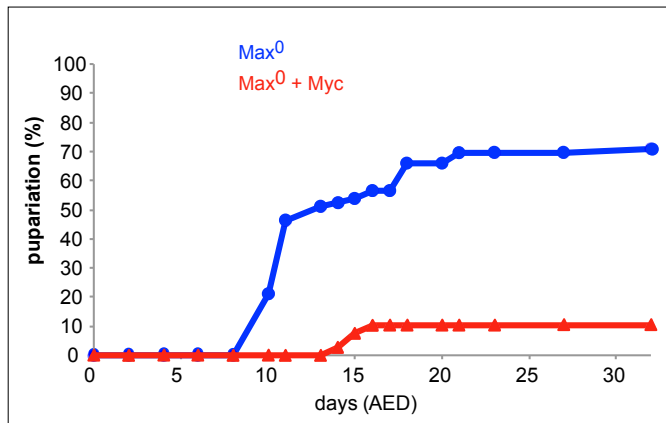
Figure 4.10: Overexpression of Myc in a Max^0 mutant background leads to pupariation block

Pupariation of Max^0 mutants with and without Myc overexpression over a period of 32 days after egg deposition (AED). The percentage of pupariated animals was calculated based on the total number of animals observed for this genotype after the heat shock. Animals were counted, transferred to a fresh vial and pupariation was monitored every day (Max^0: 76 animals; Max^0 + Myc: 77 animals).
Genotypes:
Max^0: "y w UAS-mCD8-GFP hs-FLP; +; actin>CD2>GAL4 max[1]/ max[1]"
Max^0 + Myc: "y w UAS-mCD8-GFP hs-FLP; UAS-Myc[132]/ +; actin>CD2>GAL4 max[1]/ max[1] UAS-p35"

It is unknown where Myc interferes with the ecdysone system. Heat-shock induced overexpression using the actin-GAL4 driver leads to strong ubiquitous expression of the UAS transgenes. Since ecdysone is produced in the PG, three scenarios for Myc's mode of action are possible: 1. Myc affects the ecdysone signaling pathway upstream of the PG (i.e. the signals activating the synthesis of ecdysone in the PG) or 2. directly in the PG (i.e. the ecdysone biosynthetic machinery) or 3. downstream of the PG in the target tissue in combination with 1. or 2.

To narrow down in which specific organ Myc needs to be overexpressed to cause a pupariation block as observed after ubiquitous expression, several GAL4 drivers were tested as summarized in table 4.2.1.

70

Table 4.2.1: Overview of Myc´s influence on pupariation in different tissues

The table summarizes the pupariation rate of larvae after Myc overexpression in specific tissues. The investigated GAL4 driver with the corresponding expression pattern is listed, as well as the number of experimental animals, control animals and independent repeats (in parentheses). Finally the pupariation rate of experimental animals is shown.

Relevant genotypes: "x-GAL4, UAS-Myc, UAS-p35, max/max"

("x" stands for the respective GAL4-driver listed below)

Driver	Pattern	Animals	Pupariation (%)
hs>act	ubiquitous	174, 76 (16)	32
phm	PG (weakly wing discs & tracheae)	95, 81 (7)	25
Feb36	PG & corpora allata	26, 75 (4)	77
P5015	PG	32, 36 (3)	99
spok	PG	23, 32	94
hs>act, phm-G80	ubiquitous, not PG	18, 25 (5)	44
P0206	ring gland	34, 124 (6)	74
Aug21	corpora allata	12, 53 (6)	100
C929	peptidergic neurons	54, 121 (7)	98
386Y	peptidergic neurons	39, 90 (7)	100
elav	pan-neuronal	42, 103 (7)	100
ap	wing discs	48, 59	49
CG	fat body	33, 35 (3)	94

All available PG-specific drivers (phm, Feb36, P0206, P5015, spok) were tested to investigate if Myc is acting directly in the PG but none of them caused the same phenotype as actin-GAL4 (Table 4.2.1). The low numbers of pupariated animals after overexpression with phm-GAL4 is due to the fact that most of the larvae died in L2 stage unable to undergo the molt to L3. Additionally, only 25% of the L3 escapers could pupariate suggesting that overexpression of Myc with phm-GAL4 blocks the pupariation of these animals and that Myc affects ecdysone synthesis directly in the PG. However, it is also possible that the few L3 escapers suffer damage from Myc overexpression and as a consequence, they are unable to initiate the complex process of pupariation. Therefore, several approaches were made to overcome the high lethality in L2 stage by shifting the onset of Myc overexpression to a time point shortly after the L3 molt, in analogy to what was done for the actin-GAL4 driver.

First, the temperature-dependency of GAL4 was exploited to keep ectopic Myc levels low during early development. In the beginning the larvae were incubated at 18°C for periods of 6 to 8 days and then shifted to 25°C. With the temperature shift GAL4 activity should increase and consequently Myc overexpression. Unfortunately, this approach did not rescue the larval

lethality nor the pupariation block. Second, a temperature-sensitive GAL80 transgene was introduced (y w; tub-GAL80$_{ts}$/UAS-Myc; max phm-GAL4/max UAS-p35). The animals were raised at 25°C for 4 days. Under these conditions GAL4 activity is inhibited by GAL80. After-wards the larvae were incubated at 30°C to inactivate GAL80 and allow Myc expression. Unfortunately, the long incubation at this high temperature resulted not only in lethality of the experimental animals, but also Max^0 mutants without Myc overexpression and Max wildtype animals were killed. Therefore, it was impossible to investigate pupariation in this experi-mental setup. Third, a transgene was constructed for temporally controlled Myc expression (UAS-FRT-RFP-stop-FRT-Myc), which can be activated by a heat-shock in combination with hs-FLP. Without heat-shock, the construct expresses just RFP due to the stop codon at the end of the RFP open reading frame. To test its ability to drive conditional Myc expression, the construct was activated in the presence of ap-GAL4 for expression in the wing discs. This resulted in adult flies with bent down wings or wings with necrotic patches, which is con-sistent with previously described phenotypes caused by Myc overexpression (Furrer *et al.*, 2010; Schwinkendorf and Gallant, 2009). Nevertheless, no pupariation block was observed with this construct presumably because its Myc expression is not strong enough. Finally, to rescue the lethality during L2-L3 transition caused by Myc overexpression with phm-GAL4, the L2 larvae were fed with synthetic 20-hydroxyecdysone (20E; the active form of ecdy-sone). However, this did not rescue the early larval lethality. Maybe the right timepoint to start the 20E feeding is an issue. It could be that 20E was applied too late to initiate the nec-essary processes for the molt to L3. Alternatively, the observed molting defect is not due to a lack of ecdysone but Myc overexpression leads to a different defect that kills these larvae.

Since the experiments with phm-GAL4 did not produce interpretable results, this GAL4 driver was not pursued any further. Instead, the weaker PG drivers Feb36, P0206 and P5015 as well as the stronger ones (Mai60- and spok-GAL4) were investigated (Table 4.2.1). Overex-pression of Myc with Mai60 resulted in embryonic lethality. None of the other PG-drivers caused a pupariation block suggesting that overexpression in the PG is not sufficient to in-duce the observed effect. To determine if Myc expression in the PG is even required for the non-pupariating phenotype, the actin-GAL4 driver was combined with a phm-GAL80 transgene (Table 4.2.1). This construct inhibits expression exclusively in the PG which was confirmed by GFP expression throughout the larvae but not in the PG. Animals that overex-press Myc everywhere except in the PG did not pupariate (Table 4.2.1). Meaning that Myc overexpression in the PG is not required to block pupariation, as long as Myc is overex-pressed everywhere else in the larva.

Taken together, these findings suggest that Myc is not acting directly in the PG, but instead in a different tissue which has an indirect impact on ecdysone synthesis. To address this possibility, Myc was overexpressed with several other tissue-specific GAL4 drivers. For neu-

ronal expression C929-GAL4, 386Y-GAL4 and elav-GAL4 were tested. Ap-GAL4 targets the wing discs while CG-GAL4 drives expression in the fat body. Unfortunately, none of the tested drivers produced the expected phenotype and pupariation block (Table 4.2.1). Either Myc was not overexpressed in the correct cells or the pupariation block requires the simultaneous overexpression of Myc in separate tissues. Meaning that the tissue where Myc acts to cause a pupariation block could not be identified.

4.2.2 Myc affects ecdysone biosynthesis and expression of its targets

Myc overexpression causes a phenotype very similar to mutations in the ecdysone pathway. To confirm that this pathway is affected by Myc, the mutant animals were fed with 20-hydroxyecdysone (20E; the active compound of ecdysone). This experiment was first carried out by D. Steiger (Steiger, 2007) and subsequently repeated during this thesis. Feeding of 20E rescued the pupariation block suggesting that ecdysone synthesis is affected by Myc overexpression.

To confirm this defect in 20E signaling, we tried to measure the ecdysone titers from whole larvae by mass spectrometry. Unfortunately, this approach failed probably due to insufficient sensitivity of the machine. Instead, the expression levels of the early response genes were analyzed. This serves an indirect readout for the activity of the ecdysone pathway (i.e. relative levels of 20E) because these genes are direct targets of ecdysone-bound EcR (Delanoue *et al.*, 2010). Therefore, the mRNA abundance of two early response genes, *Eip75B* and *BR-C*, was determined via qRT-PCR in whole larvae. The gene expression was compared for wildtype, Max^0 and Max^0 + Myc larvae at two timepoints during development, an early (in feeding L3 larvae) and a late timepoint (right before pupariation). In wildtype and Max^0 animals the levels of both transcripts are increased right before pupariation (Figure 4.11 B) suggesting that the ecdysone pathway is active. In contrast, in Max^0 + Myc larvae the levels of *Eip75B* stayed the same and for *BR-C* they even dropped slightly. The missing induction of the early response genes suggests that not enough ecdysone is produced in these animals.

Therefore, the structure of the organ where ecdysone is synthesized (PG) was investigated to find out if Myc overexpression damages the organ. Initially, Myc was overexpressed directly in the PG (with phm-GAL4), before it was established that the PG is not the site of Myc's action. The structure of these PGs is not grossly altered after Myc overexpression compared to control but the cell nuclei are enlarged (Figure 4.11 A right panel). An analogous phenotype was already described under enhanced Myc levels in fat body cells where it resulted from increased endoreplication (Pierce *et al.*, 2004). PGs with and without Myc overexpression were dissected for several other experiments (e.g. Figure 4.12) and the structure of both looked similar, with no obvious defect caused by Myc overexpression. Later it was also no-

ticed that the PGs looked normal when Myc was ubiquitously overexpressed except in the PG (actin-GAL4 combined with phm-GAL80).

Thus reduced ecdysone production due to a gross malformation of the PG can be excluded.
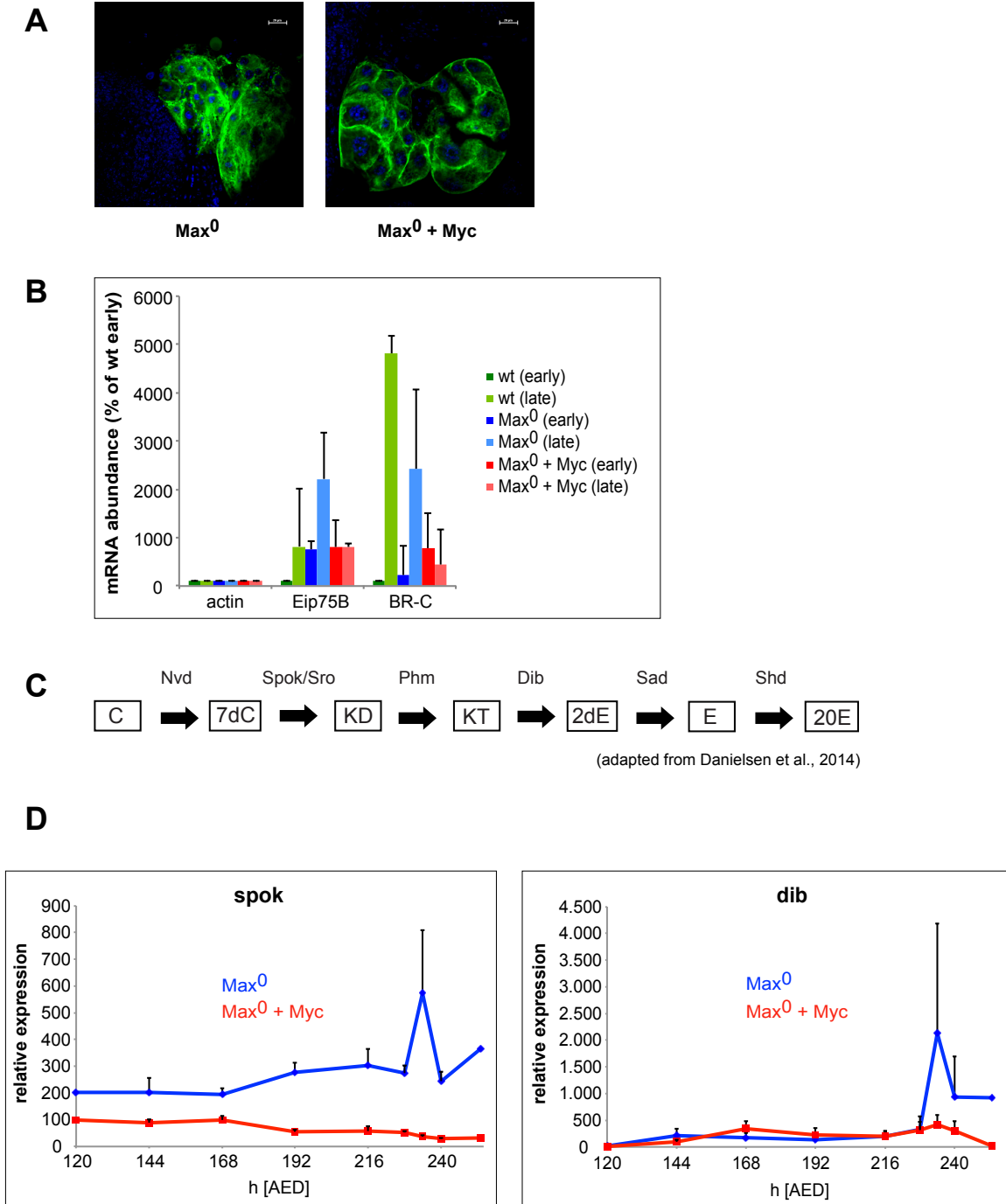
Figure 4.11: Effect of Myc overexpression on early response genes and halloween genes

A) Pictures of prothoracic glands from Max[0] animals ± Myc overexpression. Green reflects GFP expression driven by the phm-GAL4 driver. Cell nuclei are shown in blue.

B) Analysis of *Eip75B* and *BR-C* mRNA expression by qRT-PCR. Levels were determined for each genotype at an early timepoint in feeding L3 larvae (84 h AED for wildtype larvae; 144 h AED for both Max[0] mutants) and a late timepoint right before pupariation (132 h AED for wildtype larvae; 240 h AED

74

for both Max[0] mutants). The expression was normalized to the corresponding value of wildtype animals at an early timepoint. Actin5C was used as internal control. Shown are averages and SEMs from two biological replicates.

C) Scheme showing the conversion from dietary cholesterol to 20-hydroxyecdysone (adapted from Danielsen *et al.*, 2014).

D) Levels of the halloween genes spok and dib during development of Max[0] mutants with and without Myc overexpression measured by qRT-PCR. Values were normalized to actin5C of each sample and then to the value of the wt control at the first timepoint. Each data point results from one to three independent experiments, error bars indicate SEMs.

Genotypes:

A) Max[0]: "y w; +; max[1] phm-GAL4 UAS-GFP/ max[1]"

Max[0] + Myc: "y w; UAS-Myc[132]/ +; max[1] phm-GAL4 UAS-GFP/ max[1] UAS-p35"

B&D) Wt: "y w"

Max[0]: "y w UAS-mCD8-GFP hs-FLP; +; actin>CD2>GAL4 max[1]/ max[1]"

Max[0] + Myc: "y w UAS-mCD8-GFP hs-FLP; UAS-Myc[132]/ +; actin>CD2>GAL4 max[1]/ max[1] UAS-p35"

After the confirmation that the PG is intact, the Halloween genes, which are required for the synthesis of ecdysone (1.4.1), were investigated. For this purpose, the expression levels of these genes were analyzed by qRT-PCR. It was not necessary to isolate PGs, since the Halloween genes are only expressed in the PG. A heat-shock was given at 96 h AED to induce Myc expression. Afterwards, samples were collected every 6 h to 24 h until 253 h AED, a timepoint right before Max^0 mutants start to pupariate. The expression profiles of all Halloween genes were determined (except for *nvd*) and all were quite similar. Therefore, only *spok* and *dib* are shown as examples (Figure 4.11 D) and the profiles of the other genes are shown in the appendix (Figure S2). In Max^0 animals the expression of *spok* and *dib* is constant during development with a clear peak at 234 h AED. This peak is missing in larvae overexpressing Myc. For *dib* the mRNA levels of both genotypes are quite similar during development except for the peak expression at 234 h AED. In contrast *spok* levels are overall lower in Max^0 + Myc larvae. All examined Halloween genes showed a strong peak at 234 h AED in Max^0 mutants confirming that ecdysone production is enhanced at the end of larval development to induce pupariation. This peak is missing in a Myc overexpression background indicating that ecdysone is not synthesized in this genotype.

Taken together, these results show that increased Myc expression has no influence on the structure of the PG but inhibits Halloween gene expression and consequently presumably ecdysone synthesis. This leads to reduced expression of the early response genes and therefore, the signal to initiate pupariation is missing.

4.2.3 Elevated Myc levels influence the pathways involved in ecdysone synthesis

Several pathways are known to be involved in the regulation of ecdysone production in the prothoracic gland (PG) (see 1.4.2). Three of these pathways were investigated after ubiquitous Myc overexpression; unfortunately, we had no access to tools for the investigation of TGFβ signaling.

A

mTOR reporter activity

B

tGPH localization

Max^0 Max^0 + Myc

C

PTTH

Sample	PTTH level (± SEM)
wt early L3	103 (± 17)
wt late L3	91053 (± 3429)
Max^0 early L3	519 (± 58)
Max^0 late L3	22937 (± 9791)
Max^0 + Myc early L3	681 (± 32)
Max^0 + Myc late L3	1146 (± 99)

Figure 4.12: Pathways involved in ecdysone synthesis are affected by overexpression of Myc

A) Activity of a mTOR reporter in prothoracic glands (PGs) of wt and Max^0 mutant animals measured by luciferase activity. Single PGs were isolated from larvae carrying the unk-FLuc reporter which is repressible by mTOR. Max^0 mutants were collected in early L3 stage (192 h), late L3 stage (234 h) and right before pupariation (240 h). Shown is the average luciferase activity per PG ± SEM. For each genotype two to nine PGs were analyzed.

B) Pictures showing the localization of the tGPH reporter in PGs of Max^0 animals in late L3 stage (234h AED). The reporter is shown in green and the nuclei in blue. Activity of the insulin signaling pathway is reflected by the degree of membrane localization of the reporter.

C) Relative expression of PTTH measured by qRT-PCR. Levels were determined for wt animals and mutants with or without Myc overexpression early (wt: 84 h AED; Max0 mutants: 144 h AED) and late (wt: 132 h; Max0 mutants: 240 h) in L3 larval stage. Values were first normalized to actin5C for each genotype and then to „wt early L3". Averages and SEMs result from one (wt) or two (Max^0 ± Myc) biological replicates. Table depicts exact values (right panel).

Genotypes:

A) Wt: "y w"

Max^0: "y w actin>CD2>GAL4 hs-FLP; +; max[1] unk-FLuc/ max[1]"

Max^0 + Myc: "y w actin>CD2>GAL4 hs-FLP; UAS-Myc[132]/ +; max[1] unk-FLuc/ max[1] UAS-p35"

B) Max^0: "y w hs-FLP; tGPH/ +; actin>CD2>GAL4 max[1]/ max[1] UAS-p35"

Max^0 + Myc: "y w hs-FLP; tGPH/ UAS-Myc[132]; actin>CD2>GAL4 max[1]/ max[1] UAS-p35"

C) Wt: "y w"

Max^0: "y w UAS-mCD8-GFP hs-FLP; +; actin>CD2>GAL4 max[1]/ max[1]"

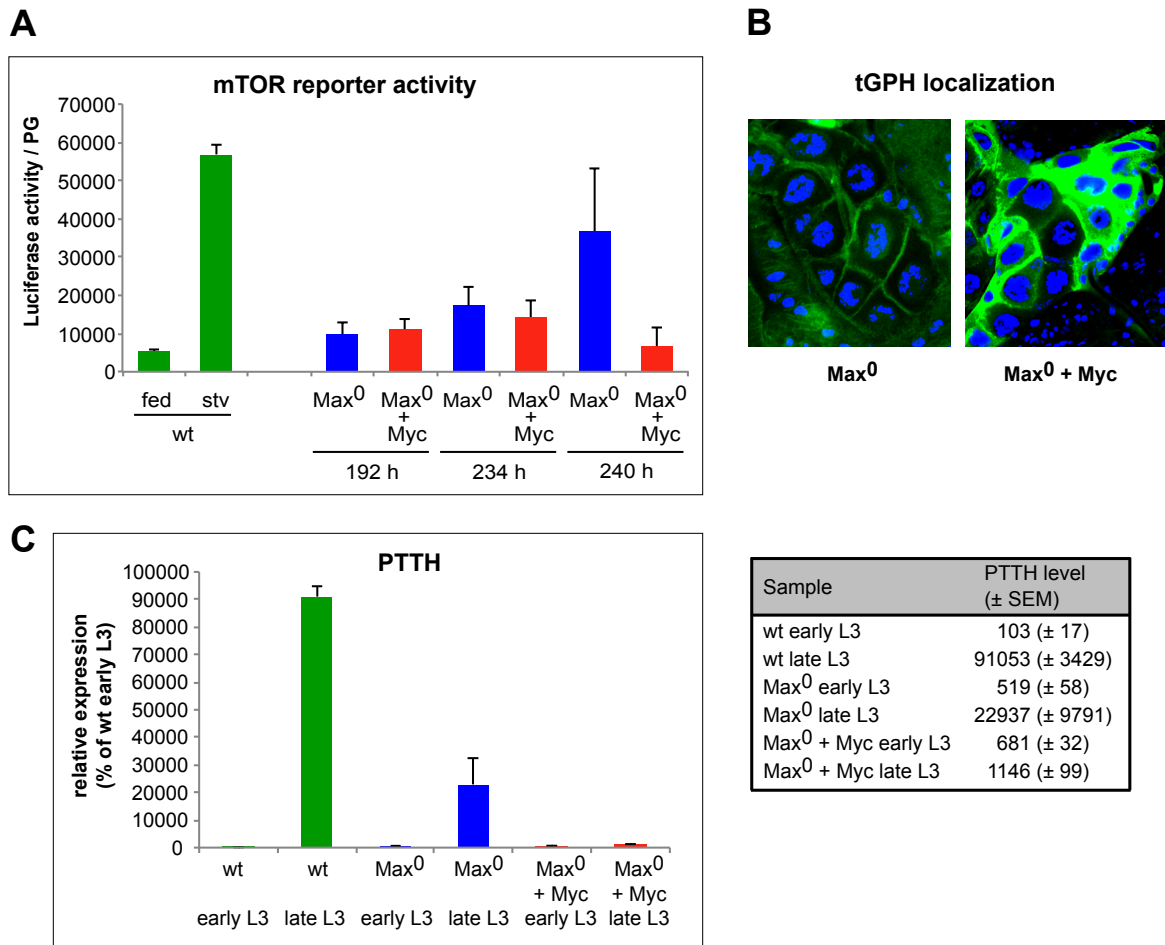Max^0 + Myc: "y w UAS-mCD8-GFP hs-FLP; UAS-Myc[132]/ +; actin>CD2>GAL4 max[1]/ max[1] UAS-p35"

First, mTOR activity was determined with the help of a transgene expressing firefly luciferase under the control of the *unkempt* (*unk*) promoter (unk-FLuc). The *unkempt* gene is repressed by mTOR and increased activity of the unk-FLuc reporter has been shown to faithfully reflect decreases in mTOR activity *in vivo* (Tiebe *et al.*, 2015). Single PGs were isolated from larvae and analyzed in a luciferase assay. Fed and starved wildtype animals were used to verify the function of the reporter (Figure 4.12 A). Under starvation conditions reporter activity is strongly increased, consistent with the notion that mTOR activity is decreased in this situation. mTOR activity was analyzed at 192, 234 and 240 hours AED in Max^0 mutants ± Myc. For some data points only two PGs were examined, so these analyses still need to be confirmed. Max^0 mutants showed an increase in luciferase signal over the examined time period (Figure 4.12 A). A corresponding decrease in mTOR activity during late L3 larval development might be expected, since the larvae stop feeding and might experience some starvation-like symptoms at this time point. In contrast, Myc overexpression did not increase reporter activity at any time point, indicating that Myc does not inhibit mTOR activity in this context but also, that the developmental decrease in mTOR activity does not take place in this genotype.

Second, the insulin/insulin-like growth factor pathway (IIS) was investigated with the tGPH reporter (Britton *et al.*, 2002). The reporter is transcriptionally controlled by tubulin and consists of a PH (pleckstrin homology)-domain fused to GFP. When the IIS pathway is active the PH-domain and therefore PH:GFP is recruited to the plasma membrane otherwise the protein is distributed throughout the cytoplasm. Larval PGs were isolated at 234 h AED, fixed with paraformaldehyde and analyzed with a confocal microscope. In Max^0 animals GFP is predominantly localized to the plasma membrane reflecting active insulin signaling (Figure 4.12 B). GFP expression is stronger in Max^0 + Myc, however, the reporter is equally distributed between the cytoplasm and the membrane. This suggests that IIS activity is reduced by elevated Myc levels. To support these findings more samples need to be analyzed and further time points should be included.

Third, defects in the PTTH pathway were analyzed. For that purpose the expression of PTTH of wildtype animals and both types of mutants at two different time points was measured by qRT-PCR. This approach revealed a dramatic increase of PTTH levels in wildtype and Max^0 mutants right before pupariation, whereas Max^0 + Myc larvae were lacking such a strong expression (Figure 4.12 C).

In conclusion, two of the pathways (IIS and PTTH) controlling ecdysone production seem to be affected by Myc overexpression. Loss of either pathway alone is probably not sufficient to cause a complete pupariation block (see 1.4.2), but the combined deficiency of pathways may very well result in the strong defect in ecdysone synthesis.

4.2.4   MycΔZ, a mutant form of Myc, causes the same phenotype as wildtype Myc

To identify molecular targets of Myc that might mediate the observed pupariation block, cell culture experiments in S2 cells were performed. A mutant form of Myc which lacks the leucine zipper (MycΔZ) and is therefore unable to dimerize with Max was used for this approach (Figure 4.13 A) (Steiger *et al.*, 2008). Before turning to cell culture this truncated form was tested for its effect on pupariation. Overexpression of such a Myc mutant in a Max wildtype background might be expected to mimick some of the effects caused by overexpression of MycWT in a Max^0 background. Surprisingly, Max wildtype animals overexpressing MycΔZ pupariated at the same time as control animals. In a wildtype background Myc overexpression is obviously not sufficient to block pupariation. It seems likely that the Max^0 background is required for Myc's effect. Therefore, the pupariation of Max^0 mutants overexpressing MycΔZ was monitored (Figure 4.13 B). The graphs for Max^0 and Max^0 + MycWT are the same as shown in Figure 4.10. After overexpression of MycΔZ only 7% of the Max^0 larvae were able to initiate pupariation before day 18 AED. This shows that MycΔZ is able to provoke the same phenotype as MycWT in this background.
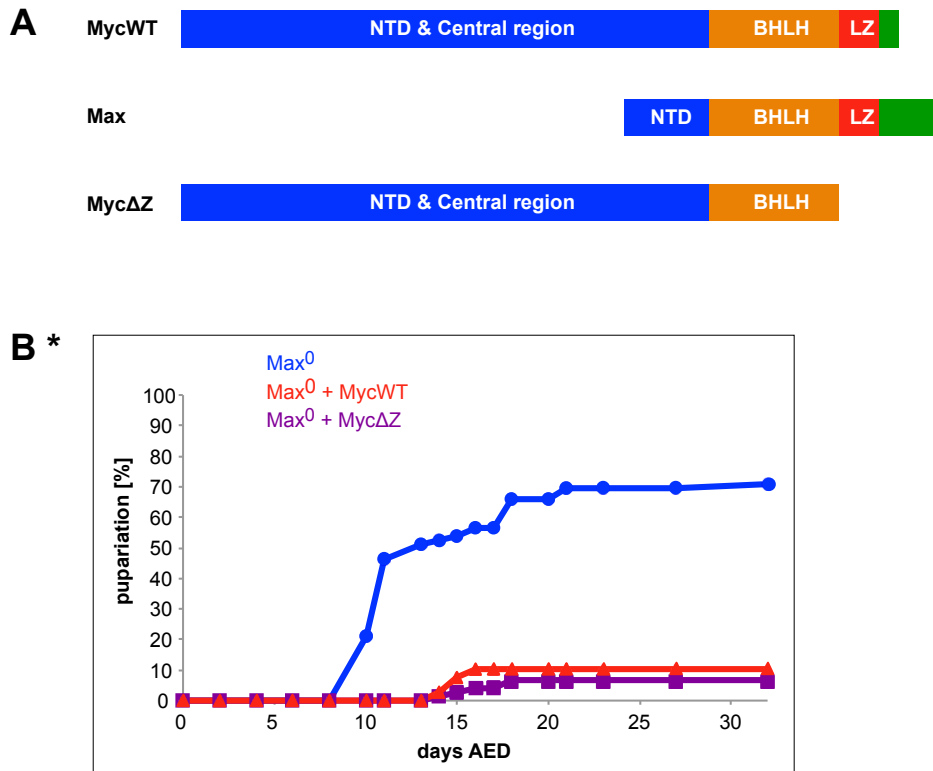
Figure 4.13: MycΔZ has the same effect on pupariation as MycWT

A) Scheme depicting the important domains of MycWT, MycΔZ and Max. The leucine zipper of MycWT enables heterodimerization with its partner protein Max. The MycΔZ construct lacks the leucine zipper and is therefore not able to dimerize with Max.

B) Pupariation of different Max^0 mutants was compared over a period of 32 days after egg deposition (AED). Overexpression of MycΔZ blocks pupariation to the same extent as does overexpression of MycWT. Percentage of pupariated animals was calculated based on the total number of animals transferred into a fresh vial after the heat shock (Max^0: 76 animals; Max^0 + MycWT: 77 animals; Max^0 + MycΔZ: 75).

* Graph for Max^0 ± MycWT was already shown in Fig. 4.10.

Genotypes:

B) Max^0: "y w UAS-mCD8-GFP hs-FLP; +; actin>CD2>GAL4 max[1]/ max[1]"

Max^0 + MycWT: "y w UAS-mCD8-GFP hs-FLP; UAS-Myc[132]/ +; actin>CD2>GAL4 max[1]/ max[1] UAS-p35"

Max^0 + MycΔZ: "y w UAS-mCD8-GFP hs-FLP; +; actin>CD2>GAL4 max[1]/ max[1] UAS-p35; UAS-HA-MycΔZ/ +"

### 4.2.5 Effect of Myc on potentially Max-independent targets

A list of 265 direct Myc targets (Herter *et al.*, 2015) was scanned for genes known to play a role during development or ecdysone synthesis (based on the literature, as well as electronic annotations) to identify genes that potentially mediate the pupariation block. This search revealed five possible candidates: the transcription factor molting defective (*mld*) (it regulates the expression of some Halloween genes (Danielsen *et al.*, 2014; Neubueser *et al.*, 2005)), the ecdysone receptor (*EcR*) and its direct target *Eip75B* (both are also involved in ecdysone synthesis (Parvy *et al.*, 2014)), the pro-apoptotic gene reaper (*rpr*) (a direct EcR target which is required for apoptotic events (Jiang *et al.*, 2000)) and the transcription factor Kruppel-homolog 1 (*Kr-h1*; another EcR target for later responses to ecdysone (Pecasse *et al.*, 2000)).

ChIP experiments were performed to verify if these genes can be bound by Myc in the absence of Max in cell culture. For this purpose S2 cells were transfected with the constructs HA-MycWT or HA-MycΔZ and processed 40 hours later. Untreated cells were used as control. The chromatin was precipitated with an HA-specific antibody or control rabbit IgGs.

The ChIP showed a strong enrichment of the investigated genes in cells transfected with MycWT compared to control cells or IgGs confirming the binding of MycWT to this targets (Figure 4.14 A). Both Myc forms bound equally strongly to *EcR* and *rpr* while binding of MycΔZ to *mld*, *Eip75B* and *Kr-h1* is reduced as compared to wildtype, but still strongly detectable. Thus, these target genes are still bound by Myc in the absence of Max.

To examine if candidate gene expression is altered in Max^0 + Myc larvae, qRT-PCR analyses were performed, starting from whole larval lysates. Such animals were compared with wildtype and Max^0 larvae at two different time points, in young feeding L3 larvae and in older L3 larvae shortly before pupariation. In wildtype animals expression of all genes was strongly increased at the second time point as compared to the first (Figure 4.14 B). Right before pupariation increased levels were also observed in Max^0 mutants for all genes except *Kr-h1*. In contrast, in Max^0 + Myc mutants the levels of *mld*, *rpr* and *Kr-h1* stayed the same and were only slightly increased for *EcR* and *Eip75B*.

Taken together, five Myc target genes with a demonstrated role in metamorphosis were identified and all of them can be bound by Myc independently of Max. Four of these genes (*mld*, *EcR*, *Eip75B* and *rpr*) are clearly reduced in their developmental expression by Myc overexpression, which raises the possibility that they are involved in the observed effect of Myc on pupariation.
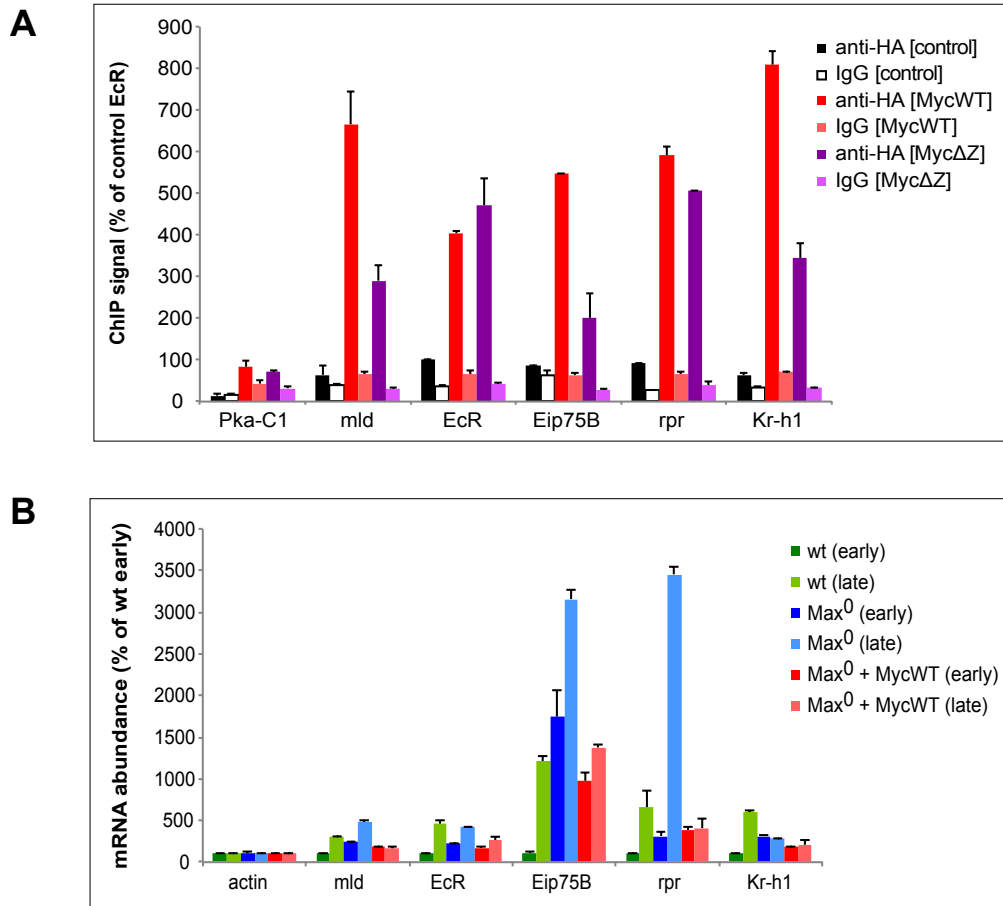
Figure 4.14: Effect of Myc on binding and expression of selected targets

Candidate genes were selected from a list of targets which are bound by Myc (defined in ChIP sequencing experiments from Herter *et al*., 2015) and which are known to be involved in development or the ecdysone pathway. Selected genes are *mld*, *EcR*, *Eip75B*, *rpr* and *Kr-h1*.

A) ChIP from control cells and cells expressing HA:MycWT or HA:MycΔZ. Cells were transfected with the indicated constructs and harvested 40 h later. Chromatin was precipitated with a HA-specific antibody and nonspecific rabbit IgGs were used as control. Averages and SEMs result from technical triplicates and were normalized to the signal for EcR of control cells.

B) Expression of candidate genes was analyzed by qRT-PCR. Transcript levels in whole larval extracts from wt, Max^0 and Max^0 + Myc at an early (wt: 84 h; Max^0 ± Myc: 144 h) and late time point (wt: 132 h; Max^0 ± Myc: 240 h) during development were compared. With the ΔΔCt method each sample was normalized to actin5C and to the values of wt at the early timepoint. Results origin from three technical replicates. Error bars indicate SEMs.

Genotypes:

B) Wt: "y w"

Max^0: "y w UAS-mCD8-GFP hs-FLP; +; actin>CD2>GAL4 max[1]/ max[1]"

Max^0 + Myc: "y w UAS-mCD8-GFP hs-FLP; UAS-Myc[132]/ +; actin>CD2>GAL4 max[1]/ max[1] UAS-p35"

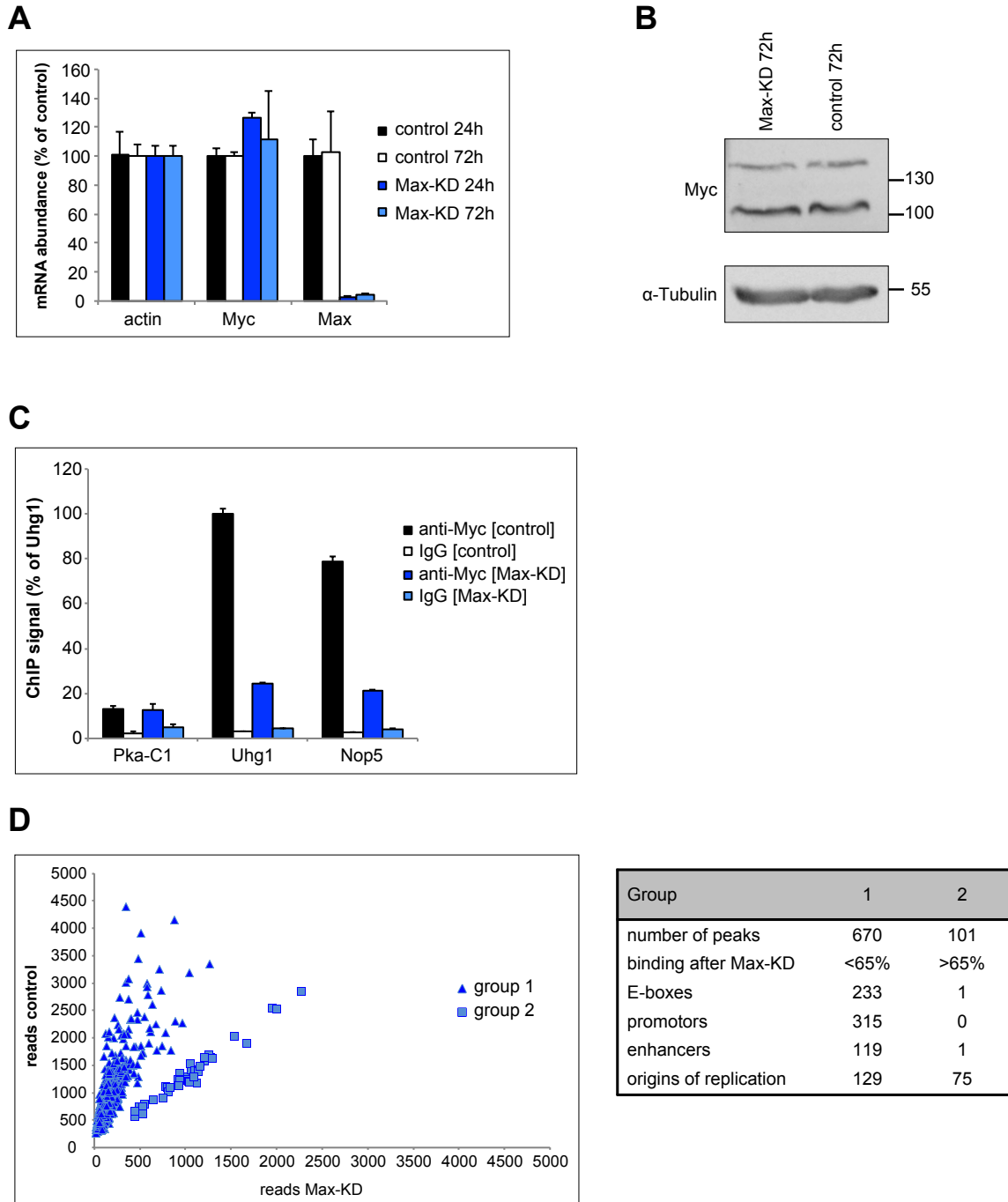### 4.2.6   Effects of Max depletion on Myc targets

As a complementary approach to explore how overexpressed MycDZ binds to its target genes, we wanted to find out which target genes are still bound by endogenous Myc upon depletion of Max. The genes analyzed above were of particular interest. For this purpose, S2 cells were either treated with dsRNA against Max or left untreated and further processed 72 hours later. The Max knockdown was verified via qRT-PCR (Figure 4.15 A) since no working anti-Max antibody is available for *Drosophila*. Max transcript levels were already strongly reduced after 24 h (97.1 ± 1.0%), indicating that Max protein levels were below 4% after 72 h because the protein has a half-life of less than 10 hours (Steiger *et al.*, 2008). The amount of Myc protein was analyzed by Western blot and shown to remain unchanged after Max knockdown (Figure 4.15 B). The chromatin of both samples was immunoprecipitated with a rabbit anti-Myc antibody or non-immune rabbit IgGs. Prior to sequencing the efficiency of the immunoprecipitation was tested by analyzing one negative (Pka-C1) and two positive (Uhg1, Nop5) Myc targets. Myc binding to the positive targets is strongly reduced after Max knockdown (Figure 4.15 C) attesting to the success of the ChIP experiment. The chromatin was further processed for sequencing. The sequencing produced 2.9 million reads for the control sample and 11.4 million reads for the Max-KD sample. Since equal read numbers of both samples are required for the analysis with the software macs only 2.9 million reads of each sample were compared. This means that most of the reads from the Max-KD had to be ignored. The analysis was repeated with the reads from the previous control sample (see 4.1.5). There the sequencing produced 7.8 million reads for the control. Therefore, less than half of the reads from the Max-KD sample had to be excluded for the second analysis. Both analyses gave similar results, therefore the one with 7.8 million reads was further analyzed.

Myc binding to the five candidate genes described above (4.2.5) was strongly reduced (between 80.8% and 86.7%) after Max knockdown. Obviously endogenous levels of Myc need Max for the binding to these sites. Nevertheless, overexpressed Myc can bind to these targets independent from Max as shown for MycDZ (4.14 A) and their expression is affected by Myc overexpression *in vivo* (Figure 4.14 B).

Apart from these genes, no obvious candidate gene was found that is absolutely Max-independent. However, the Myc binding sites clearly fall into two categories dependent on their sensitivity to Max depletion (Figure 4.15 D left panel). The first group contains 670 peaks which are strongly reduced after Max knockdown. In contrast, the second group contains 101 peaks and Max depletion had a much weaker effect. More differences between the groups were discovered during further analyses (Figure 4.15 D right panel). 233 E-boxes were found in group 1 but only one E-box in group 2. This is consistent with the notion that E-boxes are only bound by Myc:Max dimers and hence strongly affected by Max loss. Furthermore, group 1 contained many promoter (315) and enhancer sites (119) whereas in group 2

no promoter sequence and only one enhancer site was found. Since group 2 does not contain any promoter region, there is no clearly associated gene and accordingly no expression data. However, 78% of these group 2 sites overlap origins of replication (oris) compared to 18% of group 1. Myc's potential link to replication will be addressed later (see Discussion). Furthermore, group 1 contains all previously described Myc targets, none of them is found in group 2. So, Max depletion seems to affect the binding of endogenous Myc to all of its targets.

At this point, it is not clear if such a potential effect of Myc on replication is involved in the observed pupariation block or if this effect involves Myc targets that require Max for the recruitment of Myc at physiological leves but become independent of Max after Myc overexpression (as proposed for the five candidate genes described above).

A

B

C

D

Group	1	2
number of peaks	670	101
binding after Max-KD	<65%	>65%
E-boxes	233	1
promotors	315	0
enhancers	119	1
origins of replication	129	75

Figure 4.15: Max-dependence of Myc chromatin binding

A) Transcript levels of Myc and Max were measured in control and Max depleted cells by qRT-PCR. Values were normalized to actin5C of each sample and plotted relative to „control 24 h". Averages and standard deviations originate from technical triplicates.

B) Myc levels in control cells and cells incubated with Max-dsRNA for 72 h were analyzed by Western blot. α-Tubulin served as loading control.

C) ChIPs from control cells and cells after Max knockdown. Chromatin was precipitated with a rabbit anti-Myc antibody or control rabbit IgGs. Shown are averages and standard deviations from technical triplicates normalized to the signal for Uhg1 of control cells.

D) ChIP sequencing analysis of control and Max-KD cells. Shown are read numbers for Myc peaks after Max depletion in comparison to control (left panel). Reads for control are the same as used in 4.1.5. The results from further analysis of the two different groups are summarized in the table (right panel).

4.2.7 Hypoxia causes elevated Max transcript levels

The previous results show that ectopic Myc expression affects ecdysone signaling in Max^0 mutants. This situation is artificial, raising the question whether such conditions might ever occur during normal development. Various situations are known which cause an increase of Myc levels, for example tissue damage, potentially mimicking the Myc overexpression setting used throughout this work (Gallant, 2013). In contrast, circumstances leading to the complete loss of Max have not been described in the past, but a recent publication reported that Max protein levels in vertebrate cells are reduced under low oxygen conditions (hypoxia) (Kemmerer and Weigand, 2014). This might reflect a natural situation where Myc is acting in the absence of Max.
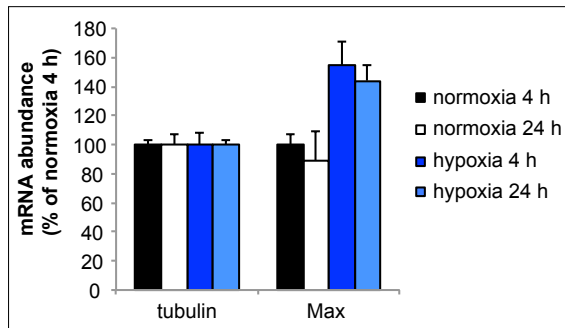
Figure 4.16: Effect of hypoxia on Max expression in S2 cells

Expression of Max was determined via qRT-PCR. S2 cells were incubated for 4 h or 24 h under normal oxygen conditions (normoxia) or low oxygen (hypoxia, 0.5% oxygen). Values were normalized to tubulin and shown in relation to Max levels of cells under normoxia for 4 h. Mean ± SD of technical duplicates are presented.

To investigate if hypoxia reduces expression of Max, S2 cells were incubated with 0.5% oxygen for 4 h and 24 h. Control cells were kept under normal oxygen conditions for the same periods. Transcript levels of Max were determined via qRT-PCR showing that Max expression was increased after 4 h of hypoxia and the levels are quite similar even after longer exposure to low oxygen (Figure 4.16). This experiment was only performed once and needs to be repeated. In addition, the influence of hypoxia on Max expression *in vivo* should be investigated. This could be done by incubating larvae under low oxygen conditions. It would be even more important to find out how hypoxia affects Max protein levels but this is difficult because none of the tested antibodies was able to recognize *Drosophila* Max.

Nevertheless, at this point there is no indication that hypoxia might constitute a situation where Max reduction plays a role during normal development.

5 Discussion

5.1 The influence of the PAF1 complex on Myc-regulated transcription

5.1.1 Atu binds directly to Myc and helps recruit it to target genes

The transcription factor Myc needs to form a heterodimer with Max for the transcriptional regulation of target genes. These dimers bind most efficiently to canonical E-box motifs but it was shown that the DNA sequence alone is not sufficient to define the targets of Myc. Several promoters without an E-box are also bound by Myc (Guo *et al.*, 2014) and the *in vitro* binding constant of Myc:Max dimers for E-boxes is not sufficient to explain the observed affinity for its target sites *in vivo* (Lorenzin *et al.*, 2016). Therefore, it was speculated that additional factors are involved in the recruitment of Myc:Max dimers independent of the sequence. WDR5 was recently shown to interact with the conserved MB IIIb domain of Myc and elimination of WDR5 impairs the binding of Myc to the majority of its targets (Thomas *et al.*, 2015). WDR5 is not the only co-factor which recruits Myc:Max complexes to their targets sequence-independently. The PAF1 complex was identified as novel Myc co-factor in *Drosophila* S2 cells (Furrer, 2008; Furrer *et al.*, 2010) and in this study here, we were able to show that the PAF1 complex has a similar role as WDR5.

Atu does not affect Myc levels, but Myc activity and it interacts directly with the central region of Myc. The N- and C-terminus of Myc are well characterized. The N-terminal part contains the Myc boxes I and II, which are involved in transcriptional activation. The C-terminus comprises the bHLHZ motif, necessary for the dimerization with Max and binding to DNA. In contrast, less is known about the central part of Myc, which harbors three conserved Myc boxes in vertebrates (MB IIIa, IIIb and IV). MB IIIa was shown to contribute to transcriptional repression by Myc (Kurland and Tansey, 2008) and MB IV is required for the binding of Myc to naked DNA (Cowling *et al.*, 2006). MB IIIb is important for the binding to WDR5 and thereby for the recruitment of Myc to DNA (Thomas *et al.*, 2015). MB IIIb is identical between vertebrate and *Drosophila* Myc, therefore one would assume that the *Drosophila* homolog of WDR5, called Wds, would bind to this motif (although this has not been experimentally addressed). Atu does not require MB IIIb for binding to Myc, therefore it seems to interact with a different region than WDR5. Although the region of Myc which mediates the binding with Atu is in close vicinity of MB IIIb. It is likely that the central part of Myc has additional important functions because of its high evolutionary conservation. Therefore, further studies are necessary to reveal these functions and further binding partners of this particular region.

A short centrally located region of Atu (aa 442 – 474) with no described function was shown to be essential for the association with Myc (Figure 4.2 C). In general, no specific structures or biochemical functions were described for Atu (Tomson and Arndt, 2013). However, a 93

aa region located in the C-terminal half of Leo1, the human homolog of Atu, is required for its binding to Paf1. This interaction mediates the binding of Leo1 to the PAF1 complex (Chu *et al.*, 2013). Since the C-terminal part of Leo1 is responsible for its association with the complex, the N-terminal and central part would be free to interact with Myc. Furthermore, it was demonstrated that the PAF1 complex binds RNA and Leo1 is essential for this binding in yeast. In strains lacking Leo1 the recruitment of PAF1 to chromatin was reduced. Altogether these data suggest that the PAF1 complex localizes to highly transcribed genes, which is also the perfect location for Myc, and this association is stabilized by the interaction of Leo1 with RNA (Dermody and Buratowski, 2010).

Several methods showed that Atu interacts with Myc *in vivo* and on chromatin. There are two different possibilities how Myc and the PAF1 complex act together to bind specifically to target genes to control their transcription. Myc can bind sequence-specifically to its targets and recruits the PAF1 complex afterwards. Or the PAF1 complex could first associated with the general transcription machinery, which leads to the subsequent recruitment of additional factors, in this case Myc. Both alternatives were investigated by depletion of individual proteins followed by ChIP of the other partners. This showed that the PAF1 complex contributes to Myc recruitment, and not the other way around.

In this thesis, the rabbit anti-Myc antibody from Santa Cruz was used for all Myc ChIPs and the following sequencing experiments. To exclude background signals resulting from unspecific binding of the antibody, we used Myc-depleted cells as control and eliminated peaks present in a HA-ChIP from naïve S2 cells. With these settings 714 Myc-bound regions were identified in S2 cells almost three times more as proposed by Herter *et al*. They found 263 binding sites of Myc in *Drosophila* S2 cells with two different antibodies, a monoclonal mouse anti-Myc and a polyclonal rabbit anti-Myc (Herter *et al.*, 2015). The different antibodies which were used might explain the varying numbers of binding sites. The commercial antibody from Santa Cruz has a higher affinity than the selfmade ones used in Herter *et al*. Surprisingly, Yang *et al*. obtained almost 4000 Myc binding sites with the antibody from Santa Cruz (Yang *et al.*, 2013). This high number of binding sites results from some background binding of the antibody which they did not realize due to missing controls, like non-immune IgGs or Myc depleted cells (Herter *et al.*, 2015). However, we consider the 714 sites identified here to be highly specific since they were strongly reduced after Myc depletion (Figure 4.7) and therefore we used them for all further analyses. 296 of these binding sites were shown to lie in close proximity to promoters and 166 close to enhancer sites, which matches with published data showing that Myc preferentially binds to promoter-proximal sequences (Herter *et al.*, 2015; Walz *et al.*, 2014). Some of the remaining sites also correspond to origins of replication (see the ChIPseq analysis after Max-KD) and the other remaining peaks have no identified functional elements.

Since the PAF1 complex associates with the general transcription machinery preferentially at active promoters, it is perfectly placed to recruit Myc to target genes. Indeed, Atu depletion significantly reduced Myc binding to target genes at promoter sites. Many of these promoters contain E-boxes which can be bound by Myc:Max dimers *in vitro*. Nevertheless, the loss of Atu reduces Myc recruitment to such E-box targets, even though the interaction of Myc:Max complexes with the DNA should not be affected. This shows that Atu or the PAF1 complex fulfills a similar function as WDR5, although the overall effect is much milder. It is possible that additional factors like WDR5 or Atu are involved in Myc's recruitment to target genes and that their impact might differ depending on the cellular background.

The strong binding reduction after Myc knockdown confirmed that Myc binds to many of the identified enhancers sites. Unexpectedly, these sites were not impaired after Atu knockdown. It is possible that the different effect on promoter and enhancer sites derives from a differential occupancy of Atu. This possibility was investigated with an HA ChIP showing that Atu is present at both sites. These results suggest that Atu is not required for the recruitment of Myc to enhancer sites, which is confusing and we do not have an explanation for this.

5.1.2   Global effects of Atu on gene expression

To investigate the consequences of Atu depletion on the transcriptomes of S2 cells, RNA sequencing experiments were carried out. The overall impact was very weak and a GSEA did not identify any specific gene set to be affected after Atu knockdown, even though Atu protein levels were strongly decreased. The comparison of all expressed genes with the gene set of direct Myc targets (see Results for definition) showed a significant decrease in gene expression. This analysis was carried out in R, which presumably follows different algorithms as GSEA. Also the genes with an E-box downstream of their transcriptional start site (see Results for definition) showed a reduced expression after Atu depletion. These findings reflect a positive effect of the PAF1 complex on gene expression, which is consistent with the reduced Myc recruitment observed after Atu depletion, but the effect is less pronounced. The differences might be explained by the findings of Jaenicke *et al*. They observed a negative effect of the PAF1 complex on the expression of Myc target genes. After knockdown of Cdc73 in hTERT-immortalized mammary epithelial cells (IMECs) gene expression was about 10% increased. They proposed that a complex of Myc and the PAF1 complex can inhibit transcription and that the accumulation of such inhibitory complexes is limited by the degradation of Myc to allow transcriptional activation (Jaenicke *et al.*, 2016). Nevertheless, the observed effect is only mild which is consistent with our findings. This might make sense if the PAF1 complex plays two roles in transcription: first a positive one in Myc recruitment and later on a negative one in transcription elongation. Depending on the situation, one or the other function might dominate and the overall output on transcription might be positive or

negative. But this output would always be weaker than either effect alone because it is always the sum of both effects. The PAF1 complex might also have such ambiguous roles in other context, and this might explain why the complex is identified variably as a positive or a negative factor, and why the effects on steady-state transcript levels are usually quite mild. Several published data show that the PAF1 complex exerts a positive effect on RNA pol II pause release and transcriptional elongation. For example, the knockout of Paf1 or Rtf1 in yeast causes a global reduction of newly synthesized mRNA (Xu *et al.*, 2017). Furthermore, in human leukemia cells (THP1) most genes are not affected by Paf1 depletion but a significant fraction (about 15%) shows an increase of paused RNA pol II at promoter-proximal sites (Yu *et al.*, 2015). In contrast, the knockdown of Paf1 caused a reduction of paused RNA pol II in another leukemia cell line (CCRF-CEM) (Yu *et al.*, 2015). And the expression of direct PAF1 complex targets was increased by less then 10% after the knockdown of Paf1 (Chen *et al.*, 2015). These data suggest a negative impact of PAF1 on transcription elongation. Yu *et al.* proposed that the differential effects of the PAF1 complex might result from differences in the genetic background or the physiological state of the corresponding cells (Yu *et al.*, 2015).

5.1.3 The PAF1 complex becomes more essential upon Myc overexpression

The PAF1 complex is an evolutionary conserved protein complex, which is involved in numerous RNA pol II-dependent transcriptional processes. The different subunits of the PAF1 complex were first identified in *S. cerevisiae* and the characterization of the corresponding genes showed that they are not essential in yeast. In contrast, in *Drosophila* existing loss-of-function mutations in all PAF1 components are lethal (Bahrampour and Thor, 2016). In this thesis, none of the knockdowns affected larval survival, with the exception of Paf1, which killed the larvae within 48 hours. After knockdown of the other components the larvae developed at least to pharate adult stage and even some viable adults were found. For Rtf1, our observation fits with published data where the knockdown of Rtf1 resulted in pupal lethality with no adult escapers (Tenney *et al.*, 2006). In contrast, much stronger phenotypes were observed for null mutants of hyx or Ctr9. The loss of hyx caused lethality during late embryogenesis (Mosimann *et al.*, 2006). The same was observed for hemizygous Ctr9 mutants. Here, few larvae hatched to L1 stage but died quickly afterwards (Bahrampour and Thor, 2016). Furthermore, the PAF1 complex is involved in Myc-dependent growth. The size of adult bristles was reduced after depletion of Paf1, Rtf1 and Atu in bristle precursor cells (Gerlach *et al.*, manuscript submitted). A similar phenotype was already described after moderate Myc reduction (Gallant *et al.*, 1996; Johnston *et al.*, 1999). Myc overexpression in imaginal disc clones leads to a strong increase in cell size. The elimination of PAF1 complex components in such clones was able to strongly diminish this overgrowth whereas the size of control clones was not affected (Gerlach *et al.*, manuscript submitted). A similar effect was ob-

served in adult eyes where overexpression of Myc caused an increase of ommatidial size. This results in overall bigger eyes and a rough appearance, because the ommatidia are disordered. Roughness of the eyes was reduced by Atu knockdown. No effect of Atu depletion was observed in eyes that do not overexpress Myc demonstrating that all the described effects are mediated by Myc. It seems reasonable to presume that the function of PAF1 becomes more essential under elevated Myc levels. This is also reflected in the gene expression profiles of wing discs. Myc-activated as well as Myc-repressed genes are affected by Atu depletion (Figure 4.9) which is consistent with the notion that Myc recruitment is impaired. Such conditions might be found in several human tumors that might be sensitive to the depletion of the PAF1 complex.

The loss of Max has a much stronger impact on the expression of Myc target genes meaning that the loss of the sequence-specific DNA binding partner is more severe for Myc (Figure 4.9). For this experiment eight day old Max^0 larvae were investigated in which essentially no Max transcripts were detected anymore by RNAseq. Eight days after egg deposition, there should be no Max protein left since the protein has a half-life of less than 10 hours (Steiger *et al.*, 2008). Myc overexpression in a Max^0 mutant background did not induce any specific targets to the same extent as in a Max wildtype background. Maybe Max is indeed needed for the chromatin-binding to all of Myc's targets. This could be explained by the postulated requirement of Max for the proper folding of Myc (Adhikary and Eilers, 2005). The Myc targets lacking an E-box motif are less affected by the loss of Max meaning that Myc retains some function in the absence of Max. So maybe Max does not contribute any specificity to these genes. Furthermore, the Myc ChIPseq in S2 cells showed that the binding of Myc to origins of replication is relatively insensitive to Max knockdown. This suggests a possible non-transcriptional function of Myc which is independent of Max.

5.2 Myc affects ecdysone synthesis and developmental transitions

5.2.1 Elevated Myc levels block pupariation by abolishing the ecdysone signal

Unexpectedly, a connection was found between the growth regulator Myc and the steroid hormone ecdysone, which controls developmental transitions. The co-overexpression of Myc and p35 in a Max^0 mutant background after the L3 molt leads to a pupariation block and this block can be rescued by feeding of 20-hydroxyecdysone (Steiger, 2007) (4.2.1 & 4.2.2). This observation suggests three possible scenarios how Myc could interfere with the ecdysone pathway: 1. upstream of the PG by influencing the signals that control ecdysone synthesis in the PG or 2. directly in the PG by affecting the biosynthetic machinery or 3. downstream of the PG in the target tissues in combination with 1. or 2.

The pupariation block caused by Myc overexpression can be rescued by ectopic ecdysone feeding, which argues against an effect of Myc downstream of the PG (hypothesis 3). Nevertheless, these animals probably have a defect in ecdysone production and this assumption was investigated by comparison of ecdysteroid levels from the different phenotypes. Unfortunately, a direct measurement of ecdysone titers from whole larvae extracts by mass spectrometry failed, probably due to insufficient sensitivity of the machine. In the future, such measurements will be attempted using ELISA or mass spectrometry with a more sensitive machine. Instead, the activity of 20E was measured indirectly by determining the mRNA levels of two direct 20E targets (*BR-C* and *Eip75B*) (see 1.4.1). Wildtype animals and Max^0 mutants show a strong increase of both transcripts right before pupariation whereas the expression levels stayed low in Max^0 + Myc animals (Figure 4.11). This indicates that ecdysone signaling is impaired in such animals. Afterwards the question was addressed whether Myc acts directly in the PG (hypothesis 2). The PG might be damaged by Myc overexpression resulting in absent ecdysone production. This speculation could not be confirmed because dissected PGs of mutants with ubiquitous Myc overexpression looked grossly normal. Even high overexpression of Myc directly in the PG (phm-GAL4) did not destroy the gland. The size and shape of these PGs is similar to control PGs of Max^0 mutants but the cell nuclei are enlarged. This might result from increased endoreplication as already described for Myc overexpression in fat body cells (Pierce *et al.*, 2004). In addition, the overexpression of Myc exclusively in the PG is not sufficient to block pupariation as shown with the different PG-specific GAL4 drivers. Also Myc overexpression everywhere but in the PG (using phm-GAL80) suggests that Myc is not even required in the PG for its effect on ecdysone (Table 4.2.1). Based on these results an effect of Myc directly in the PG (hypothesis 2) makes it highly unlikely.

Since the PG looked grossly normal, the levels of the ecdysone biosynthetic genes inside the PG were analyzed to find out why ecdysone production is missing. The Halloween genes are expressed at low levels during early and mid third instar but rise dramatically in late L3 larvae

shortly before pupariation. Such expression patterns were reported in different insect species (Danielsen *et al.*, 2014; Hentze *et al.*, 2013; Rewitz *et al.*, 2006a; Rewitz *et al.*, 2006b). In addition, the transcript levels of these genes were shown to correlate very well with the ecdysone titer in the hemolymph (Parvy *et al.*, 2005; Warren *et al.*, 2002; Warren *et al.*, 2006). Reduced transcript levels of the Halloween genes were found after depletion of various transcription factors (Danielsen *et al.*, 2014; Komura-Kawa *et al.*, 2015) and this correlated with decreased 20E levels measured by ELISA. Therefore, the expression of the Halloween genes can be used as an indirect readout for ecdysone levels. As expected, these genes are expressed at basal levels during early and mid L3 stage in Max^0 larvae and show a clear peak shortly before pupariation (Figure 4.11 D). In Max^0 + Myc larvae the expression peak of all Halloween genes is missing, confirming that Myc inhibits ecdysone production in these animals (Figure 4.11 D).

5.2.2 Signaling pathways affected by Myc overexpression

Myc overexpression was shown to affect ecdysone production, therefore the upstream signaling pathways, which regulated ecdysone synthesis in the PG, were analyzed (hypothesis 1). First of all, the mTOR pathway which showed decreased activity in control Max^0 mutants right before the onset of pupariation as reflected by the increased activity of the mTOR-repressed *unk*-reporter (Figure 4.12). Such a decrease of mTOR levels might be expected in late L3 larvae, since they stop feeding and might experience a situation resembling starvation. However, this is pure speculation since no data about mTOR activity during larval development have been published so far. In Max^0 + Myc larvae the levels of the mTOR reporter stayed similar during the investigated period, indicating that elevated Myc levels do not repress mTOR activity. A developmental decrease as observed in control larvae does not take place either. A possible explanation for the quite constant mTOR levels might be the unusual feeding behavior of Max^0 + Myc mutants. Normally, after the attainment of the critical weight, larvae stop feeding, wander around and prepare for pupariation. For Max^0 + Myc animals, it was noticed that they repeatedly leave the food for a while and come back to feed again. However, there are no reported data that altered mTOR activity has an influence on ecdysone production. Taken together, the mTOR pathway is probably not responsible for the observed pupariation block.

Second, the activity of the insulin pathway was monitored with the help of the tGPH construct. In Max^0 larvae shortly before pupariation the construct was predominantly located at the plasma membrane, indicating active insulin signaling (Figure 4.12). In Max^0 + Myc animals, tGPH was equally distributed between the cytoplasm and the membrane. Thus, Myc overexpression seems to inhibit insulin signaling in the PG, which may contribute to the observed defect in ecdysone synthesis. Furthermore, the *FOXO response element* (*FRE*)-*luc*

reporter could be used to assay the activity of FOXO and thereby of the insulin pathway. This reporter was previously shown to be a suitable tool to monitor the activity of the insulin pathway (Mirth *et al.*, 2014). Nevertheless, reduced activity of the insulin pathway alone is not sufficient to explain the developmental arrest observed after Myc overexpression. Animals experiencing reduced insulin signaling were described to prolong the larval stage and eclose as bigger flies, but metamorphosis was not completely prevented (Caldwell *et al.*, 2005; Colombani *et al.*, 2005; Mirth *et al.*, 2005).

Finally, to investigate the PTTH pathway, the transcript levels of the ligand PTTH were analyzed. Overexpression of Myc prevented the increase of PTTH transcripts which was observed in wildtype larvae and in Max^0 larvae (Figure 4.12). Hence, Myc overexpression is accompanied by a clear reduction of PTTH expression. Although PTTH is also not absolutely required for metamorphosis, a reduction of PTTH expression results in a delayed onset of metamorphosis and thereby bigger adult flies (Yamanaka *et al.*, 2013).

However, the loss of PTTH in combination with reduced insulin signaling might explain the defect in ecdysone production and the subsequent developmental arrest. A similar arrest was shown for larvae with a defect in the TGFβ / Activin pathway (Gibbens *et al.*, 2011). The knockdown of dSmad2, the sole downstream mediator of Activin signaling, resulted in reduced expression of the PTTH receptor Torso and the insulin receptor InR and eliminated the 20E peak. Reconstitution of either pathway rescued pupariation arguing that the pathways can partially substitute for each other (Gibbens *et al.*, 2011). Unfortunately, we did not have a tool to directly investigate the activity of the TGFβ / Activin pathway. The measurement of dSmad2 transcript level from whole larvae will not be helpful since dSmad2 is expressed in several tissues. However, dSmad2 levels in the PG could be measured by RNA in situ hybridization or by qRT-PCR of isolated PGs.

In addition, the overexpression of Myc was investigated in different tissues with specific GAL4 drivers that are active in neurons, fat body or wing discs (also hypothesis 1), but none of them produced the same phenotype as observed after ubiquitous expression (Table 4.2.1). Myc might need to be overexpressed in several tissues simultaneously to block pupariation.

For the different upstream pathways most of the descriptive analysis was performed during this thesis. This has identified the PTTH pathway as the main suspect and the insulin signaling pathway as an additional candidate. The next step would be a functional analysis to demonstrate that either or both of these pathways are responsible for the effect. This might involve the ectopic expression of PTTH in Max^0 + Myc larvae, or the activation of the PTTH-activated RTK signaling pathway in the PG of Max^0 + Myc larvae.

5.2.3   Molecular Myc targets that mediate the effect on ecdysone synthesis

For time reasons, we started to search for the molecular targets that mediate the Myc-dependent pupariation block in parallel to the genetic experiments discussed above. Normally, the tissue in which Myc does its harm would be identified first. Afterwards, this tissue would be isolated and used for the molecular analyses. However, the identification of the affected tissue is time consuming and has not been successful yet, therefore the molecular experiments were started in parallel using S2 cells, which are easily accessible in large quantities. Analyses of existing ChIPseq, RNAseq and electronic annotation data identified five genes that could potentially be controlled by Myc in a Max mutant background and play a role in ecdysis. The five candidate genes are *EcR*, *Eip75B*, *mld*, *Kr-h1* and *rpr* (see Results 4.2.5). ChIP experiments confirmed that all these genes are bound by a Myc mutant (MycΔZ, unable to bind Max) independently of Max. Furthermore, these genes were shown to be misregulated in Max^0 + Myc mutants (Figure 4.14). For the experiments the RNA from whole larvae was isolated and analyzed by qRT-PCR. Since all these genes are ubiquitously expressed, it was assumed that the transcript levels change in similar ways in all tissues. Nevertheless, it might be possible that an increase in a specific tissue (e.g. the PTTH neurons) is hidden by a general decrease in all other tissues. The fact that whole larvae were used for the analyses implies also that the effects of Myc were measured in a mixture of tissues (i. e. tissues that act upstream of the PG as well as tissues that act downstream of the PG). The reduced expression observed for *Kr-h1*, *Eip75*, *rpr* and *EcR* might result from tissues that react to ecdysone as discussed below. However, it is possible that Myc overexpression has a direct effect on their expression in tissues upstream of the PG. Unfortunately, the investigation of such differential effects is not possible as long as the organ in which Myc interferes with ecdysone is unknown.

In Max^0 mutants the expression of the transcription factor Kr-h1 is not increased shortly before pupariation. Since these animals pupariate normally it seems likely that Kr-h1 is not the factor which mediates the pupariation block of animals overexpressing Myc. The absence of induction of Kr-h1, Eip75B and rpr caused by Myc might be an indirect effect. Although Myc binds directly to these genes, here in this situation there might be another effect which is more important. These genes are normally induced by the binding of an ecdysone-EcR complex. Since Myc affects ecdysone production, this results in reduced gene expression. For the EcR a similar explanation is possible, because after ligand binding the EcR regulates its own expression (Gonsalves *et al.*, 2011). The most parsimonious explanation is an indirect effect of Myc mediated by reduced ecdysone synthesis. In contrast, the lack of *mld* induction seems to be a direct effect of Myc overexpression. It is possible that *mld* is partially responsible for the observed non-pupariating phenotype but it is probably not the only factor involved. *Mld* mutants have reduced ecdysone levels because of a lack of *spok* expression

(Neubueser *et al.*, 2005; Ono *et al.*, 2006). A reduction of *nvd*, *spok* and *sro* was shown after the depletion of *mld* in the PG, whereas the other Halloween genes were not affected (Danielsen *et al.*, 2014). In this study, the overexpression of Myc caused a reduction of all investigated Halloween genes (4.2.2). The experiments so far raise the possibility that *mld* is involved in mediating the effect of Myc overexpression on pupariation. The challenge for future work will be to prove this. This might involve the demonstration that depletion of *mld* can phenocopy the consequences of Myc overexpression, and/or the demonstration that ectopic expression of *mld* can overcome Myc's effect. Finally, it will be necessary to identify the tissue in which Myc interacts with *mld* to control the synthesis of ecdysone.

Myc ChIPseq of S2 cells after Max-KD was performed as another parallel approach to identify potentially Max-independent targets of Myc. Ideally, ChIPseq analyses of overexpressed Myc in the relevant tissue of Max mutant larvae would be carried out, but as mentioned above the relevant tissue is still not identified. Therefore, S2 cells were used again, as a substitute for the unknown tissue *in vivo,* where Max could also quantitatively be eliminated. A comparison with Myc ChIPseq from control cells still points to the Myc targets that might be regulated in the absence of Max (Figure 4.15).

First, the five candidate genes described above were analyzed revealing that Max knockdown strongly reduces Myc binding to all of them. This suggests that endogenous levels of Myc need Max for the binding to these genes and that Myc cannot regulate these genes in the absence of Max. Alternatively, the depletion of Max reduces Myc binding but does not eliminate it. This is because Myc is less stable in the absence of Max, not because Myc cannot bind to these targets in the absence of Max. However, if Myc is overexpressed to high enough levels, there will be enough Myc to regulate these targets. This would fit to the observation that HA:MycΔZ can bind to these genes and that Myc overexpression has a clear effect *in vivo* in Max^0 mutants (Figure 4.14). Second, the sequencing did not reveal any gene that is bound by endogenous Myc completely independently from Max, which indicates that Max knockdown affects the binding of endogenous Myc to all of its targets. It was supposed that Max might be required for the correct folding of the Myc protein which would be a potential explanation for this finding (Adhikary and Eilers, 2005). Furthermore, it is unknown if there are Myc targets that do require Max at physiological Myc levels but become partially independent of Max upon Myc overexpression as proposed for the five targets described above.

However, the binding sites of Myc show different sensitivities to Max knockdown and separate into two categories (Figure 4.15). Max depletion strongly reduced the binding of Myc in the first group and many E-box motifs were found among these binding sites. Almost all the promoters and enhancers fall into this group, and they cover the known Myc targets that

were identified by Herter *et al*. The binding sites of group 2 do not contain promoter regions and it is not clear which gene's expression they control, or whether they control any gene's expression at all. However, many of the binding sites in group 2 overlap with origins of replication (oris). Indeed, Myc has been proposed to have a transcription-independent effect on DNA replication (Dominguez-Sola *et al.*, 2007). The oris found in group 2 might mediate the effect of Myc on replication, which suggests that this potential role in replication is independent from Max. This is consistent with the observation that Myc overexpression results in larger PG cell nuclei in Max^0 mutant larvae, which is probably caused by enhanced endoreplication (Pierce *et al.*, 2004). At the moment it is not clear if a potential effect on replication is linked to the pupariation block caused by Myc overexpression.

Overexpression of MycΔZ in a Max wildtype background did not affect development or pupariation. Obviously the overexpression of Myc is not sufficient to provoke a developmental arrest in a wildtype background. The Max mutation contributes somehow to the pupariation block. Nevertheless, Myc overexpression is required for this effect in the absence of Max and overexpression of MycΔZ blocks pupariation with the same efficiency as MycWT (Figure. 4.13). This confirms that the MycΔZ protein is functional. However, MycΔZ affects pupariation only in a Max mutant background, not in a wildtype background, although MycΔZ cannot bind to Max in either situation. Together these findings strongly argue that Myc overexpression does not block pupariation through binding to some residual Max protein since MycΔZ does not bind to Max. Furthermore, the leuzine zipper is not needed for the pupariation block. This excludes the possibility that Myc interacts with any other protein through this binding site and thereby mediates the effect. Finally, this raises the question how the Max mutation contributes to this phenotype. It is possible that the reduced growth rate and the delayed development are necessary for this. We tried to mimick this with *Minute* mutants, which show a prolonged larval development (Morata and Ripoll, 1974), but even in this background the overexpression MycΔZ did not block pupariation. It might be that the developmental delay of these Minute mutants was not strong enough. However, it is assumed that the loss of Max predisposes the larvae to a Myc-induced pupariation block by some other way, but it is unknown how.

5.2.4 Hypoxia – a natural condition for Max-independent Myc functions?

Our data demonstrate that Myc overexpression has an influence on ecdysone activity in Max[0] mutants. At the moment it is not clear whether such a situation ever occurs during normal development, and if so, under which condition. Various situations were described which lead to increased Myc expression, for example tissue damage (Gallant, 2013), but conditions that cause the elimination of Max were not known. Recently, a publication showed that Max protein levels were reduced in human endothelial cells (HUVECs) after hypoxia treatment (Kemmerer and Weigand, 2014). Alternative splicing produced two *Max* mRNA isoforms during hypoxia in addition to the main form and both of these forms showed increased expression in this situation. One isoform encodes a stop codon and is therefore degraded by nonsense-mediated decay. The other isoform encodes a highly unstable protein with a very short half-life. Since both mRNA isoforms are unproductive in terms of protein expression, Kemmerer *et al*. proposed that the RNA splicing events solely serve the reduction of wildtype Max protein. In addition, a recent publication proposed that hypoxia inhibits ecdysone secretion of isolated PGs (DeLalio *et al.*, 2015). This raises the possibility that hypoxia in *Drosophila* larvae reduces Max protein levels. Furthermore, Myc protein levels might also be increased in such a situation, in part by the loss of autorepression (Goodliffe *et al.*, 2005; Steiger *et al.*, 2008). Both effects together might then reduce ecdysone synthesis and delay pupariation.

A preliminary experiment was carried out in S2 cells but did not shown any reduction of Max mRNA levels after hypoxia treatment. These connections need to be further investigated. Max transcript levels were analyzed assuming that hypoxia functions in the same way in HUVEC cells and in S2 cells. However, it is possible that hypoxia affects the protein levels of Max in both cell lines but uses different mechanisms, alternative splicing in HUVEC cells and maybe protein destabilization in S2 cells. Of couse it is also possible that hypoxia does not affect Max levels at all in S2 cells.

6 References

Adelman, K., Wei, W., Ardehali, M.B., Werner, J., Zhu, B., Reinberg, D., and Lis, J.T. (2006). Drosophila Paf1 modulates chromatin structure at actively transcribed genes. Molecular and cellular biology *26*, 250-260.

Adhikary, S., and Eilers, M. (2005). Transcriptional regulation and transformation by MYC proteins. Nat Rev Mol Cell Bio *6*, 635-645.

Arnold, C.D., Gerlach, D., Stelzer, C., Boryn, L.M., Rath, M., and Stark, A. (2013). Genome-Wide Quantitative Enhancer Activity Maps Identified by STARR-seq. Science *339*, 1074-1077.

Ayer, D.E., Kretzner, L., and Eisenman, R.N. (1993). Mad - a Heterodimeric Partner for Max That Antagonizes Myc Transcriptional Activity. Cell *72*, 211-222.

Bahrampour, S., and Thor, S. (2016). Ctr9, a Key Component of the Paf1 Complex, Affects Proliferation and Terminal Differentiation in the Developing Drosophila Nervous System. G3-Genes Genom Genet *6*, 3229-3239.

Benassayag, C., Montero, L., Colombie, N., Gallant, P., Cribbs, D., and Morello, D. (2005). Human c-Myc isoforms differentially regulate cell growth and apoptosis in Drosophila melanogaster. Molecular and cellular biology *25*, 9897-9909.

Blackwell, T.K., Huang, J., Ma, A., Kretzner, L., Alt, F.W., Eisenman, R.N., and Weintraub, H. (1993). Binding of Myc Proteins to Canonical and Noncanonical DNA-Sequences. Molecular and cellular biology *13*, 5216-5224.

Blackwell, T.K., Kretzner, L., Blackwood, E.M., Eisenman, R.N., and Weintraub, H. (1990). Sequence-Specific DNA-Binding by the C-Myc Protein. Science *250*, 1149-1151.

Blackwood, E.M., and Eisenman, R.N. (1991). Max - a Helix-Loop-Helix Zipper Protein That Forms a Sequence-Specific DNA-Binding Complex with Myc. Science *251*, 1211-1217.

Bonke, M., Turunen, M., Sokolova, M., Vaharautio, A., Kivioja, T., Taipale, M., Bjorklund, M., and Taipale, J. (2013). Transcriptional Networks Controlling the Cell Cycle. G3-Genes Genom Genet *3*, 75-90.

Bouchard, C., Dittrich, O., Kiermaier, A., Dohmann, K., Menkel, A., Eilers, M., and Luscher, B. (2001). Regulation of cyclin D2 gene expression by the Myc/Max/Mad network: Myc-dependent TRRAP recruitment and histone acetylation at the cyclin D2 promoter. Genes & development *15*, 2042-2047.

Bradford, M.M. (1976). A rapid and sensitive method for the quantitation of microgram quantities of protein utilizing the principle of protein-dye binding. Analytical biochemistry *72*, 248-254.

Bridges, C.B. (1935). Drosophila melanogaster: Legend for symbols, mutants, valuations. Drosophila Information Service *3*, 5-19.

Britton, J.S., Lockwood, W.K., Li, L., Cohen, S.M., and Edgar, B.A. (2002). Drosophila's insulin/P13-kinase pathway coordinates cellular metabolism with nutritional conditions. Developmental cell *2*, 239-249.

Caldwell, P.E., Walkiewicz, M., and Stern, M. (2005). Ras activity in the Drosophila prothoracic gland regulates body size and developmental rate via ecdysone release (vol 15, pg 1785, 2005). Current Biology *15*, 2175-2175.

Chen, F.X., Woodfin, A.R., Gardini, A., Rickels, R.A., Marshall, S.A., Smith, E.R., Shiekhattar, R., and Shilatifard, A. (2015). PAF1, a Molecular Regulator of Promoter-Proximal Pausing by RNA Polymerase II. Cell *162*, 1003-1015.

Chu, X.L., Qin, X.H., Xu, H.S., Li, L., Wang, Z., Li, F.Z., Xie, X.Q., Zhou, H., Shen, Y.Q., and Long, J.F. (2013). Structural insights into Paf1 complex assembly and histone binding. Nucleic Acids Res *41*, 10619-10629.

Colombani, J., Andersen, D.S., and Leopold, P. (2012). Secreted Peptide Dilp8 Coordinates Drosophila Tissue Growth with Developmental Timing. Science *336*, 582-585.

Colombani, J., Bianchini, L., Layalle, S., Pondeville, E., Dauphin-Villemant, C., Antoniewski, C., Carre, C., Noselli, S., and Leopold, P. (2005). Antagonistic actions of ecdysone and insulins determine final size in Drosophila. Science *310*, 667-670.

Conacci-Sorrell, M., Ngouenet, C., and Eisenman, R.N. (2010). Myc-Nick: A Cytoplasmic Cleavage Product of Myc that Promotes alpha-Tubulin Acetylation and Cell Differentiation. Cell *142*, 480-493.

Cowling, V.H., Chandriani, S., Whitfield, M.L., and Cole, M.D. (2006). A conserved Myc protein domain, MBIV, regulates DNA binding, apoptosis, transformation, and G(2) arrest (vol 26, 4226, 2006). Molecular and cellular biology *26*, 5201-5201.

Crisucci, E.M., and Arndt, K.M. (2012). Paf1 Restricts Gcn4 Occupancy and Antisense Transcription at the ARG1 Promoter. Molecular and cellular biology *32*, 1150-1163.

Dan, H.C., Sun, M., Yang, L., Feldman, R.I., Sui, X.M., Ou, C.C., Nellist, M., Yeung, R.S., Halley, D.J.J., Nicosia, S.V.*, et al.* (2002). Phosphatidylinositol 3-kinase/Akt pathway regulates tuberous sclerosis tumor suppressor complex by phosphorylation of tuberin. Journal of Biological Chemistry *277*, 35364-35370.

Dang, C.V. (2013). MYC, metabolism, cell growth, and tumorigenesis. Cold Spring Harbor perspectives in medicine *3*.

Dang, C.V., Barrett, J., Villagarcia, M., Resar, L.M.S., Kato, G.J., and Fearon, E.R. (1991). Intracellular Leucine Zipper Interactions Suggest C-Myc Hetero-Oligomerization. Molecular and cellular biology *11*, 954-962.

Danielsen, E.T., Moeller, M.E., Dorry, E., Komura-Kawa, T., Fujimoto, Y., Troelsen, J.T., Herder, R., O'Connor, M.B., Niwa, R., and Rewitz, K.F. (2014). Transcriptional control of steroid biosynthesis genes in the Drosophila prothoracic gland by ventral veins lacking and knirps. PLoS genetics *10*, e1004343.

Davis, A.C., Wims, M., Spotts, G.D., Hann, S.R., and Bradley, A. (1993). A Null C-Myc Mutation Causes Lethality before 10.5 Days of Gestation in Homozygotes and Reduced Fertility in Heterozygous Female Mice. Genes & development *7*, 671-682.

de la Cova, C., Abril, M., Bellosta, P., Gallant, P., and Johnston, L.A. (2004). Drosophila myc regulates organ size by inducing cell competition. Cell *117*, 107-116.

DeLalio, L.J., Dion, S.M., Bootes, A.M., and Smith, W.A. (2015). Direct effects of hypoxia and nitric oxide on ecdysone secretion by insect prothoracic glands. Journal of insect physiology *76*, 56-66.

Delanoue, R., Slaidina, M., and Leopold, P. (2010). The Steroid Hormone Ecdysone Controls Systemic Growth by Repressing dMyc Function in Drosophila Fat Cells. Developmental cell *18*, 1012-1021.

Dermody, J.L., and Buratowski, S. (2010). Leo1 Subunit of the Yeast Paf1 Complex Binds RNA and Contributes to Complex Recruitment. Journal of Biological Chemistry *285*, 33671-33679.

Dominguez-Sola, D., Ying, C.Y., Grandori, C., Ruggiero, L., Chen, B., Li, M.Y., Galloway, D.A., Gu, W., Gautier, J., and Dalla-Favera, R. (2007). Non-transcriptional control of DNA replication by c-Myc. Nature *448*, 445-U443.

Eilers, M., and Eisenman, R.N. (2008). Myc's broad reach. Genes & development *22*, 2755-2766.

Frank, S.R., Parisi, T., Taubert, S., Fernandez, P., Fuchs, M., Chan, H.M., Livingston, D.M., and Amati, B. (2003). MYC recruits the TIP60 histone acetyltransferase complex to chromatin. Embo Rep *4*, 575-580.

Furrer, M. (2008). Characterization of novel cofactors in Myc-dependent transcription regulation. In Mathematisch-naturwissenschaftliche Fakultät (Zürich: Universität Zürich), pp. 146.

Furrer, M., Balbi, M., Albarca-Aguilera, M., Gallant, M., Herr, W., and Gallant, P. (2010). Drosophila Myc interacts with host cell factor (dHCF) to activate transcription and control growth. The Journal of biological chemistry *285*, 39623-39636.

Gallant, P. (2009). Drosophila Myc. Advances in cancer research *103*, 111-144.

Gallant, P. (2013). Myc function in Drosophila. Cold Spring Harbor perspectives in medicine *3*, a014324.

Gallant, P., Shiio, Y., Cheng, P.F., Parkhurst, S.M., and Eisenman, R.N. (1996). Myc and Max homologs in Drosophila. Science *274*, 1523-1527.

Garelli, A., Gontijo, A.M., Miguela, V., Caparros, E., and Dominguez, M. (2012). Imaginal Discs Secrete Insulin-Like Peptide 8 to Mediate Plasticity of Growth and Maturation. Science *336*, 579-582.

Garen, A., Kauvar, L., and Lepesant, J.A. (1977). Roles of Ecdysone in Drosophila Development. Proceedings of the National Academy of Sciences of the United States of America *74*, 5099-5103.

Gargano, B., Amente, S., Majello, B., and Lania, L. (2007). P-TEFb is a crucial co-factor for Myc transactivation. Cell cycle *6*, 2031-2037.

Geminard, C., Rulifson, E.J., and Leopold, P. (2009). Remote Control of Insulin Secretion by Fat Cells in Drosophila. Cell metabolism *10*, 199-207.

Gibbens, Y.Y., Warren, J.T., Gilbert, L.I., and O'Connor, M.B. (2011). Neuroendocrine regulation of Drosophila metamorphosis requires TGFbeta/Activin signaling. Development *138*, 2693-2703.

Gilbert, L.I. (2004). Halloween genes encode P450 enzymes that mediate steroid hormone biosynthesis in Drosophila melanogaster. Mol Cell Endocrinol *215*, 1-10.

Gilbert, L.I., Rybczynski, R., and Warren, J.T. (2002). Control and biochemical nature of the ecdysteroidogenic pathway. Annual review of entomology *47*, 883-916.

Gonsalves, S.E., Neal, S.J., Kehoe, A.S., and Westwood, J.T. (2011). Genome-wide examination of the transcriptional response to ecdysteroids 20-hydroxyecdysone and ponasterone A in Drosophila melanogaster. Bmc Genomics *12*.

Goodliffe, J.M., Wieschaus, E., and Cole, M.D. (2005). Polycomb mediates Myc autorepression and its transcriptional control of many loci in Drosophila. Genes & development *19*, 2941-2946.

Grewal, S.S., Li, L., Orian, A., Eisenman, R.N., and Edgar, B.A. (2005). Myc-dependent regulation of ribosomal RNA synthesis during Drosophila development. Nat Cell Biol *7*, 295-U109.

Gronke, S., Clarke, D.F., Broughton, S., Andrews, T.D., and Partridge, L. (2010). Molecular evolution and functional characterization of Drosophila insulin-like peptides. PLoS genetics *6*, e1000857.

Guccione, E., Martinato, F., Finocchiaro, G., Luzi, L., Tizzoni, L., Dall'Olio, V., Zardo, G., Nervi, C., Bernard, L., and Amati, B. (2006). Myc-binding-site recognition in the human genome is determined by chromatin context. Nat Cell Biol *8*, 764-U225.

Guo, J.N., Li, T.D., Schipper, J., Nilson, K.A., Fordjour, F.K., Cooper, J.J., Gordan, R., and Price, D.H. (2014). Sequence specificity incompletely defines the genome-wide occupancy of Myc. Genome biology *15*.

Hann, S.R. (2014). MYC Cofactors: Molecular Switches Controlling Diverse Biological Outcomes. Cold Spring Harbor perspectives in medicine *4*.

Hentze, J.L., Moeller, M.E., Jorgensen, A.F., Bengtsson, M.S., Bordoy, A.M., Warren, J.T., Gilbert, L.I., Andersen, O., and Rewitz, K.F. (2013). Accessory Gland as a Site for Prothoracicotropic Hormone Controlled Ecdysone Synthesis in Adult Male Insects. Plos One *8*.

Herbst, A., Hemann, M.T., Tworkowski, K.A., Salghetti, S.E., Lowe, S.W., and Tansey, W.P. (2005). A conserved element in Myc that negatively regulates its proapoptotic activity. Embo Rep *6*, 177-183.

Herbst, A., Salghetti, S.E., Kim, S.Y., and Tansey, W.P. (2004). Multiple cell-type-specific elements regulate Myc protein stability. Oncogene *23*, 3863-3871.

Herter, E.K., Stauch, M., Gallant, M., Wolf, E., Raabe, T., and Gallant, P. (2015). snoRNAs are a novel class of biologically relevant Myc targets. BMC biology *13*, 25.

Hill, R.J., Billas, I.M.L., Bonneton, F., Graham, L.D., and Lawrence, M.C. (2013). Ecdysone Receptors: From the Ashburner Model to Structural Biology. Annual Review of Entomology, Vol 58 *58*, 251-+.

Hulf, T., Bellosta, P., Furrer, M., Steiger, D., Svensson, D., Barbour, A., and Gallant, P. (2005). Whole-genome analysis reveals a strong positional bias of conserved dMyc-dependent E-boxes. Molecular and cellular biology *25*, 3401-3410.

Hurlin, P.J., Queva, C., and Eisenman, R.N. (1997). Mnt: A novel max-interacting protein and myc antagonist. Curr Top Microbiol *224*, 115-121.

Hurlin, P.J., Queva, C., Koskinen, P.J., Steingrimsson, E., Ayer, D.E., Copeland, N.G., Jenkins, N.A., and Eisenman, R.N. (1995). Mad3 and Mad4 - Novel Max-Interacting Transcriptional Repressors That Suppress C-Myc Dependent Transformation and Are Expressed during Neural and Epidermal Differentiation. Embo Journal *14*, 5646-5659.

Hurlin, P.J., Steingrimsson, E., Copeland, N.G., Jenkins, N.A., and Eisenman, R.N. (1999). Mga, a dual-specificity transcription factor that interacts with Max and contains a T-domain DNA-binding motif. Embo Journal *18*, 7019-7028.

Ikeya, T., Galic, M., Belawat, P., Nairz, K., and Hafen, E. (2002). Nutrient-dependent expression of insulin-like peptides from neuroendocrine cells in the CNS contributes to growth regulation in Drosophila. Current Biology *12*, 1293-1300.

Ingvarsson, S., Asker, C., Axelson, H., Klein, G., and Sumegi, J. (1988). Structure and Expression of B-Myc, a New Member of the Myc Gene Family. Molecular and cellular biology *8*, 3168-3174.

Jaehning, J.A. (2010). The Paf1 complex: platform or player in RNA polymerase II transcription? Biochimica et biophysica acta *1799*, 379-388.

Jaenicke, L.A., von Eyss, B., Carstensen, A., Wolf, E., Xu, W., Greifenberg, A.K., Geyer, M., Eilers, M., and Popov, N. (2016). Ubiquitin-Dependent Turnover of MYC Antagonizes MYC/PAF1C Complex Accumulation to Drive Transcriptional Elongation. Molecular cell *61*, 54-67.

Jiang, C., Lamblin, A.F., Steller, H., and Thummel, C.S. (2000). A steroid-triggered transcriptional hierarchy controls salivary gland cell death during Drosophila metamorphosis. Molecular cell *5*, 445-455.

Johnston, L.A., Prober, D.A., Edgar, B.A., Eisenman, R.N., and Gallant, P. (1999). Drosophila myc regulates cellular growth during development. Cell *98*, 779-790.

Kemmerer, K., and Weigand, J.E. (2014). Hypoxia reduces MAX expression in endothelial cells by unproductive splicing. FEBS letters *588*, 4784-4790.

Kiessling, A., Sperl, B., Hollis, A., Eick, D., and Berg, T. (2006). Selective inhibition of c-Myc/Max dimerization and DNA binding by small molecules. Chem Biol *13*, 745-751.

Kim, J., Guermah, M., and Roeder, R.G. (2010). The human PAF1 complex acts in chromatin transcription elongation both independently and cooperatively with SII/TFIIS. Cell *140*, 491-503.

Kluding, C.N.-V.E.W.H. (1984). Mutations affecting the pattern of the larval cuticle in Drosophila melanogaster. Roux's Archives of Developmental Biology *193*, 267-282.

Kohl, N.E., Kanda, N., Schreck, R.R., Bruns, G., Latt, S.A., Gilbert, F., and Alt, F.W. (1983). Transposition and Amplification of Oncogene-Related Sequences in Human Neuroblastomas. Cell *35*, 359-367.

Komura-Kawa, T., Hirota, K., Shimada-Niwa, Y., Yamauchi, R., Shimell, M., Shinoda, T., Fukamizu, A., O'Connor, M.B., and Niwa, R. (2015). The Drosophila Zinc Finger Transcription Factor Ouija Board Controls Ecdysteroid Biosynthesis through Specific Regulation of spookier. PLoS genetics *11*.

Kretzner, L., Blackwood, E.M., and Eisenman, R.N. (1992). Myc and Max Proteins Possess Distinct Transcriptional Activities. Nature *359*, 426-429.

Kurland, J.F., and Tansey, W.P. (2008). Myc-mediated transcriptional repression by recruitment of histone deacetylase. Cancer Res *68*, 3624-3629.

Layalle, S., Arquier, N., and Leopold, P. (2008). The TOR Pathway Couples Nutrition and Developmental Timing in Drosophila. Developmental cell *15*, 568-577.

Li, H., Handsaker, B., Wysoker, A., Fennell, T., Ruan, J., Homer, N., Marth, G., Abecasis, G., Durbin, R., and Genome Project Data Processing, S. (2009). The Sequence Alignment/Map format and SAMtools. Bioinformatics *25*, 2078-2079.

Lin, C.Y., Loven, J., Rahl, P.B., Paranal, R.M., Burge, C.B., Bradner, J.E., Lee, T.I., and Young, R.A. (2012). Transcriptional Amplification in Tumor Cells with Elevated c-Myc. Cell *151*, 56-67.

Loo, L.W.M., Secombe, J., Little, J.T., Carlos, L.S., Yost, C., Cheng, P.F., Flynn, E.A., Edgar, B.A., and Eisenman, R.N. (2005). The transcriptional repressor dMnt is a regulator of growth in Drosophila melanogaster. Molecular and cellular biology *25*, 7078-7091.

Lorenzin, F., Benary, U., Baluapuri, A., Walz, S., Jung, L.A., von Eyss, B., Kisker, C., Wolf, J., Eliers, M., and Wolf, E. (2016). Different promoter affinities account for specificity in MYC-dependent gene regulation. eLife *5*.

Luo, J.N., Lushchak, O.V., Goergen, P., Williams, M.J., and Nassel, D.R. (2014). Drosophila Insulin-Producing Cells Are Differentially Modulated by Serotonin and Octopamine Receptors and Affect Social Behavior. Plos One *9*.

Luscher, B., and Vervoorts, J. (2012). Regulation of gene transcription by the oncoprotein MYC. Gene *494*, 145-160.

Mahani, A., Henriksson, J., and Wright, A.P.H. (2013). Origins of Myc Proteins - Using Intrinsic Protein Disorder to Trace Distant Relatives. Plos One *8*.

Manning, B.D., Tee, A.R., Logsdon, M.N., Blenis, J., and Cantley, L.C. (2002). Identification of the tuberous sclerosis complex-2 tumor suppressor gene product tuberin as a target of the phosphoinositide 3-Kinase/Akt pathway. Molecular cell *10*, 151-162.

Mao, D.Y.L., Watson, J.D., Yan, P.S., Barsyte-Lovejoy, D., Khosravi, F., Wong, W.W.L., Farnham, P.J., Huang, T.H.M., and Penn, L.Z. (2003). Analysis of Myc bound loci identified by CpG island arrays shows that Max is essential for Myc-dependent repression. Current Biology *13*, 882-886.

McBrayer, Z., Ono, H., Shimell, M., Parvy, J.P., Beckstead, R.B., Warren, J.T., Thummel, C.S., Dauphin-Villement, C., Gilbert, L.I., and O'Connor, M.B. (2007). Prothoracicotropic hormone regulates developmental timing and body size in Drosophila. Developmental cell *13*, 857-871.

McDuff, F.O., Naud, J.F., Montagne, M., Sauve, S., and Lavigne, P. (2009). The Max homodimeric b-HLH-LZ significantly interferes with the specific heterodimerization between the c-Myc and Max b-HLH-LZ in absence of DNA: a quantitative analysis. J Mol Recognit *22*, 261-269.

McMahon, S.B., Van Buskirk, H.A., Dugan, K.A., Copeland, T.D., and Cole, M.D. (1998). The novel ATM-related protein TRRAP is an essential cofactor for the c-Myc and E2F oncoproteins. Cell *94*, 363-374.

McMahon, S.B., Wood, M.A., and Cole, M.D. (2000). The essential cofactor TRRAP recruits the histone acetyltransferase hGCN5 to c-Myc. Molecular and cellular biology *20*, 556-562.

Mirth, C., Truman, J.W., and Riddiford, L.M. (2005). The role of the prothoracic gland in determining critical weight for metamorphosis in Drosophila melanogaster. Current biology : CB *15*, 1796-1807.

Mirth, C.K., Tang, H.Y., Makohon-Moore, S.C., Salhadar, S., Gokhale, R.H., Warner, R.D., Koyama, T., Riddiford, L.M., and Shingleton, A.W. (2014). Juvenile hormone regulates body size and perturbs insulin signaling in Drosophila. Proceedings of the National Academy of Sciences of the United States of America *111*, 7018-7023.

Montero, L., Muller, N., and Gallant, P. (2008). Induction of apoptosis by Drosophila Myc. Genesis *46*, 104-111.

Morata, G., and Ripoll, P. (1974). Minutes: Mutants of Drosophila Autonomously Affecting Cell Division Rate. Developmental biology *42*, 211-221.

Mosimann, C., Hausmann, G., and Basler, K. (2006). Parafibromin/Hyrax activates Wnt/Wg target gene transcription by direct association with beta-catenin/Armadillo. Cell *125*, 327-341.

Mullis, K., Faloona, F., Scharf, S., Saiki, R., Horn, G., and Erlich, H. (1986). Specific enzymatic amplification of DNA in vitro: the polymerase chain reaction. Cold Spring Harbor symposia on quantitative biology *51 Pt 1*, 263-273.

Nakaoka, T., Iga, M., Yamada, T., Koujima, I., Takeshima, M., Zhou, X.Y., Suzuki, Y., Ogihara, M.H., and Kataoka, H. (2017). Deep sequencing of the prothoracic gland transcriptome reveals new players in insect ecdysteroidogenesis. Plos One *12*.

Nau, M.M., Brooks, B.J., Battey, J., Sausville, E., Gazdar, A.F., Kirsch, I.R., Mcbride, O.W., Bertness, V., Hollis, G.F., and Minna, J.D. (1985). L-Myc, a New Myc-Related Gene Amplified and Expressed in Human Small Cell Lung-Cancer. Nature *318*, 69-73.

Neubueser, D., Warren, J.T., Gilbert, L.I., and Cohen, S.M. (2005). molting defective is required for ecdysone biosynthesis. Developmental biology *280*, 362-372.

Nie, Z.Q., Hu, G.Q., Wei, G., Cui, K.R., Yamane, A., Resch, W., Wang, R.N., Green, D.R., Tessarollo, L., Casellas, R.*, et al.* (2012). c-Myc Is a Universal Amplifier of Expressed Genes in Lymphocytes and Embryonic Stem Cells. Cell *151*, 68-79.

Niwa, Y.S., and Niwa, R. (2014). Neural control of steroid hormone biosynthesis during development in the fruit fly Drosophila melanogaster. Genes Genet Syst *89*, 27-34.

Ono, H., Rewitz, K.F., Shinoda, T., Itoyama, K., Petryk, A., Rybczynski, R., Jarcho, M., Warren, J.T., Marques, G., Shimell, M.J.*, et al.* (2006). Spook and Spookier code for stage-specific components of the ecdysone biosynthetic pathway in Diptera. Developmental biology *298*, 555-570.

Orian, A., van Steensel, B., Delrow, J., Bussemaker, H.J., Li, L., Sawado, T., Williams, E., Loo, L.W.M., Cowley, S.M., Yost, C.*, et al.* (2003). Genomic bindin by the Drosophila Myc, Max, Mad/Mnt transcription factor network. Genes & development *17*, 1101-1114.

Parvy, J.P., Blais, C., Bernard, F., Warren, J.T., Petryk, A., Gilbert, L.I., O'Connor, M.B., and Dauphin-Villemant, C. (2005). A role for beta FTZ-F1 in regulating ecdysteroid titers during post-embryonic development in Drosophila melanogaster. Developmental biology *282*, 84-94.

Parvy, J.P., Wang, P., Garrido, D., Maria, A., Blais, C., Poidevin, M., and Montagne, J. (2014). Forward and feedback regulation of cyclic steroid production in Drosophila melanogaster. Development *141*, 3955-3965.

Pecasse, F., Beck, Y., Ruiz, C., and Richards, G. (2000). Kruppel-homolog, a stage-specific modulator of the prepupal ecdysone response, is essential for Drosophila metamorphosis. Developmental biology *221*, 53-67.

Petryk, A., Warren, J.T., Marques, G., Jarcho, M.P., Gilbert, L.I., Kahler, J., Parvy, J.P., Li, Y.T., Dauphin-Villemant, C., and O'Connor, M.B. (2003). Shade is the Drosophila P450 enzyme that mediates the hydroxylation of ecdysone to the steroid insect molting hormone 20-hydroxyecdysone. Proceedings of the National Academy of Sciences of the United States of America *100*, 13773-13778.

Peukert, K., Staller, P., Schneider, A., Carmichael, G., Hanel, F., and Eilers, M. (1997). An alternative pathway for gene regulation by Myc. Embo Journal *16*, 5672-5686.

Pierce, S.B., Yost, C., Anderson, S.A.R., Flynn, E.M., Delrow, J., and Eisenman, R.N. (2008). Drosophila growth and development in the absence of dMyc and dMnt. Developmental biology *315*, 303-316.

Pierce, S.B., Yost, C., Britton, J.S., Loo, L.W., Flynn, E.M., Edgar, B.A., and Eisenman, R.N. (2004). dMyc is required for larval growth and endoreplication in Drosophila. Development *131*, 2317-2327.

Qiu, H.F., Hu, C.H., Wong, C.M., and Hinnebusch, A.G. (2006). The Spt4p subunit of yeast DSIF stimulates association of the Paf1 complex with elongating RNA polymerase II. Molecular and cellular biology *26*, 3135-3148.

Quinlan, A.R., and Hall, I.M. (2010). BEDTools: a flexible suite of utilities for comparing genomic features. Bioinformatics *26*, 841-842.

Rahl, P.B., Lin, C.Y., Seila, A.C., Flynn, R.A., McCuine, S., Burge, C.B., Sharp, P.A., and Young, R.A. (2010). c-Myc Regulates Transcriptional Pause Release. Cell *141*, 432-445.

Rajan, A., and Perrimon, N. (2012). Drosophila Cytokine Unpaired 2 Regulates Physiological Homeostasis by Remotely Controlling Insulin Secretion. Cell *151*, 123-137.

Rewitz, K.F., Rybczynski, R., Warren, J.T., and Gilbert, L.I. (2006a). The Halloween genes code for cytochrome P450 enzymes mediating synthesis of the insect moulting hormone. Biochem Soc T *34*, 1256-1260.

Rewitz, K.F., Rybczynski, R., Warren, J.T., and Gilbert, L.I. (2006b). Identification, characterization and developmental expression of Halloween genes encoding P450 enzymes mediating ecdysone biosynthesis in the tobacco hornworm, Manduca sexta. Insect Biochem Molec *36*, 188-199.

Rewitz, K.F., Yamanaka, N., Gilbert, L.I., and O'Connor, M.B. (2009). The Insect Neuropeptide PTTH Activates Receptor Tyrosine Kinase Torso to Initiate Metamorphosis. Science *326*, 1403-1405.

Riddiford, L.M. (1993). Hormone Receptors and the Regulation of Insect Metamorphosis. Receptor *3*, 203-209.

Sabo, A., Kress, T.R., Pelizzola, M., de Pretis, S., Gorski, M.M., Tesi, A., Morelli, M.J., Bora, P., Doni, M., Verrecchia, A.*, et al.* (2014). Selective transcriptional regulation by Myc in cellular growth control and lymphomagenesis. Nature *511*, 488-+.

Schneider, I. (1972). Cell lines derived from late embryonic stages of Drosophila melanogaster. Journal of embryology and experimental morphology *27*, 353-365.

Schreiber-Agus, N., Stein, D., Chen, K., Goltz, J.S., Stevens, L., and DePinho, R.A. (1997). Drosophila Myc is oncogenic in mammalian cells and plays a role in the diminutive phenotype. Proceedings of the National Academy of Sciences of the United States of America *94*, 1235-1240.

Schwinkendorf, D., and Gallant, P. (2009). The conserved Myc box 2 and Myc box 3 regions are important, but not essential, for Myc function in vivo. Gene *436*, 90-100.

Sheiness, D., Fanshier, L., and Bishop, J.M. (1978). Identification of Nucleotide-Sequences Which May Encode Oncogenic Capacity of Avian Retrovirus Mc29. J Virol *28*, 600-610.

Shi, X.M., Finkelstein, A., Wolf, A.J., Wade, P.A., Burton, Z.F., and Jaehning, J.A. (1996). Paf1p, an RNA polymerase II-associated factor in Saccharomyces cerevisiae, may have both positive and negative roles in transcription. Molecular and cellular biology *16*, 669-676.

Spradling, A.C., Stern, D., Beaton, A., Rhem, E.J., Laverty, T., Mozden, N., Misra, S., and Rubin, G.M. (1999). The Berkeley Drosophila Genome Project gene disruption project: Single P-element insertions mutating 25% of vital drosophila genes. Genetics *153*, 135-177.

Squazzo, S.L., Costa, P.J., Lindstrom, D.L., Kumer, K.E., Simic, R., Jennings, J.L., Link, A.J., Arndt, K.M., and Hartzog, G.A. (2002). The Paf1 complex physically and functionally associates with transcription elongation factors in vivo. The EMBO journal *21*, 1764-1774.

Steiger, D. (2007). Analysis of the Max Network in Drosophila (Zuerich: University of Zuerich), pp. 173.

Steiger, D., Furrer, M., Schwinkendorf, D., and Gallant, P. (2008). Max-independent functions of Myc in Drosophila melanogaster. Nature genetics *40*, 1084-1091.

Sugiyama, A., Kume, A., Nemoto, K., Lee, S.Y., Asami, Y., Nemoto, F., Nishimura, S., and Kuchino, Y. (1989). Isolation and Characterization of S-Myc, a Member of the Rat Myc Gene Family. Proceedings of the National Academy of Sciences of the United States of America *86*, 9144-9148.

Tenney, K., Gerber, M., Ilvarsonn, A., Schneider, J., Gause, M., Dorsettt, D., Eissenberg, J.C., and Shilatifard, A. (2006). Drosophila Rtf1 functions in histone methylation, gene expression, and Notch signaling. Proceedings of the National Academy of Sciences of the United States of America *103*, 11970-11974.

Thomas, L.R., Wang, Q., Grieb, B.C., Phan, J., Foshage, A.M., Sun, Q., Olejniczak, E.T., Clark, T., Dey, S., Lorey, S.*, et al.* (2015). Interaction with WDR5 promotes target gene recognition and tumorigenesis by MYC. Molecular cell *58*, 440-452.

Tiebe, M., Lutz, M., De La Garza, A., Buechling, T., Boutros, M., and Teleman, A.A. (2015). REPTOR and REPTOR-BP Regulate Organismal Metabolism and Transcription Downstream of TORC1. Developmental cell *33*, 272-284.

Tomson, B.N., and Arndt, K.M. (2013). The many roles of the conserved eukaryotic Paf1 complex in regulating transcription, histone modifications, and disease states. Bba-Gene Regul Mech *1829*, 116-126.

Trumpp, A., Refaeli, Y., Oskarsson, T., Gasser, S., Murphy, M., Martin, G.R., and Bishop, J.M. (2001). c-Myc regulates mammalian body size by controlling cell number but not cell size. Nature *414*, 768-773.

Vaque, J.P., Fernandez-Garcia, B., Garcia-Sanz, P., Ferrandiz, N., Bretones, G., Calvo, F., Crespo, P., Marin, M.C., and Leon, J. (2008). c-Myc inhibits Ras-mediated differentiation of pheochromocytoma cells by blocking c-Jun up-regulation. Mol Cancer Res *6*, 325-339.

Vennstrom, B., Sheiness, D., Zabielski, J., and Bishop, J.M. (1982). Isolation and Characterization of C-Myc, a Cellular Homolog of the Oncogene (V-Myc) of Avian Myelocytomatosis Virus Strain-29. J Virol *42*, 773-779.

Wade, P.A., Werel, W., Fentzke, R.C., Thompson, N.E., Leykam, J.F., Burgess, R.R., Jaehning, J.A., and Burton, Z.F. (1996). A novel collection of accessory factors associated with yeast RNA polymerase II. Protein Expres Purif *8*, 85-90.

Walz, S., Lorenzin, F., Morton, J., Wiese, K.E., von Eyss, B., Herold, S., Rycak, L., Dumay-Odelot, H., Karim, S., Bartkuhn, M.*, et al.* (2014). Activation and repression by oncogenic MYC shape tumour-specific gene expression profiles (vol 511, pg 483, 2014). Nature *516*.

Warren, J.T., Petryk, A., Marques, G., Jarcho, M., Parvy, J.P., Dauphin-Villemant, C., O'Connor, M.B., and Gilbert, L.I. (2002). Molecular and biochemical characterization of two P450 enzymes in the ecdysteroidogenic pathway of Drosophila melanogaster. Proceedings of the National Academy of Sciences of the United States of America *99*, 11043-11048.

Warren, J.T., Petryk, A., Marques, G., Parvy, J.P., Shinoda, T., Itoyama, K., Kobayashi, J., Jarcho, M., Li, Y.T., O'Connor, M.B.*, et al.* (2004). Phantom encodes the 25-hydroxylase of Drosophila melanogaster and Bombyx mori: a P450 enzyme critical in ecdysone biosynthesis. Insect Biochem Molec *34*, 991-1010.

Warren, J.T., Yerushalmi, Y., Shimell, M.J., O'Connor, M.B., Restifo, L.L., and Gilbert, L.I. (2006). Discrete pulses of molting hormone, 20-hydroxyecdysone, during late larval development of Drosophila melanogaster: correlations with changes in gene activity. Developmental dynamics : an official publication of the American Association of Anatomists *235*, 315-326.

Wert, M., Kennedy, S., Palfrey, H.C., and Hay, N. (2001). Myc drives apoptosis in PC12 cells in the absence of Max. Oncogene *20*, 3746-3750.

Wood, M.A., McMahon, S.B., and Cole, M.D. (2000). An ATPase/helicase complex is an essential cofactor for oncogenic transformation by c-Myc. Molecular cell *5*, 321-330.

Xu, Y., Bernecky, C., Lee, C.T., Maier, K.C., Schwalb, B., Tegunov, D., Plitzko, J.M., Urlaub, H., and Cramer, P. (2017). Architecture of the RNA polymerase II-Paf1C-TFIIS transcription elongation complex. Nature communications *8*, 15741.

Yamanaka, N., Rewitz, K.F., and O'Connor, M.B. (2013). Ecdysone control of developmental transitions: lessons from Drosophila research. Annual review of entomology *58*, 497-516.

Yang, J.P., Sung, E., Donlin-Asp, P.G., and Corces, V.G. (2013). A subset of Drosophila Myc sites remain associated with mitotic chromosomes colocalized with insulator proteins. Nature communications *4*.

Youn, M.Y., Yoo, H.S., Kim, M.J., Hwang, S.Y., Choi, Y., Desiderio, S.V., and Yoo, J.Y. (2007). hCTR9, a component of Paf1 complex, participates in the transcription of interleukin 6-responsive genes through regulation of STAT3-DNA interactions. Journal of Biological Chemistry *282*, 34727-34734.

Yu, M., Yang, W., Ni, T., Tang, Z., Nakadai, T., Zhu, J., and Roeder, R.G. (2015). RNA polymerase II-associated factor 1 regulates the release and phosphorylation of paused RNA polymerase II. Science *350*, 1383-1386.

Zhang, Y., Liu, T., Meyer, C.A., Eeckhoute, J., Johnson, D.S., Bernstein, B.E., Nusbaum, C., Myers, R.M., Brown, M., Li, W.*, et al.* (2008). Model-based analysis of ChIP-Seq (MACS). Genome biology *9*, R137.

Zhu, B., Zheng, Y., Pham, A.D., Mandal, S.S., Erdjument-Bromage, H., Tempst, P., and Reinberg, D. (2005). Monoubiquitination of human histone H2B: The factors involved and their roles in HOX gene regulation. Molecular cell *20*, 601-611.

7 Appendix

## 7.1 Supplemental figures

A

B

C
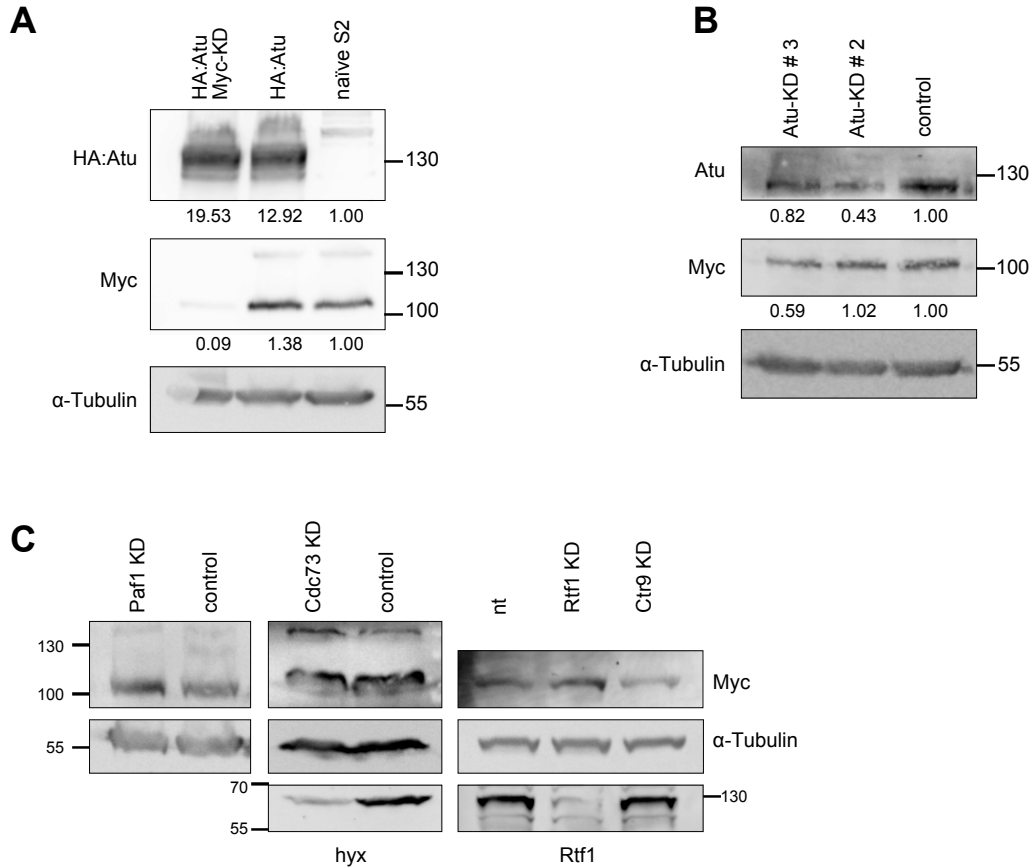
Figure S1: Western blots of PAF1 complex components

A) Western blot displaying HA:Atu induction and Myc depletion. The proteins were visualized with anti-HA and anti-Myc antibodies. α-Tubulin was used as a loading control. The blot belongs to Figure 4.4 A.

B) Western blot confirming Atu depletion. The blot was probed with antibodies against Atu and Myc. α-Tubulin served as loading control. This blot belongs to Figure 4.4 C.

C) Western blot analysis of endogenous Myc levels after depletion of different PAF1 complex components and confirmation of the knockdown. The blots were probed with the indicated antibodies. α-Tubulin was used as loading control. These blots belong to Figure 4.5 B.
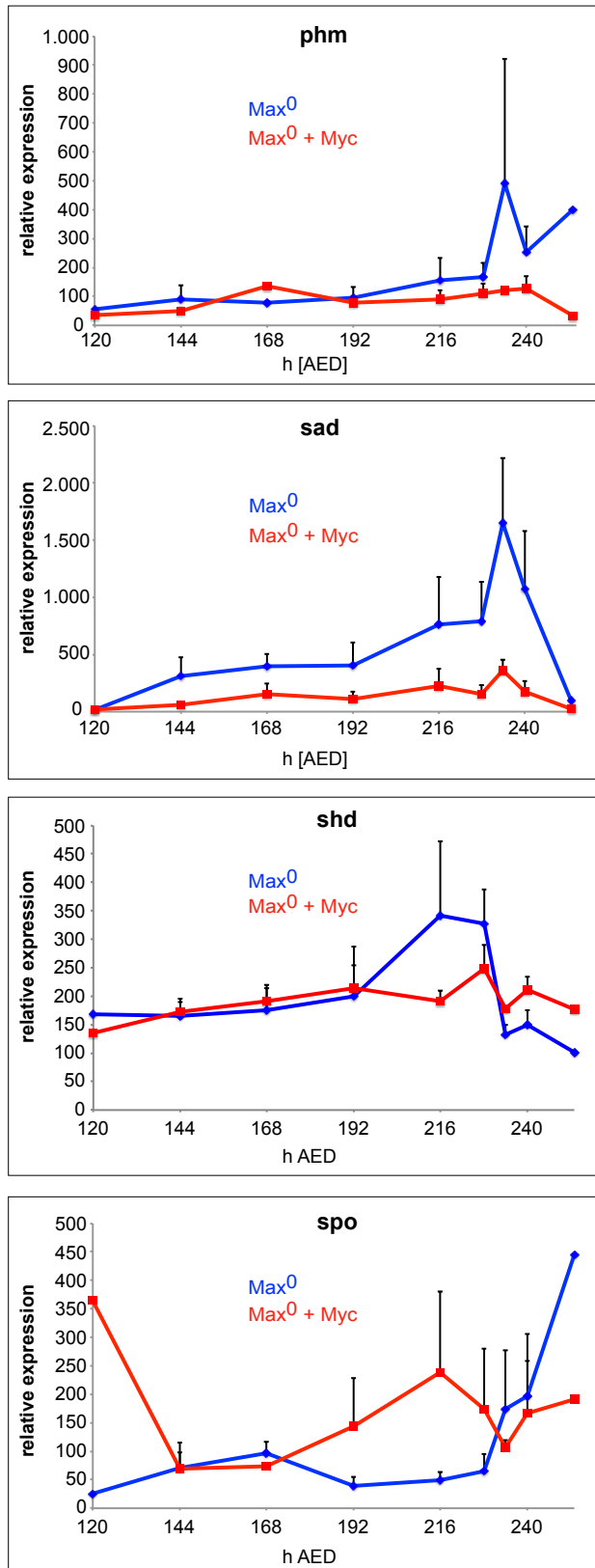
Figure S2: Expression levels of additional Halloween genes

Levels of the Halloween genes *phm*, *sad*, *shd*, and *spo* during development of Max[0] mutants with and without Myc overexpression measured by qRT-PCR. Values were normalized to actin5C of each sample and then to the value of the wt control at the first timepoint. Each data point results from one to three independent experiments, error bars indicate SEM.

7.2 Abbreviations

Prefixes	
p	pico
n	nano
µ	micro
m	milli
c	centi
k	kilo

Units	
°C	degree celsius
A	ampere
Da	dalton
g	gram
h	hour
l	liter
m	meter
min	minute
M	mol/l
OD	optical density
s	second
U	unit
V	volts
v/v	volumer per volume
w/v	weight per volume

Proteins, protein domains and other biomolecules	
A	adenine
aa	amino acid
bp	basepair(s)
bHLH	basic helix-loop-helix
C	cytosine
cDNA	complementary DNA
dATP	deoxyadenosine triphosphate
dCTP	deoxycytidine triphosphate
dGTP	deoxyguanosine triphosphate
dTTP	deoxythymidine triphosphate

DNA	deoxyribonucleic acid
dNTPs	deoxyribonucleoside triphosphates
dsRNA	double stranded RNA
FRT	flipase recombination target
G	guanine
GFP	green fluorescent protein
HRP	horseradish peroxidase
nt	nucleotide(s)
ORF	open reading frame
RNA	ribonucleic acid
LZ	leucine zipper
T	thymine
UAS	upstream activating sequence
UTR	untranslated region

Chemicals and solutions

APS	ammoniumpersulfate
BSA	bovine serum albumine
ddH$_2$O	bidestilled water
DMSO	dimethylsulfoxide
EDTA	ethylendiamintetraacetate
FBS	fetal bovine serum
PBS	phosphate-buffered saline
SDS	sodium dodecyl sulfate
TAE	
TBS	Tris-buffered saline
TBS-T	Tris-buffered saline with tween-20
TE	Tris-EDTA-buffer
TEMED	N,N,N',N'-tetramethylethylendiamine
Tris	Tris-(hydroxymethyl)-aminomethan

Other abbreviations

ChIP	chromatin immunoprecipitation
ChIP-seq	chromatin immunoprecipitation followed by deep sequencing
E. coli	*Escherichia coli*
e.g.	for example

hs	heat shock
IP	immunoprecipitation
PAGE	polyacrylamide-gelelectrophoresis
PCR	polymerase chain reaction
pers. com.	personal communication
qPCR	quantitative PCR
qRT-PCR	quantitative Reverse Transcriptase PCR
RNAi	RNA interference
rpm	rotations per minute
RT	room temperature
SC	Santa Cruz
o./n.	overnight; 16-20 h
WT	wildtype
ΔZ	depleted leucine zipper

7.3 Acknowledgements

First of all, I would like to thank my supervisor, Prof. Dr. Peter Gallant, for the opportunity to work on this project. I am very grateful for his encouragement and support throughout this project and for his open ear whenever I had problems.

I would also like to thank my committee members Prof. Dr. Christian Wegener and Prof. Dr. Thomas Raabe for their support in my progress over the years.

I would like to thank all present and former members of the Gallant lab for a wonderful working atmosphere: Eva Herter, Oriel Carreno, Maria Piera, Katharina Grund-Müller, Maria Gallant, André Kutschke and Dirk Birkel.

Furthermore, I want to thank all members of the Eilers, Schulze, Wolf and Diefenbacher group for countless discussions and technical help.

A big "thank you" to Eva, Francesca and Apoorva for correcting my thesis.

A special thanks to Eva, Oriel, Anne, Francesca, Francesca, Jiajia, Irem, Gabriele, Theresa, Isabelle and Apoorva for the great time we spent together, also outside the lab. Thank you for the coffee breaks, movie nights and dinners we enjoyed together.

I want to thank my whole family for their continuous support and love! Thank you!

Finally, I especially want to thank Martin. I am so thankful for your love, your encouragement and that you always believed in me, even when I didn´t believe in myself. Thank you for always being by my side!

7.4 Curriculum vitae

7.5 Affidavit

I hereby confirm that my thesis entitled **"Influence of Myc-interacting proteins on transcription and development"** is the result of my own work. I did not receive any help or support from commercial consultants. All sources and/or materials applied are listed and specified in the thesis.

Furthermore, I confirm that this thesis has not yet been submitted as part of another examination process neither in identical nor in similar form.

Würzburg, 30.06.2017

Place, Date   Signature

7.6 Eidesstattliche Erklärung

Hiermit erkläre ich an Eides statt, die Dissertation **"Der Einfluss von Myc-interagierenden Proteinen auf Transkription und Entwicklung"** eigenständig, d.h. insbesondere selbständig und ohne Hilfe eines kommerziellen Promotionsberaters, angefertigt und keine anderen als die von mir angegebenen Quellen und Hilfsmittel verwendet zu haben.

Ich erkläre außerdem, dass die Dissertation weder in gleicher noch in ähnlicher Form bereits in einem anderen Prüfungsverfahren vorgelegen hat.

Würzburg, 30.06.2017

Ort, Datum   Unterschrift